



The
University
Of
Sheffield.

This is a repository copy of *Improved reconstruction of highly boosted τ -lepton pairs in the $\tau\tau \rightarrow (\mu\nu\mu\nu\tau)(\text{hadrons} + \nu\tau)$ decay channels with the ATLAS detector*.

White Rose Research Online URL for this paper:

<https://eprints.whiterose.ac.uk/228622/>

Version: Published Version

Article:

Aad, G. orcid.org/0000-0002-6665-4934, Aakvaag, E. orcid.org/0000-0001-7616-1554, Abbott, B. orcid.org/0000-0002-5888-2734 et al. (2881 more authors) (2025) Improved reconstruction of highly boosted τ -lepton pairs in the $\tau\tau \rightarrow (\mu\nu\mu\nu\tau)(\text{hadrons} + \nu\tau)$ decay channels with the ATLAS detector. *The European Physical Journal C*, 85 (6). 706. ISSN 1434-6044

<https://doi.org/10.1140/epjc/s10052-025-14012-4>

Reuse

This article is distributed under the terms of the Creative Commons Attribution (CC BY) licence. This licence allows you to distribute, remix, tweak, and build upon the work, even commercially, as long as you credit the authors for the original work. More information and the full terms of the licence here:
<https://creativecommons.org/licenses/>

Takedown

If you consider content in White Rose Research Online to be in breach of UK law, please notify us by emailing eprints@whiterose.ac.uk including the URL of the record and the reason for the withdrawal request.



Improved reconstruction of highly boosted τ -lepton pairs in the $\tau\tau \rightarrow (\mu\nu_\mu\nu_\tau)(\text{hadrons} + \nu_\tau)$ decay channels with the ATLAS detector

ATLAS Collaboration*

CERN, 1211 Geneva 23, Switzerland

Received: 20 December 2024 / Accepted: 26 February 2025

© CERN for the benefit of the ATLAS Collaboration 2025

Abstract This paper presents a new τ -lepton reconstruction and identification procedure at the ATLAS detector at the Large Hadron Collider, which leads to significantly improved performance in the case of physics processes where a highly boosted pair of τ -leptons is produced and one τ -lepton decays into a muon and two neutrinos (τ_μ), and the other decays into hadrons and one neutrino (τ_{had}). By removing the muon information from the signals used for reconstruction and identification of the τ_{had} candidate in the boosted pair, the efficiency is raised to the level expected for an isolated τ_{had} . The new procedure is validated by selecting a sample of highly boosted $Z \rightarrow \tau_\mu \tau_{\text{had}}$ candidates from the data sample of 140 fb^{-1} of proton–proton collisions at 13 TeV recorded with the ATLAS detector. Good agreement is found between data and simulation predictions in both the $Z \rightarrow \tau_\mu \tau_{\text{had}}$ signal region and in a background validation region. The results presented in this paper demonstrate the effectiveness of the τ_{had} reconstruction with muon removal in enhancing the signal sensitivity of the boosted $\tau_\mu \tau_{\text{had}}$ channel at the ATLAS detector.

Contents

1	Introduction
2	ATLAS detector
3	Data and simulated event samples
3.1	Simulated samples for the development of the method
3.2	Data and simulated samples for the validation of the method
4	Development of the boosted τ_{had}^N reconstruction method
4.1	Muon removal and re-reconstruction of the τ_{had} candidate
4.2	Performance of the method

5	Validation of the τ_{had}^N method in the $Z \rightarrow \tau_\mu \tau_{\text{had}}$ final states
5.1	Z -boson kinematic reconstruction
5.2	Event selection
5.3	Systematic uncertainties
5.4	Results
6	Conclusions
	References

1 Introduction

The τ -lepton is the heaviest known lepton, with a mass of 1.777 GeV, and a lifetime of 2.9×10^{-13} s [1]. It has a 35% probability of decaying leptonically into a lighter lepton and two neutrinos: $\tau \rightarrow e\nu_e\nu_\tau$ or $\tau \rightarrow \mu\nu_\mu\nu_\tau$ (denoted τ_μ), collectively referred to as τ_{lep} . In the remaining 65% of cases, the τ -lepton decays hadronically (τ_{had}) into one or more charged hadrons and zero or more neutral hadrons, plus one neutrino. Thus, the fraction of τ -lepton pairs resulting in a $\tau_\mu \tau_{\text{had}}$ final state is 23%.

The standard ATLAS τ_{had} reconstruction and identification procedure [2–5] starts with the reconstruction of the visible decay products of a τ_{had} candidate ($\tau_{\text{had-vis}}$), which is seeded by a jet clustered using the anti- k_t algorithm [6,7] with a radius parameter $R = 0.4$.¹ The jet reconstruction algorithm operates on the topological calorimeter cells [8] calibrated to the local hadronic energy scale [9]. This seed

¹ ATLAS uses a right-handed coordinate system with its origin at the nominal interaction point (IP) in the centre of the detector and the z -axis along the beam pipe. The x -axis points from the IP to the centre of the LHC ring, and the y -axis points upwards. Polar coordinates (r, ϕ) are used in the transverse plane, ϕ being the azimuthal angle around the z -axis. The pseudorapidity is defined in terms of the polar angle θ as $\eta = -\ln \tan(\theta/2)$ and is equal to the rapidity $y = \frac{1}{2} \ln \left(\frac{E+p_z}{E-p_z} \right)$ in the relativistic limit. Angular distance is measured in units of $\Delta R \equiv \sqrt{(\Delta y)^2 + (\Delta\phi)^2}$.

* e-mail: atlas.publications@cern.ch

jet is referred to as τ_{seed} jet. Only τ_{seed} jets with transverse momentum $p_T > 5 \text{ GeV}$ and pseudorapidity $|\eta| < 2.5$ are considered. Dedicated algorithms [5] are run to identify the production vertex, associating and classifying reconstructed inner detector tracks, and calibrating the energy of the τ_{had} candidate. Tracks that have passed the τ_{seed} jet association requirements are classified into four categories: ‘Tau Tracks’, ‘Conversion Tracks’, ‘Isolation Tracks’ and ‘Fake Tracks’. Only ‘Tau Tracks’ are used to determine the number of charged decay products and thus the charge of the τ lepton. After reconstruction, the τ_{had} candidate is classified by the τ_{had} identification algorithm (TauID), a recurrent neural network (RNN) classifier [4], to determine its likelihood of being the decay product of a τ_{had} . Several working points, ‘Tight’, ‘Medium’, ‘Loose’ and ‘VeryLoose’, are then defined based on optimised requirements on the RNN score with different τ_{had} identification efficiencies [4].

The standard TauID algorithm is efficient unless activity from other particles is found inside the τ_{seed} jet. One of these cases is when a pair of τ -leptons originates from a highly boosted resonance and the decay products of the two τ -leptons are reconstructed within the radius of a single τ_{seed} jet. The reconstruction and identification of boosted systems in which both τ -leptons decay hadronically is achieved by searching for hadronic τ -like substructure using a boosted decision tree within a large radius seed jet [10]. In this analysis, the decay into the $\tau_\mu \tau_{\text{had}}$ final state is considered.

Muon reconstruction [11] in the ATLAS detector is based on the information from the inner tracking detector (ID) and the muon spectrometer (MS), complemented by calorimeter data. The reconstruction begins by identifying tracks in the MS, followed by matching these with tracks in the ID. In cases where a candidate can be made from ID and MS tracks, a combined fit is performed, taking into account the energy loss in the calorimeters. This study considers muons satisfying the ‘Medium’ identification working point [11], which ensures a combined muon where the ID track matches the MS signature. The minimum ionising nature of the muon and the fact that the muon reconstruction is independent of its isolation [11] enables the possibility of removing the ID track and clusters produced by the muon from the τ_{seed} jet produced by a boosted $\tau_\mu \tau_{\text{had}}$ system. The kinematic variables that are subsequently supplied to the TauID algorithm are re-calculated without the interference of the muon. The τ_{had} reconstructed with this method is referred to as τ_{had}^μ .

The τ_{had}^μ method was developed using simulated events corresponding to a beyond the Standard Model (BSM) process with a high-mass graviton [12] decaying into two Higgs bosons as signal. Before using this technique in future BSM searches, it is important to demonstrate its performance using a Standard Model (SM) process. As a validation for the new method, the production of two τ -leptons originating from

a highly boosted Z boson giving the final state of interest, $Z \rightarrow \tau_\mu \tau_{\text{had}}$, is used.

This paper is organised as follows. The ATLAS detector is described briefly in Sect. 2. The data and simulated samples are described in Sect. 3. The development of the boosted τ_{had}^μ method is described in Sect. 4. The analysis methods and the results for the $Z \rightarrow \tau_\mu \tau_{\text{had}}$ validation are described in Sect. 5. Finally, the conclusions are given in Sect. 6.

2 ATLAS detector

The ATLAS detector [13] at the Large Hadron Collider (LHC) [14] is a multipurpose particle detector with a forward–backward symmetric cylindrical geometry and a near 4π coverage in solid angle. It consists of an ID surrounded by a thin superconducting solenoid providing a 2 T axial magnetic field, electromagnetic (EM) and hadronic calorimeters, and a MS. The inner tracking detector covers the pseudorapidity range $|\eta| < 2.5$. It consists of silicon pixel, silicon microstrip, and transition radiation tracking detectors. Lead/liquid-argon (LAr) sampling calorimeters provide EM energy measurements with high granularity within the region $|\eta| < 3.2$. A steel/scintillator-tile hadronic calorimeter covers the central pseudorapidity range ($|\eta| < 1.7$). The endcap and forward regions are instrumented with LAr calorimeters for EM and hadronic energy measurements up to $|\eta| = 4.9$. The MS surrounds the calorimeters and is based on three large superconducting air-core toroidal magnets with eight coils each. The field integral of the toroids ranges between 2.0 and 6.0 T m across most of the detector. The MS includes a system of precision tracking chambers up to $|\eta| = 2.7$ and fast detectors for triggering up to $|\eta| = 2.4$. The luminosity is measured mainly by the LUCID-2 [15] detector, which is located close to the beampipe. A two-level trigger system is used to select events [16]. The first-level trigger is implemented in hardware and uses a subset of the detector information to accept events at a rate below 100 kHz. This is followed by a software-based trigger that reduces the accepted event rate to 1 kHz on average depending on the data-taking conditions. A software suite [17] is used in data simulation, in the reconstruction and analysis of real and simulated data, in detector operations, and in the trigger and data acquisition systems of the experiment.

3 Data and simulated event samples

3.1 Simulated samples for the development of the method

Monte Carlo (MC) simulated event samples [18] of signal and backgrounds are used to develop the τ_{had}^μ method and to evaluate the τ_{had} reconstruction and identification efficiency.

cies, as well as the background rejection power. The signal samples consist of BSM gravitons [12] decaying into a pair of Higgs bosons, with the hypothetical graviton mass ranging from 1 to 5 TeV. For this study, the SM Higgs bosons are constrained to decay into a pair of τ -leptons. The signal process is referred to as $G \rightarrow HH \rightarrow 4\tau$.

High- p_T , semileptonically decaying heavy-flavour hadrons may produce a detector signature that has some similarities with the signal sample of boosted $\tau_\mu \tau_{\text{had}}$ pairs, since the invariant mass of the charm hadron produced in the semileptonic decay of a bottom hadron is comparable to the τ -lepton mass. The top-antitop-quark process ($t\bar{t}$) is used to model this type of background.

The $G \rightarrow HH \rightarrow 4\tau$ signal samples were simulated using the MADGRAPH5_AMC@NLO [19] generator using matrix elements (ME) at leading-order (LO) in quantum chromodynamics (QCD) with the NNPDF2.3LO [20] parton distribution function (PDF) set. The production of $t\bar{t}$ events was modelled using the POWHEG BOX v2 [21–24] generator at next-to-leading order (NLO) in QCD with the NNPDF3.0NLO [25] PDF set and the h_{damp} parameter² set to $1.5 m_{\text{top}}$ [26].

PYTHIA 8.230 [27] with the A14 [28] set of tuned parameters (tune) and NNPDF2.3LO PDF set was used for the simulation of the parton showering and hadronisation for both the $G \rightarrow HH \rightarrow 4\tau$ samples and the $t\bar{t}$ samples. The decays of bottom and charm hadrons were performed by EVTGEN 1.6.0 [29]. The effect of multiple interactions in the same and neighbouring bunch crossings (pile-up) was modelled by overlaying the original hard-scattering event with simulated inelastic proton–proton collisions generated by PYTHIA 8.186 [30] with the A3 tune [31] and the MSTW2008LO PDF set [32]. The MC samples were reweighted so that the pile-up distribution matches the one observed in the data. All MC samples were passed through the ATLAS detector simulation based on GEANT4 [33].

3.2 Data and simulated samples for the validation of the method

For the $Z \rightarrow \tau_\mu \tau_{\text{had}}$ validation analysis, the Run 2 data sample collected in proton–proton collisions at the LHC with $\sqrt{s} = 13$ TeV and a 25 ns bunch crossing interval is used. The integrated luminosity of the sample recorded while all relevant components of the ATLAS detector were operating normally corresponds to 140 fb^{-1} [34,35].

Simulated samples provide predictions for both signal and background processes. As described in Sect. 3.1, the simulation includes the effect of pile-up and the detector response. All MC samples undergo calibrations and corrections to match the performance in data. EVTGEN 1.6.0 [29] was used again to decay bottom and charm hadrons. The rest of this section gives details of the specific MC samples used in this study.

The dominant production channel of the boosted $Z \rightarrow \tau_\mu \tau_{\text{had}}$ final states, a Z boson produced in association with jets, was modelled using the SHERPA 2.2.14 [36] generator for the $Z \rightarrow \tau\tau$ channel, while SHERPA 2.2.11 was used to model $Z \rightarrow \ell\ell$ ($\ell = e, \mu$) decays. The ME calculations ranged from NLO in QCD for final states with up to two additional parton emissions to LO in QCD for up to five additional parton emissions. The MEs were merged with the SHERPA parton shower following the MEPS@LO [37] prescription and using the NNPDF3.0NNLO [25] PDF set. The production of W bosons with jets, and the production of WW , WZ , and ZZ boson pairs, were simulated using SHERPA 2.2.11 with configurations similar to those used in the $Z+\text{jets}$ sample. Measurements of the distribution of Z -boson transverse momentum (p_T^Z) using light-lepton pair events at $\sqrt{s} = 13$ TeV [38] indicate that SHERPA 2.2.11 underestimates the cross-section for $p_T^Z > 100$ GeV by approximately 10% [39]. The simulation of initial-state QCD radiation is expected to be the same in the SHERPA 2.2.14 samples used in this study. A 10% correction is therefore applied to the predicted event yields for $Z \rightarrow \tau\tau$ in the validation analysis, with the full size of this correction quoted as a systematic uncertainty.

The production of $t\bar{t}$ events was modelled using the same configuration as the one used for the method development as in Sect. 3.1. Single-top t -channel production was modelled using the POWHEG BOX v2 [22–24,40] generator at NLO in QCD using the four-flavour scheme and the corresponding NNPDF3.0NLO PDF set. The associated production of top quarks with W bosons (tW) was modelled using the POWHEG BOX v2 generator at NLO in QCD using the five-flavour scheme and the NNPDF3.0NLO PDF set. The diagram removal scheme [41] was used to remove interference and overlap with $t\bar{t}$ production. In both cases the generated events were interfaced to PYTHIA 8.230 using the A14 tune and the NNPDF2.3LO PDF set.

The production of Higgs bosons via gluon–gluon fusion and vector–boson fusion was modeled following the configuration detailed in Ref. [42].

² The h_{damp} parameter is a resummation damping factor and one of the parameters that controls the matching of POWHEG matrix elements to the parton shower and thus effectively regulates the high-transverse-momentum radiation against which the $t\bar{t}$ system recoils.

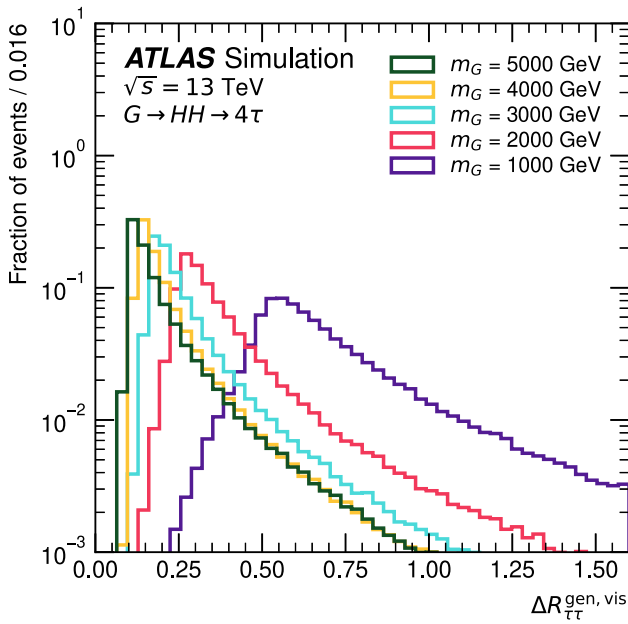


Fig. 1 The distributions of the $\Delta R_{\tau\tau}^{\text{gen},\text{vis}}$ for the generator-level $\tau_\mu \tau_{\text{had}}$ pair in $G \rightarrow HH \rightarrow 4\tau$ signal events, with graviton masses m_G ranging from 1000 to 5000 GeV

4 Development of the boosted τ_{had}^μ reconstruction method

4.1 Muon removal and re-reconstruction of the τ_{had} candidate

The τ_{had}^μ method was developed with simulated $G \rightarrow HH \rightarrow 4\tau$ signal samples with generator-level information used to evaluate the performance of the method. The angular distance at the generator-level between the $\tau_{\text{had-vis}}$ and the muon is measured by $\Delta R_{\tau\tau}^{\text{gen},\text{vis}}$. In Fig. 1, the $\Delta R_{\tau\tau}^{\text{gen},\text{vis}}$ distributions of the $\tau_\mu \tau_{\text{had}}$ pairs in the $G \rightarrow HH \rightarrow 4\tau$ samples are presented.

For $\Delta R_{\tau\tau}^{\text{gen},\text{vis}} < 0.4$, it is more likely that the muon will be reconstructed inside the τ_{seed} jet.

In this study, MC generator-level information is used to match generated $\tau_\mu \tau_{\text{had}}$ pairs with their reconstructed counterparts. The reconstructed τ_{seed} jet is generator-matched if at least one ID track matches the muon from the τ_{lep} decay or the charged hadron(s) from the τ_{had} decay. Only τ_{seed} jets originating from a boosted $\tau_\mu \tau_{\text{had}}$ pair are considered. Other τ_{seed} jets, such as those associated with QCD jets, are neglected. The MC generator-level visible τ -lepton decay products are required to satisfy the requirements $p_T > 20$ GeV and $|\eta| < 2.5$ to ensure that the τ_{seed} jets are within the tracking acceptance of the ATLAS detector.

Below the $\Delta R_{\tau\tau}^{\text{gen},\text{vis}} < 0.4$ threshold, the standard τ_{had} reconstruction and identification efficiencies drop significantly. Figure 2 shows the combined reconstruction and iden-

tification efficiencies of the standard ATLAS τ_{had} reconstruction and TauID algorithms as a function of $\Delta R_{\tau\tau}^{\text{gen},\text{vis}}$ for generator-level 1-prong and 3-prong τ_{had} in $\tau_\mu \tau_{\text{had}}$ pairs. Here ‘n-prong’ denotes the number of charged hadrons that originate from the τ_{had} decay. The ‘ $N_{\text{trk}}^{\text{reco}} = 1$ or 3’ lines shows the efficiency of a generator-level 1-prong or 3-prong τ_{had} being reconstructed with the correct number of associated charged-particle tracks. The efficiency for a τ_{seed} jet to be reconstructed from a $\tau_\mu \tau_{\text{had}}$ pair remains high for all values of $\Delta R_{\tau\tau}^{\text{gen},\text{vis}}$. However, the efficiencies for all standard TauID working points drop significantly in both the 1-prong and 3-prong cases when $\Delta R_{\tau\tau}^{\text{gen},\text{vis}} < 0.4$. The tighter the working point, the greater the fractional loss in efficiency due to the presence of the nearby muon. The performance of the standard TauID algorithm is set as the baseline in this study.

The muon’s nature as a minimum ionising particle, combined with the fact that its reconstruction is independent of its isolation [11], provides a motivation for excluding the ID track and calorimeter clusters associated with any nearby muon from the standard ATLAS τ_{had} reconstruction algorithm. By removing these contributions, the τ_{seed} jet would better represent only the $\tau_{\text{had-vis}}$, improving the accuracy of the TauID algorithm. Specifically, the ID track and clusters associated with a reconstructed muon that satisfies the ‘Medium’ muon identification working point are removed if the track or cluster is found within the reconstructed τ_{seed} jet. For calorimeter energy clusters, the algorithm checks if the energy of the cluster associated with the muon is compatible with the expected energy loss [43] from its interactions with the calorimeters between the ID and the MS and removes the cluster only when this is the case. After the muon removal, the standard τ_{had} reconstruction algorithm is re-run on the τ_{seed} jet. In this way, the relevant TauID variables for the τ_{had} candidate can be calculated without the muon component.

4.2 Performance of the method

Figure 3 shows the combined reconstruction and identification efficiencies after the muon removal as a function of $\Delta R_{\tau\tau}^{\text{gen},\text{vis}}$ for generator-level 1-prong and 3-prong $\tau_\mu \tau_{\text{had}}$ pairs for all working points. The reconstruction and identification efficiencies after the muon removal show a considerable improvement compared to those shown in Fig. 2. The signal efficiency is recovered almost completely for every working point for both 1-prong and 3-prong τ_{had} . In the 3-prong cases, the efficiency of TauID is limited by the accurate reconstruction of the correct number of tracks associated with the highly boosted τ_{had} candidates.

Roughly 95% of the τ_{seed} jets have a muon removed in the region where $\Delta R_{\tau\tau}^{\text{gen},\text{vis}} < 0.4$. This can be expected given the 97% efficiency of the ‘Medium’ muon working point,

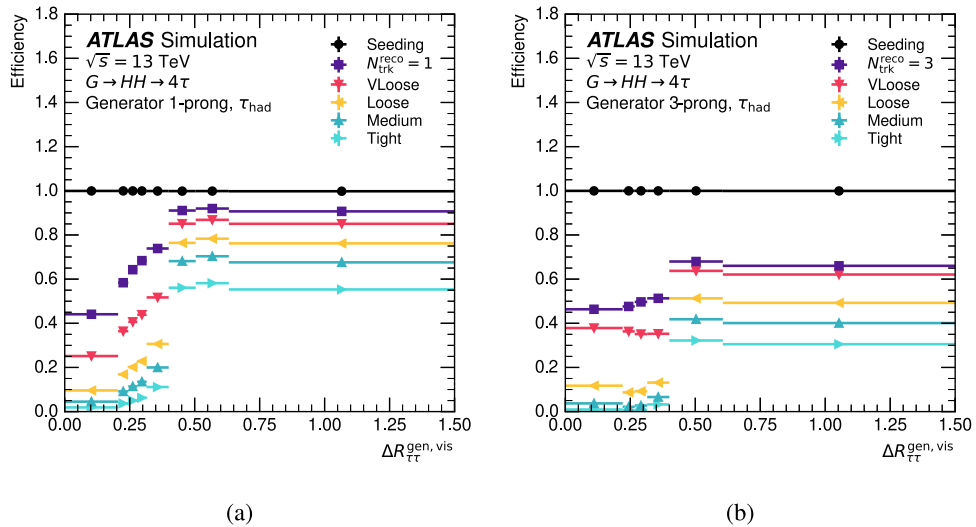


Fig. 2 The combined reconstruction and identification efficiencies of the standard ATLAS TauID for generator-level **a** 1-prong and **b** 3-prong $\tau_\mu \tau_{\text{had}}$ pairs at all working points as a function of $\Delta R_{\tau\tau}^{\text{gen,vis}}$. The ‘Seed-ing’ line shows the efficiency of a τ_{seed} jet that matches a generator-level $\tau_\mu \tau_{\text{had}}$ pair being reconstructed; the ‘ $N_{\text{trk}}^{\text{reco}} = 1$ or 3’ line shows the

efficiency of a generator-level τ_{had} being reconstructed with the correct number of associated charged-particle tracks. The ‘VLoose’, ‘Loose’, ‘Medium’, and ‘Tight’ lines show the efficiencies of the TauID working points

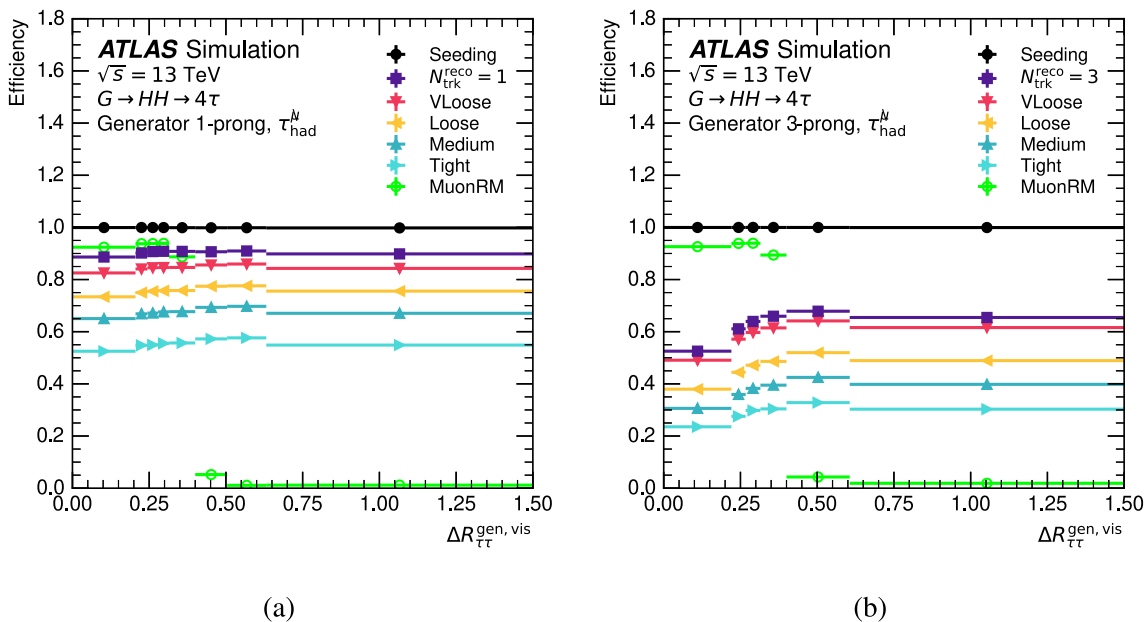


Fig. 3 The combined reconstruction and TauID efficiencies after the muon removal for generator-level **a** 1-prong and **b** 3-prong $\tau_\mu \tau_{\text{had}}$ pairs at all working points as a function of $\Delta R_{\tau\tau}^{\text{gen,vis}}$. The ‘Seeding’ line shows the efficiency of a τ_{seed} jet that matches a generator-level $\tau_\mu \tau_{\text{had}}$ pair being reconstructed; the ‘ $N_{\text{trk}}^{\text{reco}} = 1$ or 3’ line shows the efficiency of a generator-level τ_{had} being reconstructed with the correct number of

associated charged-particle tracks. The ‘VLoose’, ‘Loose’, ‘Medium’, and ‘Tight’ lines show the efficiencies of the TauID working points. The ‘MuonRM’ line shows the efficiency of a muon being identified and removed from the τ_{seed} jet. The transitions of the ‘MuonRM’ line between $0.35 < \Delta R_{\tau\tau}^{\text{gen,vis}} < 0.45$ is due to limited detector resolution in the direction of the reconstructed $\tau_{\text{had-vis}}$ and muon

with a dip below 90% in the region where the generator-level $|\eta|$ of the $\tau_{\text{had-vis}}$ is $|\eta|^{\text{gen,vis}} < 0.1$. This is illustrated in Fig. 4, which shows the signal efficiencies of the TauID working points after the muon removal as a function of $|\eta|^{\text{gen,vis}}$ for generator-level 1-prong and 3-prong τ_{seed} jets with $\Delta R_{\tau\tau}^{\text{gen,vis}} < 0.4$. The slight decrease in muon removal efficiency in the low $|\eta|^{\text{gen,vis}}$ region is caused by the non-instrumented regions of the MS.

The signal identification efficiencies at all working points of the standard ATLAS TauID are tuned to show minimum dependency on the generator-level p_T of the $\tau_{\text{had-vis}}$ ($p_{T,\tau}^{\text{gen,vis}}$) and pile-up [5]. The stability of the TauID working point efficiencies, after the muon removal, against these variables are shown in Fig. 5. To focus on the objects of interest, only generator-level $\tau_\mu \tau_{\text{had}}$ pairs with the muon identified inside the τ_{seed} jet and removed ($\Delta R_{\tau\tau}^{\text{reco}} < 0.4$) are included in these plots. For comparison, the TauID working point efficiencies as a function of the same variables for τ_{seed} objects in which muon removal is not required ($\Delta R_{\tau\tau}^{\text{gen,vis}} > 0.45$) are shown in Fig. 6. Similar behaviour is observed in Figs. 5 and 6. The improved performance and good stability across different working points demonstrate that, after the muon removal, the TauID RNN receives as input the signal τ_{seed} jet as if it were a τ_{had} that is isolated (free from interference of surrounding particles).

After the removal of the overlapping muon, the precision with which the four-momentum of the τ_{seed} jet is reconstructed improves significantly. Figure 7a shows the distributions of the difference between the generated and reconstructed η (residuals) before and after the muon removal. Compared to the performance before muon removal, the η residuals that correspond to the 68% percentile (core resolution) improves by a factor of 15. The distributions of the $\tau_{\text{had-vis}}$ p_T residuals (p_T/p_T^{gen}) are shown in Fig. 7b. These results agree well with those reported for isolated τ_{had} in Ref. [44], further demonstrating the effectiveness of the muon removal method.

Having demonstrated that the reconstruction and identification efficiencies are significantly improved by the τ_{had} method, the background rejection power is studied. The production of $t\bar{t}$ events is considered as a source of high- p_T heavy-flavour jets, which represents an example background to the τ_{had} signal. The background rejection at the ‘Medium’ TauID working point, which is defined as the ratio of the total number of reconstructed τ_{had} candidates before muon removal to the number of false positives before or after muon removal, are shown in Fig. 8, as functions of the reconstructed $\tau_{\text{had-vis}}$ p_T . For the background rejection figures, the event selections are mostly based on the reconstructed properties instead of the generator-level information. A τ_{seed} jet recon-

structed in the background sample is required to have reconstructed $20 \text{ GeV} < p_T < 300 \text{ GeV}$, $|\eta| < 2.5$, and to not be generator-matched to a τ_{had} from the semileptonic decay of a bottom or top quark. In addition, a reconstructed muon is required to be found inside the τ_{seed} jet. The τ_{had} candidates in which no muon is present are not considered in Fig. 8, as identical TauID results would be expected for these cases.

It is likely that after removing the muon, the number of reconstructed charged-particle tracks inside the τ_{seed} jet decreases by one compared to the standard reconstruction. Thus the background compositions of τ_{had} candidates reconstructed with the τ_{had}^μ method are different from the standard τ_{had} candidates. The background rejection power decreases slightly in the 3-prong case compared to the standard TauID algorithm. Without the presence of the muon within the τ_{seed} in the case of background events, the TauID algorithm finds it more challenging to reject semileptonic heavy-flavour jets. The 1-prong background rejection power increases slightly in the low- p_T region after removal of the muon due to fewer τ_{had} candidates being reconstructed after the muon removal.

The signal efficiency observed in the $G \rightarrow HH \rightarrow 4\tau$ samples and the background rejection power observed in the $t\bar{t}$ sample are combined to form the so-called receiver operating characteristic (ROC) curves. In addition to the same reconstruction level selections as the background τ_{seed} jets discussed previously, the τ_{seed} jets in the signal samples are required to be generator-matched to the $\tau_\mu \tau_{\text{had}}$ pairs. To minimise the bias introduced by the misalignment of the signal and background momentum spectra, the background events are reweighted so that the p_T distribution of the background sample matches that of the signal samples. The ROC curves illustrating the performance with and without muon removal are shown in Fig. 9. An order-of-magnitude performance gain is seen across the spectrum for both the 1-prong and 3-prong cases when the muon removal is applied.

To demonstrate the performance of the τ_{had}^μ method in reconstructing and identifying individual di- τ systems within the $G \rightarrow HH \rightarrow 4\tau$ process, Fig. 10 presents the combined τ_{had} reconstruction and identification efficiencies as a function of the generated graviton mass. The efficiencies correspond to the identification of individual di- τ systems originating from Higgs boson decays.

Compared to the standard ATLAS TauID algorithm, the τ_{had}^μ method demonstrates a complete recovery of the identification efficiency for both the 1-prong and 3-prong τ_{had} decays for high-mass $G \rightarrow HH \rightarrow 4\tau$ events, to the level expected for isolated τ_{had} candidates reconstructed with the standard TauID algorithm.

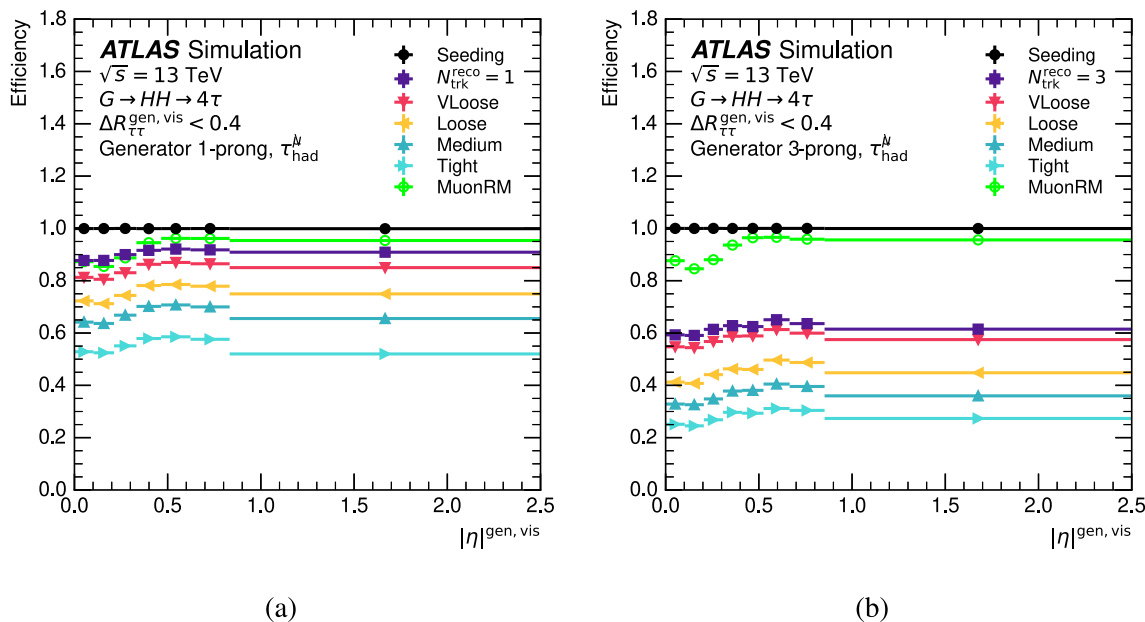


Fig. 4 The combined reconstruction and TauID efficiencies after the muon removal for generator-level **a** 1-prong and **b** 3-prong $\tau_\mu \tau_{\text{had}}$ pairs at all working points as a function of $|\eta|^{gen, \text{vis}}$ for τ_{seed} jets with $\Delta R_{\tau\tau}^{\text{gen, vis}} < 0.4$. The ‘Seeding’ line shows the efficiency of a τ_{seed} jet that matches a generator-level $\tau_\mu \tau_{\text{had}}$ pair being reconstructed; the

$N_{\text{trk}}^{\text{reco}} = 1$ or 3’ line shows the efficiency of a generator-level τ_{had} being reconstructed with the correct number of associated charged-particle tracks. The ‘VLoose’, ‘Loose’, ‘Medium’, and ‘Tight’ lines show the efficiencies of the TauID working points. The ‘MuonRM’ line shows the efficiency of a muon being identified and removed from the τ_{seed} jet

5 Validation of the τ_{had}^μ method in the $Z \rightarrow \tau_\mu \tau_{\text{had}}$ final states

The τ_{had}^μ method was developed for searches for high-mass BSM physics, such as the $G \rightarrow HH$ process, as described in Sect. 4. However, it is useful to validate its performance by considering a SM process and data from proton-proton collisions. In this paper, the Drell-Yan production of a Z boson in association with high- p_T jets from initial-state QCD radiation is considered as a validation process.

5.1 Z -boson kinematic reconstruction

The detector signature of the boosted $Z \rightarrow \tau_\mu \tau_{\text{had}}$ process includes one hadronically decaying τ -lepton and a muon, in association with significant missing transverse momentum (\vec{p}_T^{miss}) from the neutrinos produced in the two τ -lepton decays. The \vec{p}_T^{miss} , with magnitude E_T^{miss} , is estimated as the negative vector sum of the transverse momentum of all identified hard physics objects [45]. Tracks not associated with any such object are included in the soft term.

In this kinematic regime, the τ_{had} and the muon are likely to be reconstructed within the same τ_{seed} jet. In well measured events, the vector sum of the transverse momenta of the three neutrinos dominates the measured \vec{p}_T^{miss} , which in the azimuthal direction lies between the observed muon and

the τ_{had} candidate in most cases. Also, on average, the \vec{p}_T^{miss} should be closer in azimuth to the muon, because the τ_{lep} decay produces two neutrinos and the τ_{had} decay only one.

Without incorporating \vec{p}_T^{miss} , reconstructing the Z -boson invariant mass is not possible. However, it is possible to approximate the momenta of the neutrinos using the collinear approximation [46] as follows:

- the transverse momenta of the three neutrinos dominate the measured \vec{p}_T^{miss} , and other contributions are negligible;
- each τ -lepton is sufficiently boosted such that the neutrino (or pair of neutrinos) produced in its decay is collinear with its visible decay products.

These assumptions allow the reconstruction of the momenta of the neutrino (or pair of neutrinos) produced in the decay of each τ -lepton.³

Together with the momenta of the visible decay products, this procedure allows the momenta of the two τ -leptons,

³ In events in which the \vec{p}_T^{miss} lies outside the azimuthal angle between the visible decay products of the τ -leptons, the \vec{p}_T^{miss} is projected onto the direction of the nearest visible decay, and the neutrino momentum associated with the other τ -lepton is set to zero. Furthermore, events for which collinear reconstruction is not possible, i.e., with \vec{p}_T^{miss} deviating by more than 90° from the muon or the τ_{had}^μ in $\Delta\phi$, are discarded.

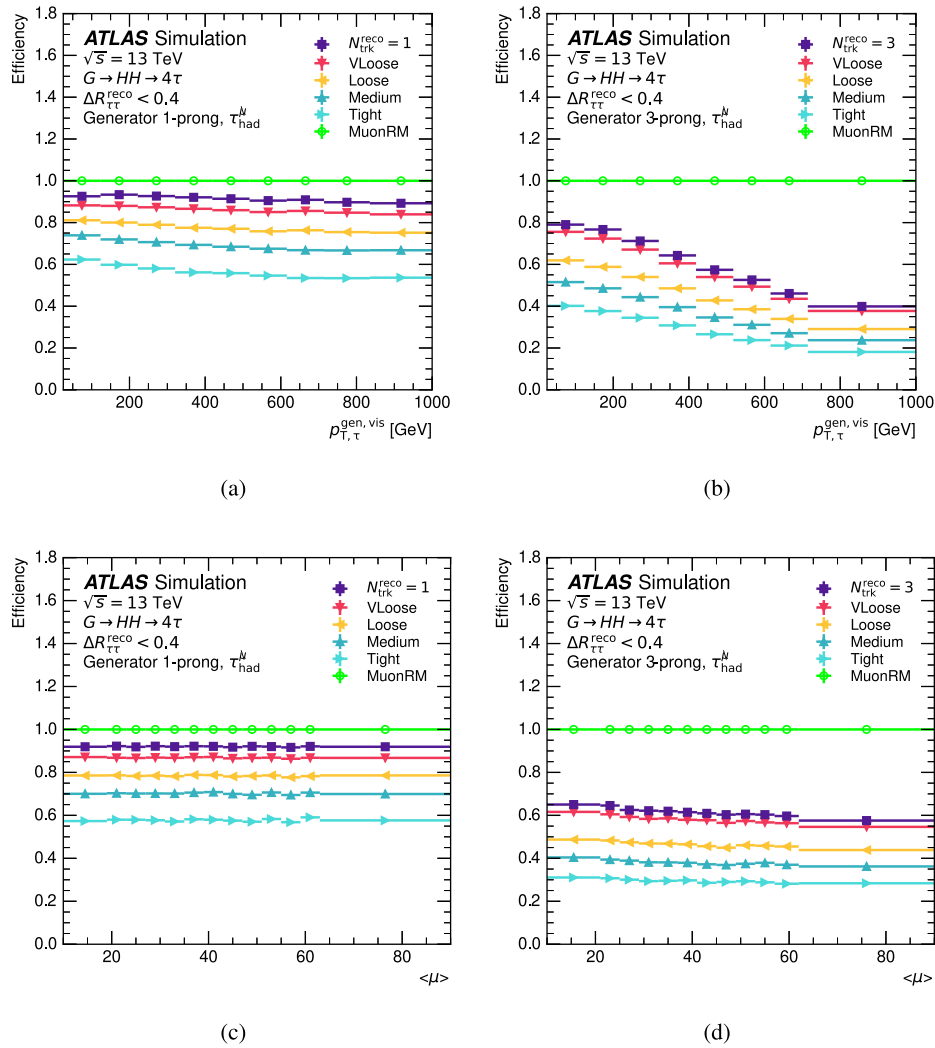


Fig. 5 The signal efficiencies of the TauID working points as a function of **a**, **b** the generator-level transverse momentum $p_{T,\tau}^{\text{gen,vis}}$ and **c**, **d** the average number of interactions per bunch crossing $\langle \mu \rangle$ for generator-level 1-prong and 3-prong τ_{seed} jets when the muon is identified inside the τ_{seed} jet and removed ($\Delta R_{\tau\tau}^{\text{reco}} < 0.4$). The ‘ $N_{\text{trk}}^{\text{reco}} = 1$ or 3’ line shows the efficiency of a generator-level τ_{had} being reconstructed with

the correct number of associated charged-particle tracks. The ‘VLoose’, ‘Loose’, ‘Medium’, and ‘Tight’ lines show the efficiencies of the TauID working points. The ‘MuonRM’ line shows the efficiency of a muon being identified and removed from the τ_{seed} , and is by definition 1.0 for all subfigures

and hence the transverse momentum ($p_{T,\mu-\text{had}}^{\text{col}}$), and mass ($m_{\mu-\text{had}}^{\text{col}}$) of the system produced by the decay of the Z boson, to be reconstructed. The jets recoiling against the Z boson are reconstructed using the anti- k_t algorithm with a radius parameter $R = 0.4$ that uses particle flow objects [47] as input. These jets are then calibrated using simulation and data a to a precision of order 1% for central jets.

5.2 Event selection

Candidate events are required to have been triggered by an un-prescaled single-muon trigger [48] or an un-prescaled

E_T^{miss} trigger [49]. The thresholds of the p_T required to fire each trigger varied for different data-taking periods. For the single muon trigger, the p_T requirement for triggers selecting isolated muons ranged from 20 to 26 GeV, while the p_T threshold for muon trigger without isolation requirements remained constant at 50 GeV. The E_T^{miss} triggers had a threshold of 70 GeV for the 2015 data-taking period and remained constant at 110 GeV for the rest of Run 2. Approximately 97% of $Z \rightarrow \tau_\mu \tau_{\text{had}}$ simulated events that satisfy the final signal selection criteria satisfy the trigger selection.

For the signal region (SR) selection, events satisfying the trigger requirements are required to have at least one muon removal τ_{had} object which satisfies $p_T > 15$ GeV, one or

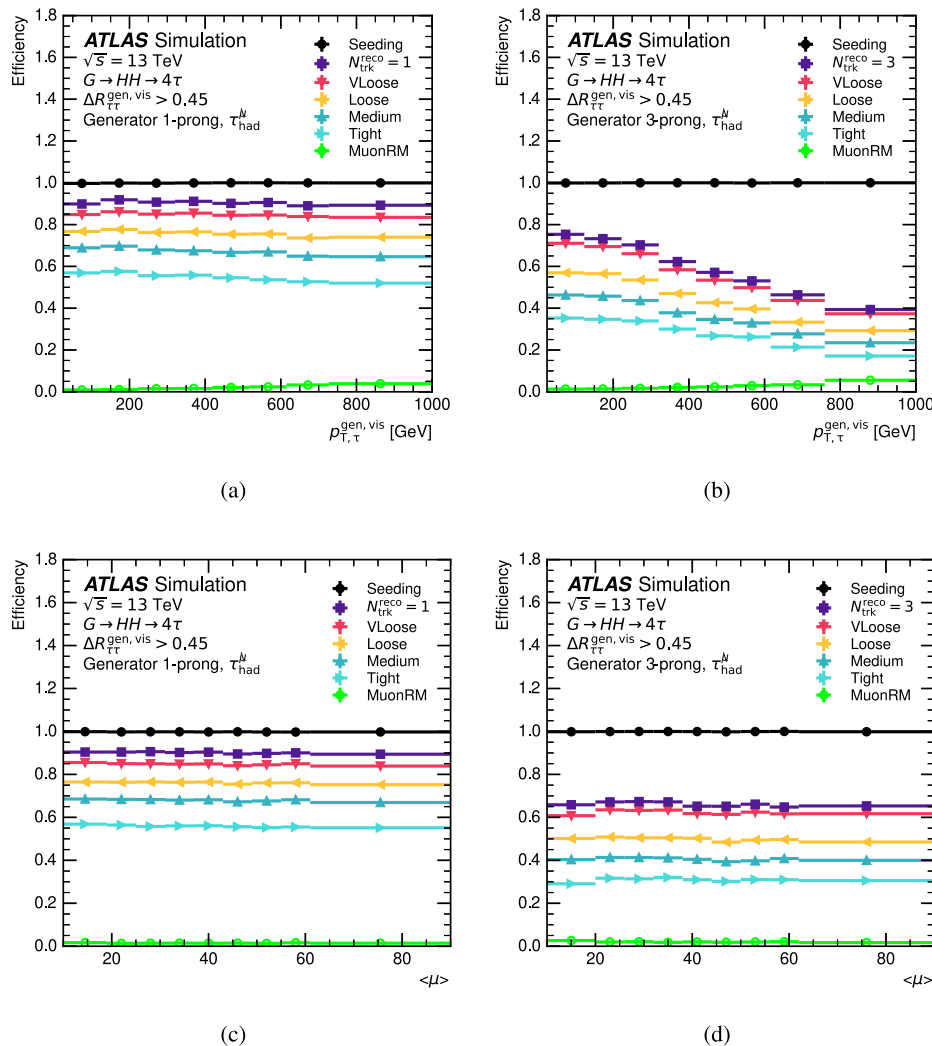


Fig. 6 The signal efficiencies of the TauID working points as a function of **a, b** the generator-level $p_{T,\tau}^{\text{gen},\text{vis}}$ and **c, d** the average number of interactions per bunch crossing ($\langle \mu \rangle$) for the generator-level 1-prong and 3-prong τ_{seed} jets with $\Delta R_{\tau\tau}^{\text{gen},\text{vis}} > 0.45$. In this region, the muon removal should not affect the results. The ‘Seeding’ line shows the efficiency of a τ_{seed} jet that matches to a generator-level $\tau_\mu \tau_{\text{had}}$ pair being reconstructed; the ‘ $N_{\text{trk}}^{\text{reco}} = 1$ or 3’ line shows the efficiency of

a generator-level τ_{had} being reconstructed with the correct number of associated charged-particle tracks. The ‘VLoose’, ‘Loose’, ‘Medium’, and ‘Tight’ lines show the efficiencies of the TauID working points. The ‘MuonRM’ line shows the efficiency of a muon being identified and removed from the τ_{seed} jet, and is expected to be low in high $\Delta R_{\tau\tau}^{\text{gen},\text{vis}}$ region

three reconstructed charged-particle tracks with charge summing to one, and a TauID jet RNN score > 0.1 , excluding $1.37 < |\eta| < 1.52$ and $|\eta| > 2.5$. This selection implies that at least one reconstructed muon satisfying the ‘Medium’ working point is inside the cone of each selected τ_{had}^μ candidate. Additionally, the muon must have $p_T > 10 \text{ GeV}$ and opposite charge to the τ_{had}^μ candidate. In this study, the overlap removal between muons and τ_{had} candidates is turned off as the default overlap removal algorithm as described in Ref. [42] would remove some of the τ_{had}^μ candidates even if the muon removal method is successful. To suppress background from events containing heavy-flavour jets, events are

rejected if they contain any jet that satisfies the DL1d based b -tagging algorithm at an 85% efficiency working point [50]. The signed $\Delta\phi$ between the muon and $\vec{p}_{\text{T}}^{\text{miss}}$ ($\Delta\phi_{\mu-\text{MET}}^{\text{signed}}$) is required to be $-0.1 < \Delta\phi_{\mu-\text{MET}}^{\text{signed}} < 0.4$. The sign of $\Delta\phi_{\mu-\text{MET}}^{\text{signed}}$ is determined by the direction of the τ_{had}^μ candidate. If the $\vec{p}_{\text{T}}^{\text{miss}}$ is inside the opening angle of the muon and the τ_{had} candidate or if the $\vec{p}_{\text{T}}^{\text{miss}}$ is outside the opening angle but closer to the muon, then the sign is positive; otherwise, it is negative. Since the focus of the analysis is the boosted $Z \rightarrow \tau_\mu \tau_{\text{had}}$ process, a loose requirement $m_{\mu-\text{had}}^{\text{col}} > 40 \text{ GeV}$, and a requirement $p_{T,\mu-\text{had}}^{\text{col}} > 250 \text{ GeV}$

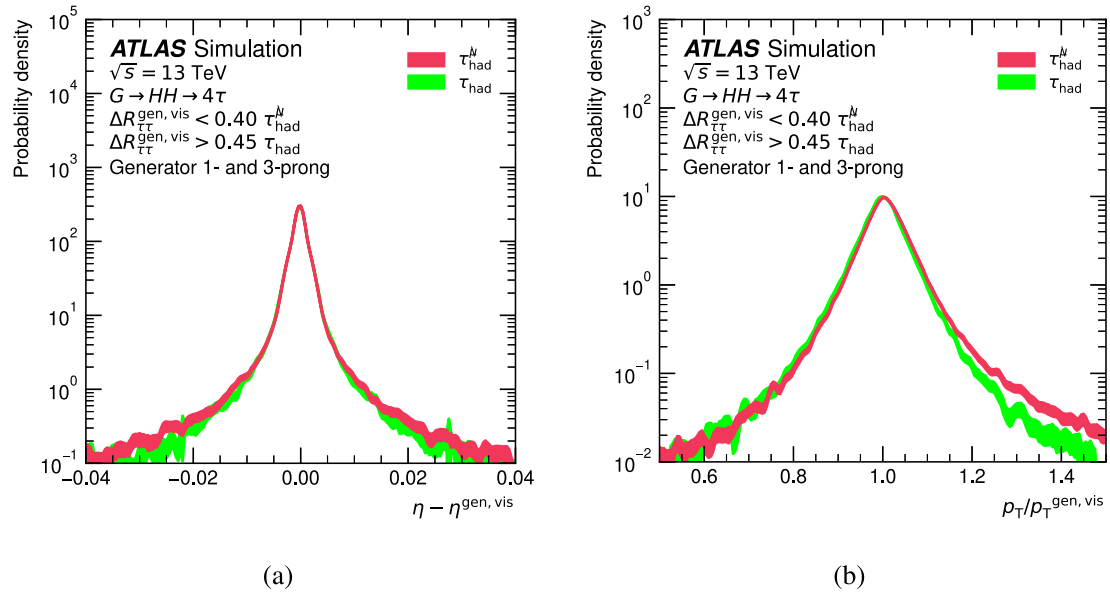


Fig. 7 The distributions of the residuals for **a** η and **b** p_T after calibrations with standard τ_{had} candidates and $\Delta R_{\tau\tau}^{\text{gen, vis}} > 0.45$ and with τ_{had}^μ candidates and $\Delta R_{\tau\tau}^{\text{gen, vis}} < 0.4$. The bands represent the statistical uncertainties

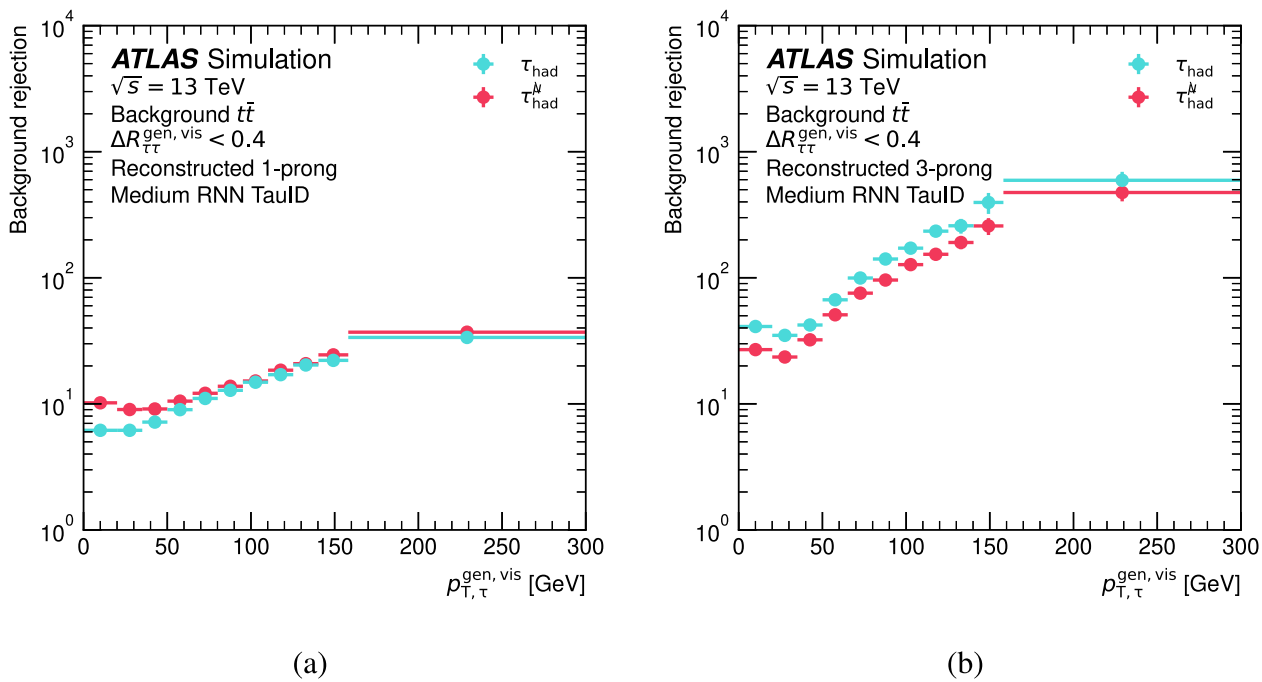


Fig. 8 The background rejection for τ_{seed} jets originating from semileptonic b -hadron decays in $t\bar{t}$ events at the ‘Medium’ TauID working point, as a function of the reconstructed p_T for **a** the reconstructed 1-prong candidates and **b** the reconstructed 3-prong candidates

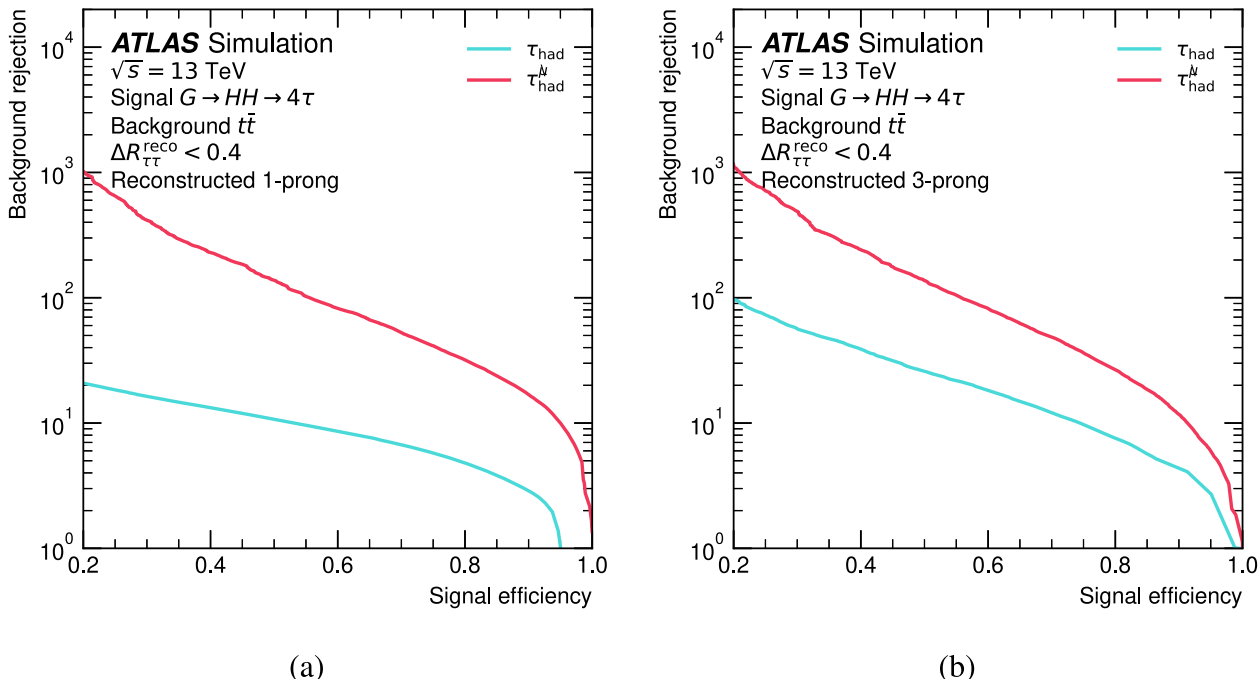


Fig. 9 Background rejection as a function of signal efficiency with and without muon removal for **a** the reconstructed 1-prong candidates and **b** the reconstructed 3-prong candidates. For the background sample, $t\bar{t}$

events are used. The combination of all $G \rightarrow HH \rightarrow 4\tau$ samples with m_G ranging from 1 to 5 TeV is used as the signal sample

are applied. A validation region (VR) is defined with the same selection requirements as the SR, except that the muon and τ_{had}^{μ} candidate are required to have the same charge, and there is no requirement on $\Delta\phi_{\mu-\text{MET}}^{\text{signed}}$ or the number of jets satisfying the b -tagging criteria. The VR is designed with enough statistical power for testing the background modelling. These tests confirm that multi-jets events contribute negligibly to the background in both the SR and VR, making it an unlikely source of significant background mismodelling. Table 1 summarises the event selection requirements for the SR and VR respectively.

Figures 11 and 12 illustrate the distributions of the TauID jet RNN score and $p_{\text{T}}^{\text{col}}_{\mu-\text{had}}$ in the SR and VR. As shown in both figures, the data and MC predictions agree well in both the SR and VR. Due to the $m_{\mu-\text{had}}^{\text{col}} > 40$ GeV requirement, the kinematics of the selection produce a peak in the $p_{\text{T}}^{\text{col}}_{\mu-\text{had}}$ distribution around 500 GeV. This highlights the fact that the τ_{had}^{μ} reconstruction picks up $\tau_{\mu}\tau_{\text{had}}$ pairs only with a sufficiently high boost.

5.3 Systematic uncertainties

The dominant source of systematic uncertainty in the comparison between the observed and expected yields in the SR is the modelling of the cross-section for Z -boson produc-

tion. As discussed in Sect. 3, a +10% correction is applied to the predicted values for $Z(\rightarrow \tau\tau) + \text{jets}$ events, with the full size of this correction quoted as a systematic uncertainty. The most significant sources of experimental systematic uncertainties are related to TauID and τ -lepton energy scale (4%) [3, 4], jet energy scale and resolution (2%) [51], $E_{\text{T}}^{\text{miss}}$ (2%) [45], and luminosity (0.83%) [35].

5.4 Results

To understand the performance improvement relative to the standard ATLAS τ_{had} reconstruction and identification, Fig. 13 shows multiple comparisons of the data and MC predictions for $m_{\mu-\text{had}}^{\text{col}}$ distributions corresponding to various signal selections; Fig. 13a corresponds to the SR selections defined in Sect. 5.2; Fig. 13b corresponds to the SR^{std} , which uses the standard ATLAS τ_{had} candidates, without the muon removal, but otherwise corresponds to the same event selection as the SR; Fig. 13c corresponds to the SR_{tight} , which imposes an additional ‘Tight’ RNN TauID requirement on the τ_{had}^{μ} candidates, but otherwise corresponds to the SR selection; and Fig. 13d corresponds to the $\text{SR}_{\text{tight}}^{\text{std}}$, which imposes an additional ‘Tight’ RNN TauID requirement and uses the standard τ_{had} candidates, without muon removal.

The collinear mass reconstruction of the di- τ system is quite effective as it clearly shows the peak corresponding to

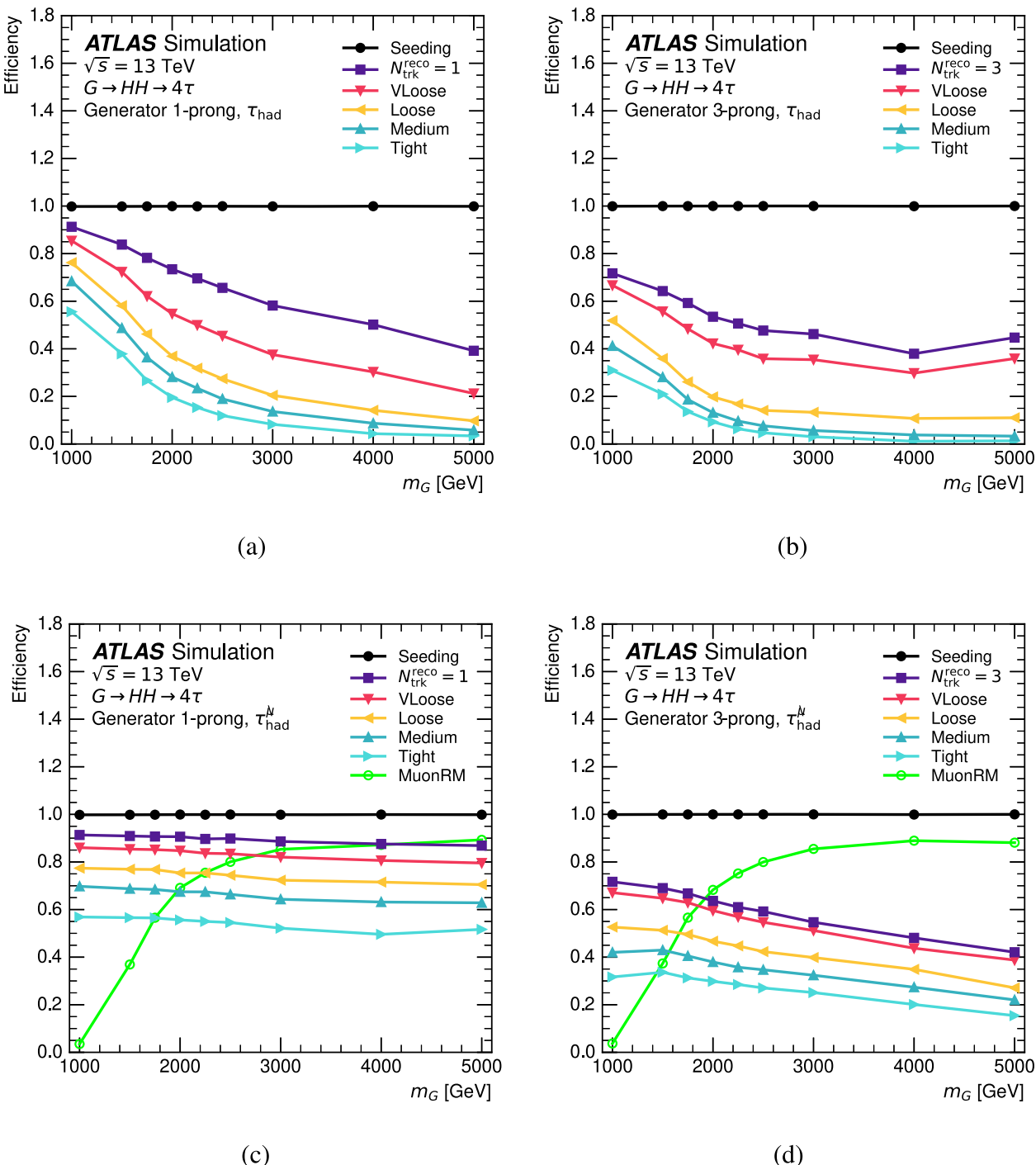


Fig. 10 The signal efficiencies of the TauID working points, as a function of m_G , for generator-level **a** 1-prong and **b** 3-prong τ_{had} with the standard ATLAS TauID algorithm and for generator-level **c** 1-prong and **d** 3-prong τ_{had} with the τ_{had}^μ method. The efficiencies shown correspond to the identification of individual di- τ systems originating from Higgs boson decays. The ‘Seeding’ line shows the efficiency of a τ_{seed}

jet that matches a generator-level $\tau_\mu \tau_{\text{had}}$ pair being reconstructed. The ‘ $N_{\text{trk}}^{\text{reco}} = 1$ or 3’ line shows the efficiency of a generator-level τ_{had} being reconstructed with the correct number of associated charged-particle tracks. The ‘VLoose’, ‘Loose’, ‘Medium’, and ‘Tight’ lines show the efficiencies of the TauID working points. The ‘MuonRM’ line shows the efficiency of a muon being identified and removed from the τ_{seed}

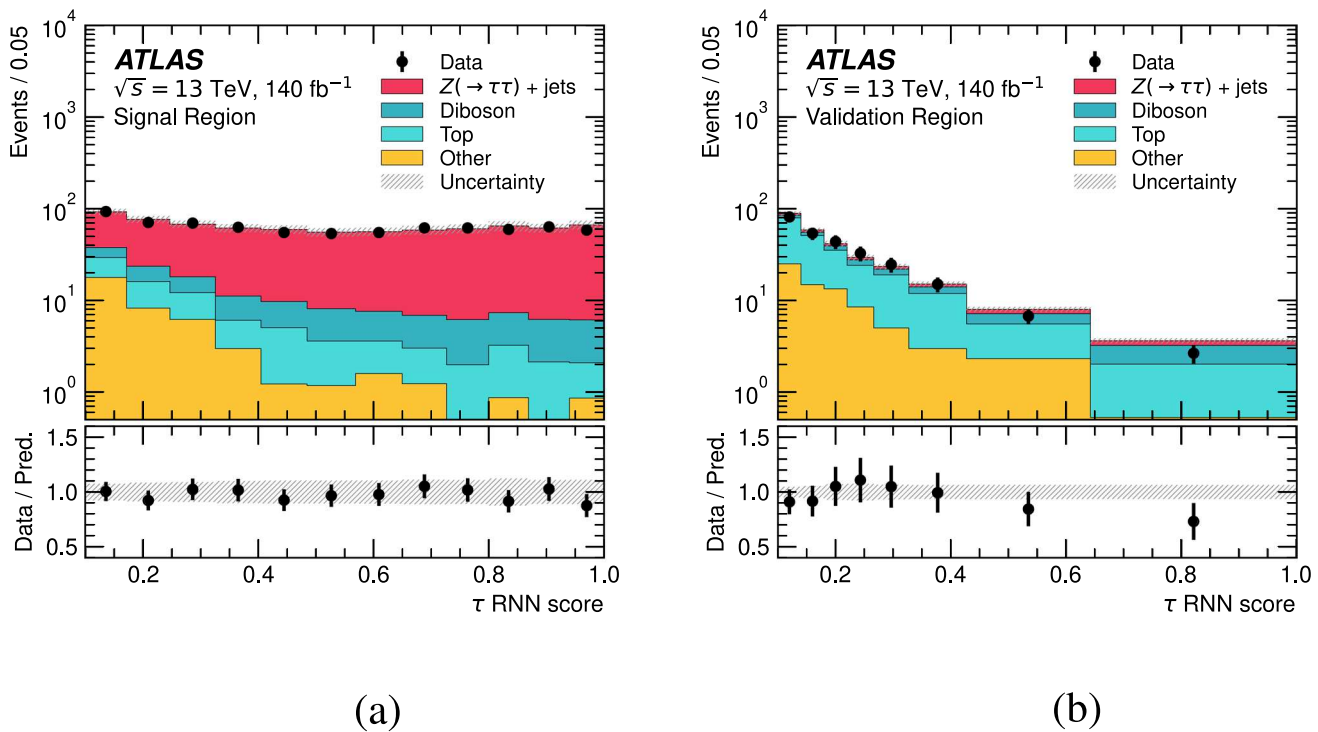


Fig. 11 The distribution of the TauID jet RNN score for τ_{had}^{μ} **a** in the SR and **b** in the VR. ‘ $Z(\rightarrow \tau\tau) + \text{jets}$ ’ represents the contributions from the signal process. ‘Top’ represents the predicted contributions from the $t\bar{t}$, single-top-quark, and tW processes. ‘Diboson’ indicates

the contributions from WW , WZ , and ZZ processes. ‘Other’ includes the contributions from the $Z(\rightarrow \ell\ell) + \text{jets}$, $W + \text{jets}$, and Higgs boson processes. The uncertainties shown include both statistical and systematic sources

the Z boson mass in Fig. 13a. The shape of the $m_{\mu-\text{had}}^{\text{col}}$ distribution for signal Drell–Yan events is very different from that seen in inclusive production [52], with a much larger fraction of the signal events in the region $40 \text{ GeV} < m_{\mu-\text{had}}^{\text{col}} < 70 \text{ GeV}$ compared to that at the Z boson peak. This pattern arises due to the steep fall in the $m_{\mu-\text{had}}^{\text{col}}$ distribution for Drell–Yan production, along with the narrowing opening angle of boosted $\tau_{\mu}\tau_{\text{had}}$ systems as $m_{\mu-\text{had}}^{\text{col}}$ decreases.

Table 2 shows the event yields in the data, as well as the predicted contributions from signal and background processes, corresponding to the various signal and validation selection criteria defined previously. Compared with the standard TauID, the τ_{had}^{μ} method results in around three times more signal events in the SR, accompanied by an increase in the number of background events. In the SR_{tight} the number of signal events is about five times higher than when using

Table 1 Summary of event selection requirements

	Object	Signal region	Validation region
τ_{had}^{μ} candidate	$p_{\text{T}} > 15 \text{ GeV}$ TauID jet RNN score > 0.1 $ \eta < 1.37$ or $1.52 < \eta < 2.5$ 1 or 3 charged-particle tracks	$p_{\text{T}} > 15 \text{ GeV}$ TauID jet RNN score > 0.1 $ \eta < 1.37$ or $1.52 < \eta < 2.5$ 1 or 3 charged-particle tracks	
Muon	‘Medium’ working point $p_{\text{T}} > 10 \text{ GeV}$	‘Medium’ working point $p_{\text{T}} > 10 \text{ GeV}$	
$\tau_{\mu}\tau_{\text{had}}$ pair	no b -tagged jet at 85% efficiency working point $-0.1 < \Delta\phi_{\mu-\text{MET}}^{\text{signed}} < 0.4$ $m_{\mu-\text{had}}^{\text{col}} > 40 \text{ GeV}$ $p_{\text{T}}_{\mu-\text{had}}^{\text{col}} > 250 \text{ GeV}$	–	
	opposite charge muon and τ_{had}^{μ} candidates	same charge muon and τ_{had}^{μ} candidates	

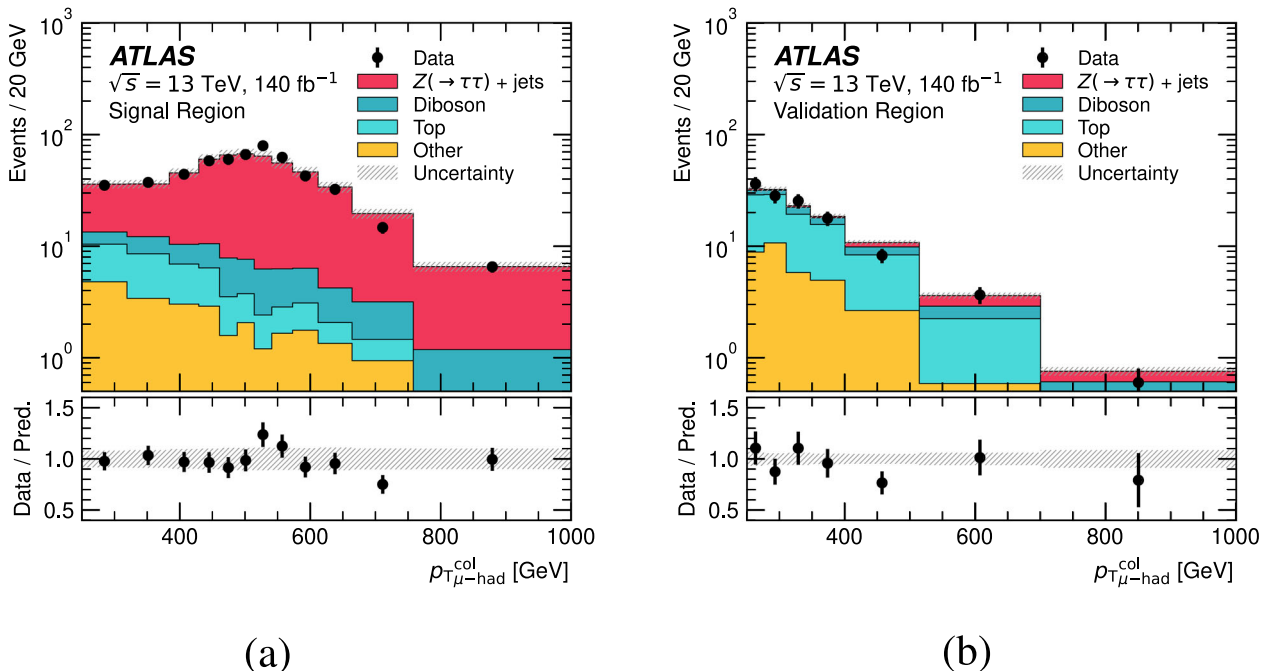


Fig. 12 The distribution of the $p_{\mu-\text{had}}^{\text{col}}$ **a** in the SR, and **b** in the VR. ‘ $Z(\rightarrow \tau\tau) + \text{jets}$ ’ represents the contributions from the signal process. ‘Diboson’ indicates the contributions from WW , WZ , and ZZ processes. ‘Top’ represents the predicted contributions from the $t\bar{t}$, single-

top-quark, and tW processes. ‘Other’ includes the contributions from the $Z(\rightarrow \ell\ell) + \text{jets}$, $W + \text{jets}$, and Higgs boson processes. The uncertainties shown include both statistical and systematic sources

the standard τ_{had} candidates, with a corresponding rise in background events as well.

Subtracting the expected background yield in the SR of 223 ± 5 events gives a measured yield for $Z \rightarrow \tau_\mu \tau_{\text{had}}$ of 920 ± 34 events. This can be compared with the expected yield for $Z \rightarrow \tau_\mu \tau_{\text{had}}$ of 945 ± 8 (stat.) ± 114 (syst.) events. Adding all sources of statistical and systematic uncertainty results in a total uncertainty of 12%. The same calculations are performed in the SR_{tight}. The ratio of data to prediction is 0.97 ± 0.12 in the SR, and 0.96 ± 0.12 in the SR_{tight}.

6 Conclusions

In this paper, the reconstruction of a highly boosted pair of τ -leptons is considered, in which one τ -lepton decays into a muon plus two neutrinos and the other τ -lepton decays hadronically, with the visible decay products overlapping. In such cases, the standard ATLAS reconstruction and identification algorithms for hadronically decaying τ -leptons fail due to the presence of the nearby muon.

The development of a muon removal procedure for τ_{had} candidates (denoted τ_{had}^{μ}) using samples of high-mass $G \rightarrow HH \rightarrow 4\tau$ events is described. The τ_{had}^{μ} method recovers the τ_{had} reconstruction and identification efficiencies to the

expected level for isolated τ_{had} decays at all τ -lepton identification working points. The measurement precision for the charge and kinematic properties of the visible τ_{had} system is similarly recovered. The background rejection power is studied using heavy-flavour jets from top-quark decays and shows no degradation relative to the standard algorithm for τ_{had} identification. The τ_{had}^{χ} method is validated by selecting a sample of highly boosted $Z \rightarrow \tau_\mu \tau_{\text{had}}$ final states using a data set of proton–proton collisions at $\sqrt{s} = 13$ TeV collected with the ATLAS detector at the LHC, and corresponding to an integrated luminosity of 140 fb^{-1} . Good agreement is found between data and simulation in both the $Z \rightarrow \tau_\mu \tau_{\text{had}}$ signal region and a background-rich validation region. The ratio of the observed and predicted event yields in the signal region is found to be consistent with unity within an uncertainty of 12%.

The results presented in this paper demonstrate the effectiveness of the τ_{had}^{μ} method in enhancing the signal sensitivity of the boosted $\tau_\mu \tau_{\text{had}}$ channel. The observed good agreement between data and simulation in the $Z \rightarrow \tau_\mu \tau_{\text{had}}$ signal region reaffirms the robustness of the newly developed reconstruction method.

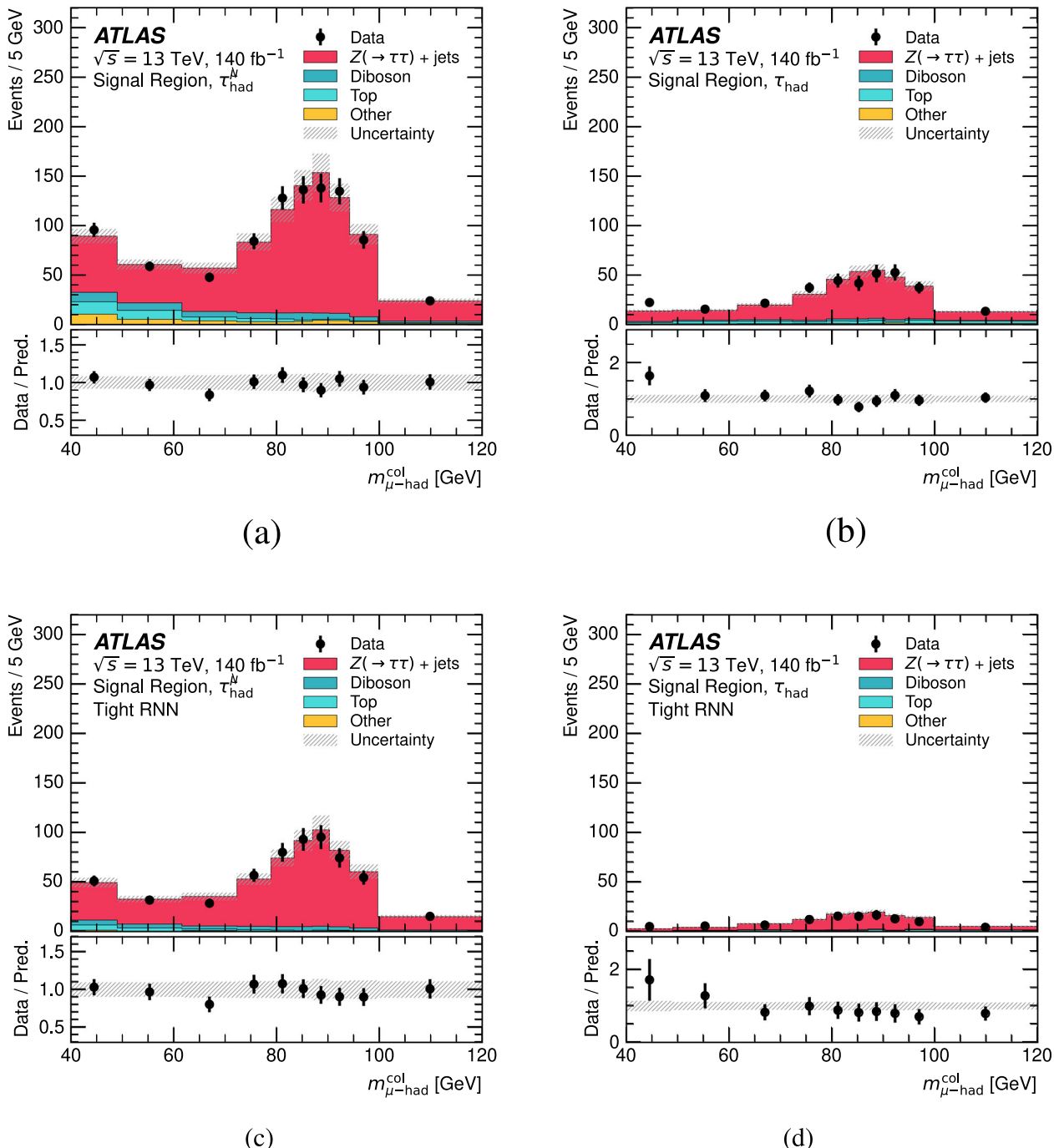


Fig. 13 The distributions of $m_{\mu\text{-had}}^{\text{col}}$ corresponding to the various signal region selection criteria defined in the text: **a** SR, **b** SR^{std}, **c** SR_{tight}, and **d** SR_{tight}^{std}. ‘ $Z(\rightarrow \tau\tau) + \text{jets}$ ’ represents the contributions from the signal process. ‘Diboson’ indicates the contributions from WW , WZ ,

and ZZ processes. ‘Top’ represents the predicted contributions from the $t\bar{t}$, single-top-quark, and tW processes. ‘Other’ includes the contributions from the $Z(\rightarrow \ell\ell) + \text{jets}$, $W + \text{jets}$, and Higgs boson processes. The uncertainties shown include both statistical and systematic sources

Table 2 Event yields for different event selection criteria, as defined in the text. The uncertainties quoted are statistical only

	SR	SR ^{std}	SR _{tight}	SR _{tight} ^{std}	VR
$Z \rightarrow \tau\tau$	945 ± 8	325 ± 4	633 ± 7	117 ± 2	20 ± 1
Diboson	91 ± 1	25 ± 1	50 ± 1	9 ± 0	38 ± 1
Top	68 ± 3	53 ± 3	26 ± 2	21 ± 2	164 ± 5
Other	65 ± 4	17 ± 2	12 ± 2	5 ± 1	76 ± 4
Total predicted	1168 ± 10	420 ± 5	721 ± 8	153 ± 3	297 ± 7
Data	1143	435	698	133	281

Acknowledgements We thank CERN for the very successful operation of the LHC and its injectors, as well as the support staff at CERN and at our institutions worldwide without whom ATLAS could not be operated efficiently. The crucial computing support from all WLCG partners is acknowledged gratefully, in particular from CERN, the ATLAS Tier-1 facilities at TRIUMF/SFU (Canada), NDGF (Denmark, Norway, Sweden), CC-IN2P3 (France), KIT/GridKA (Germany), INFN-CNAF (Italy), NL-T1 (Netherlands), PIC (Spain), RAL (UK) and BNL (USA), the Tier-2 facilities worldwide and large non-WLCG resource providers. Major contributors of computing resources are listed in Ref. [ATL-SOFT-PUB-2025-001]. We gratefully acknowledge the support of ANPCyT, Argentina; YerPhI, Armenia; ARC, Australia; BMWFW and FWF, Austria; ANAS, Azerbaijan; CNPq and FAPESP, Brazil; NSERC, NRC and CFI, Canada; CERN; ANID, Chile; CAS, MOST and NSFC, China; Minciencias, Colombia; MEYS CR, Czech Republic; DNRF and DNSRC, Denmark; IN2P3-CNRS and CEA-DRF/IRFU, France; SRNSFG, Georgia; BMBF, HGF and MPG, Germany; GSRI, Greece; RGC and Hong Kong SAR, China; ICHEP and Academy of Sciences and Humanities, Israel; INFN, Italy; MEXT and JSPS, Japan; CNRST, Morocco; NWO, Netherlands; RCN, Norway; MNiSW, Poland; FCT, Portugal; MNE/IFA, Romania; MSTDNI, Serbia; MSSR, Slovakia; ARIS and MVZI, Slovenia; DS/ NRF, South Africa; MICIU/AEI, Spain; SRC and Wallenberg Foundation, Sweden; SERI, SNSF and Cantons of Bern and Geneva, Switzerland; NSTC, Taipei; TENMAK, Türkiye; STFC/UKRI, United Kingdom; DOE and NSF, United States of America. Individual groups and members have received support from BCKDF, CANARIE, CRC and DRAC, Canada; CERN-CZ, FORTE and PRIMUS, Czech Republic; COST, ERC, ERDF, Horizon 2020, ICSC-NextGenerationEU and Marie Skłodowska-Curie Actions, European Union; Investissements d’Avenir Labex, Investissements d’Avenir Idex and ANR, France; DFG and AvH Foundation, Germany; Herakleitos, Thales and Aristeia programmes co-financed by EU-ESF and the Greek NSRF, Greece; BSF-NSF and MINERVA, Israel; NCN and NAWA, Poland; La Caixa Banking Foundation, CERCA Programme Generalitat de Catalunya and PROMETEO and GenT Programmes Generalitat Valenciana, Spain; Göran Gustafssons Stiftelse, Sweden; The Royal Society and Leverhulme Trust, United Kingdom. In addition, individual members wish to acknowledge support from Armenia: Yerevan Physics Institute (FAPERJ); CERN: European Organization for Nuclear Research (CERN DOCT); Chile: Agencia Nacional de Investigación y Desarrollo (FONDECYT 1230812, FONDECYT 1230987, FONDECYT 1240864); China: Chinese Ministry of Science and Technology (MOST-2023YFA1605700, MOST-2023YFA1609300), National Natural Science Foundation of China (NSFC-12175119, NSFC 12275265, NSFC-12075060); Czech Republic: Czech Science Foundation (GACR - 24-11373S), Ministry of Education Youth and Sports (FORTE CZ.02.01.01/00/22_008/0004632), PRIMUS Research Programme (PRIMUS/21/SCI/017); EU: H2020 European Research Council (ERC - 101002463); European Union: European Research Council (ERC - 948254, ERC 101089007, ERC, BARD, 101116429), European Union, Future Artificial Intelligence

Research (FAIR-NextGenerationEU PE00000013), Italian Center for High Performance Computing, Big Data and Quantum Computing (ICSC, NextGenerationEU); France: Agence Nationale de la Recherche (ANR-20-CE31-0013, ANR-21-CE31-0013, ANR-21-CE31-0022, ANR-22-EDIR-0002); Germany: Baden-Württemberg Stiftung (BW Stiftung-Postdoc Eliteprogramme), Deutsche Forschungsgemeinschaft (DFG - 469666862, DFG - CR 312/5-2); Italy: Istituto Nazionale di Fisica Nucleare (ICSC, NextGenerationEU), Ministero dell’Università e della Ricerca (PRIN - 20223N7F8K - PNRR M4.C2.1.1); Japan: Japan Society for the Promotion of Science (JSPS KAKENHI JP22H01227, JSPS KAKENHI JP22H04944, JSPS KAKENHI JP22KK0227, JSPS KAKENHI JP23KK0245); Netherlands: Netherlands Organisation for Scientific Research (NWO Veni 2020 - VI.Veni.202.179); Norway: Research Council of Norway (RCN-314472); Poland: Ministry of Science and Higher Education (IDUB AGH, POB8, D4 no 9722), Polish National Agency for Academic Exchange (PPN/PPO/2020/1/00002/U/00001), Polish National Science Centre (NCN 2021/42/E/ST2/00350, NCN OPUS 2023/51/B/ST2/02507, NCN OPUS nr 2022/47/B/ST2/03059, NCN UMO-2019/34/E/ST2/00393, NCN & H2020 MSCA 945339, UMO-2020/37/B/ST2/01043, UMO-2021/40/C/ST2/00187, UMO-2022/47/O/ST2/00148, UMO-2023/49/B/ST2/04085, UMO-2023/51/B/ST2/00920, UMO-2024/53/N/ST2/00869); Slovenia: Slovenian Research Agency (ARIS grant J1-3010); Spain: Generalitat Valenciana (Artemisa, FEDER, IDIFEDER/2018/048), Ministry of Science and Innovation (MCIN & NextGenEU PCI2022-135018-2, MCIN & FEDER PID2021-125273NB, RYC2019-028510-I, RYC2020-030254-I, RYC2021-031273-I, RYC2022-038164-I); Sweden: Carl Trygger Foundation (Carl Trygger Foundation CTS 22:2312), Swedish Research Council (Swedish Research Council 2023-04654, VR 2018-00482, VR 2022-03845, VR 2022-04683, VR 2023-03403, VR grant 2021-03651), Knut and Alice Wallenberg Foundation (KAW 2018.0458, KAW 2019.0447, KAW 2022.0358); Switzerland: Swiss National Science Foundation (SNSF - PCEFP2_194658); United Kingdom: Leverhulme Trust (Leverhulme Trust RPG-2020-004), Royal Society (NIF-R1-231091); United States of America: U.S. Department of Energy (ECA DE-AC02-76SF00515), Neubauer Family Foundation.

Data Availability Statement Data cannot be made available for reasons disclosed in the data availability statement. [Authors’ comment: The public release of data supporting the findings of this article will follow the CERN Open Data Policy [CERN-OPEN-2020-013]. Inquiries about plots and tables associated with this article can be addressed to atlas.publications@cern.ch.]

Code Availability Statement Code/software cannot be made available for reasons disclosed in the code availability statement. [Authors’ comment: ATLAS collaboration software is open source, and all code necessary to recreate an analysis is publicly available. The Athena (<http://gitlab.cern.ch/atlas/athena>) software repository provides all code needed for calibration and uncertainty application, with configuration files that are also publicly available via Docker containers and cvmfs.

The specific code and configurations written in support of this analysis are not public; however, these are internally preserved.]

Open Access This article is licensed under a Creative Commons Attribution 4.0 International License, which permits use, sharing, adaptation, distribution and reproduction in any medium or format, as long as you give appropriate credit to the original author(s) and the source, provide a link to the Creative Commons licence, and indicate if changes were made. The images or other third party material in this article are included in the article's Creative Commons licence, unless indicated otherwise in a credit line to the material. If material is not included in the article's Creative Commons licence and your intended use is not permitted by statutory regulation or exceeds the permitted use, you will need to obtain permission directly from the copyright holder. To view a copy of this licence, visit <http://creativecommons.org/licenses/by/4.0/>.

Funded by SCOAP³.

References

- S. Navas, Particle Data Group et al., Review of particle physics. Phys. Rev. D **110**, 030001 (2024). <https://doi.org/10.1103/PhysRevD.110.030001>
- ATLAS Collaboration, Identification and energy calibration of hadronically decaying tau leptons with the ATLAS experiment in pp collisions at $\sqrt{s} = 8$ TeV. Eur. Phys. J. C **75**, 303 (2015). <https://doi.org/10.1140/epjc/s10052-015-3500-z>. arXiv:1412.7086 [hep-ex]
- ATLAS Collaboration, Measurement of the tau lepton reconstruction and identification performance in the ATLAS experiment using pp collisions at $\sqrt{s} = 13$ TeV. ATLAS-CONF-2017-029 (2017). <https://cds.cern.ch/record/2261772>
- ATLAS Collaboration, Identification of hadronic tau lepton decays using neural networks in the ATLAS experiment. ATL-PHYS-PUB-2019-033 (2019). <https://cds.cern.ch/record/2688062>
- ATLAS Collaboration, Reconstruction, Identification, and calibration of hadronically decaying tau leptons with the ATLAS detector for the LHC Run 3 and reprocessed Run 2 data. ATL-PHYS-PUB-2022-044 (2022). <https://cds.cern.ch/record/2827111>
- M. Cacciari, G.P. Salam, G. Soyez, The anti- k_t jet clustering algorithm. JHEP **04**, 063 (2008). <https://doi.org/10.1088/1126-6708/2008/04/063>. arXiv:0802.1189 [hep-ph]
- M. Cacciari, G.P. Salam, G. Soyez, FastJet user manual. Eur. Phys. J. C **72**, 1896 (2012). <https://doi.org/10.1140/epjc/s10052-012-1896-2>. arXiv:1111.6097 [hep-ph]
- ATLAS Collaboration, Topological cell clustering in the ATLAS calorimeters and its performance in LHC Run 1. Eur. Phys. J. C **77**, 490 (2017). <https://doi.org/10.1140/epjc/s10052-017-5004-5>. arXiv:1603.02934 [hep-ex]
- T. Barillari et al., Local hadronic calibration. ATL-LARG-PUB-2009-001-2 (2008). <https://cds.cern.ch/record/1112035>
- ATLAS Collaboration, Reconstruction and identification of boosted di- τ systems in a search for Higgs boson pairs using 13 TeV proton–proton collision data in ATLAS. ATLAS-CONF-2020-012 (2020). <https://cds.cern.ch/record/2719518>
- ATLAS Collaboration, Muon reconstruction and identification efficiency in ATLAS using the full Run 2 pp collision data set at $\sqrt{s} = 13$ TeV. Eur. Phys. J. C **81**, 578 (2021). <https://doi.org/10.1140/epjc/s10052-021-09233-2>. arXiv:2012.00578 [hep-ex]
- L. Randall, R. Sundrum, Large mass hierarchy from a small extra dimension. Phys. Rev. Lett. **83**, 3370 (1999). <https://doi.org/10.1103/physrevlett.83.3370>. arXiv:9905221 [hep-ph]
- ATLAS Collaboration, The ATLAS experiment at the CERN large hadron collider. JINST **3**, S08003 (2008). <https://doi.org/10.1088/1748-0221/3/08/S08003>
- L. Evans, P. Bryant, L.H.C. Machine, JINST **3**, S08001 (2008). <https://doi.org/10.1088/1748-0221/3/08/S08001>
- G. Avoni et al., The new LUCID-2 detector for luminosity measurement and monitoring in ATLAS. JINST **13**, P07017 (2018). <https://doi.org/10.1088/1748-0221/13/07/P07017>
- ATLAS Collaboration, Performance of the ATLAS trigger system in 2015. Eur. Phys. J. C **77**, 317 (2017). <https://doi.org/10.1140/epjc/s10052-017-4852-3>. arXiv:1611.09661 [hep-ex]
- ATLAS Collaboration, Software and computing for Run 3 of the ATLAS experiment at the LHC. (2024). arXiv:2404.06335 [hep-ex]
- ATLAS Collaboration, The ATLAS simulation infrastructure. Eur. Phys. J. C **70**, 823 (2010). <https://doi.org/10.1140/epjc/s10052-010-1429-9>. arXiv:1005.4568 [physics.ins-det]
- J. Alwall et al., The automated computation of tree-level and next-to-leading order differential cross sections, and their matching to parton shower simulations. JHEP **07**, 079 (2014). [https://doi.org/10.1007/JHEP07\(2014\)079](https://doi.org/10.1007/JHEP07(2014)079). arXiv:1405.0301 [hep-ph]
- NNPDF Collaboration, R.D. Ball et al., Parton distributions with LHC data. Nucl. Phys. B **867**, 244 (2013). <https://doi.org/10.1016/j.nuclphysb.2012.10.003>. arXiv:1207.1303 [hep-ph]
- S. Frixione, G. Ridolfi, P. Nason, A positive-weight next-to-leading-order Monte Carlo for heavy flavour hadroproduction. JHEP **09**, 126 (2007). <https://doi.org/10.1088/1126-6708/2007/09/126>. arXiv:0707.3088 [hep-ph]
- P. Nason, A new method for combining NLO QCD with shower Monte Carlo algorithms. JHEP **11**, 040 (2004). <https://doi.org/10.1088/1126-6708/2004/11/040>. arXiv:hep-ph/0409146
- S. Frixione, P. Nason, C. Oleari, Matching NLO QCD computations with parton shower simulations: the POWHEG method. JHEP **11**, 070 (2007). <https://doi.org/10.1088/1126-6708/2007/11/070>. arXiv:0709.2092 [hep-ph]
- S. Alioli, P. Nason, C. Oleari, E. Re, A general framework for implementing NLO calculations in shower Monte Carlo programs: the POWHEG BOX. JHEP **06**, 043 (2010). [https://doi.org/10.1007/JHEP06\(2010\)043](https://doi.org/10.1007/JHEP06(2010)043). arXiv:1002.2581 [hep-ph]
- NNPDF Collaboration, R.D. Ball et al., Parton distributions for the LHC run II. JHEP **04**, 040 (2015). [https://doi.org/10.1007/JHEP04\(2015\)040](https://doi.org/10.1007/JHEP04(2015)040). arXiv:1410.8849 [hep-ph]
- ATLAS Collaboration, Studies on top-quark Monte Carlo modelling for Top2016. ATL-PHYS-PUB-2016-020 (2016). <https://cds.cern.ch/record/2216168>
- T. Sjöstrand et al., An introduction to PYTHIA 8.2. Comput. Phys. Commun. **191**, 159 (2015). <https://doi.org/10.1016/j.cpc.2015.01.024>. arXiv:1410.3012 [hep-ph]
- ATLAS Collaboration, ATLAS Pythia 8 tunes to 7 TeV data. ATL-PHYS-PUB-2014-021 (2014). <https://cds.cern.ch/record/1966419>
- D.J. Lange, The EvtGen particle decay simulation package. Nucl. Instrum. Methods A **462**, 152 (2001). [https://doi.org/10.1016/S0168-9002\(01\)00089-4](https://doi.org/10.1016/S0168-9002(01)00089-4)
- T. Sjöstrand, S. Mrenna, P. Skands, A brief introduction to PYTHIA 8.1. Comput. Phys. Commun. **178**, 852 (2008). <https://doi.org/10.1016/j.cpc.2008.01.036>. arXiv:0710.3820 [hep-ph]
- ATLAS Collaboration, The Pythia 8 A3 tune description of ATLAS minimum bias and inelastic measurements incorporating the Donnachie–Landshoff diffractive model. ATL-PHYS-PUB-2016-017 (2016). <https://cds.cern.ch/record/2206965>
- A.D. Martin, W.J. Stirling, R.S. Thorne, G. Watt, Parton distributions for the LHC. Eur. Phys. J. C **63**, 189 (2009). <https://doi.org/10.1140/epjc/s10052-009-1072-5>. arXiv:0901.0002 [hep-ph]
- S. Agostinelli et al., GEANT4 – a simulation toolkit. Nucl. Instrum. Methods A **506**, 250 (2003). [https://doi.org/10.1016/S0168-9002\(03\)01368-8](https://doi.org/10.1016/S0168-9002(03)01368-8)

34. ATLAS Collaboration, ATLAS data quality operations and performance for 2015–2018 data-taking. *JINST* **15**, P04003 (2020). <https://doi.org/10.1088/1748-0221/15/04/P04003>. arXiv:1911.04632 [physics.ins-det]
35. ATLAS Collaboration, Luminosity determination in pp collisions at $\sqrt{s} = 13\text{ TeV}$ using the ATLAS detector at the LHC. *Eur. Phys. J. C* **83**, 982 (2023). <https://doi.org/10.1140/epjc/s10052-023-11747-w>. arXiv:2212.09379 [hep-ex]
36. E. Bothmann et al., Event generation with Sherpa 2.2. *SciPost Phys.* **7**, 034 (2019). <https://doi.org/10.21468/SciPostPhys.7.3.034>. arXiv:1905.09127 [hep-ph]
37. S. Höche, F. Krauss, S. Schumann, F. Siegert, QCD matrix elements and truncated showers. *JHEP* **05**, 053 (2009). <https://doi.org/10.1088/1126-6708/2009/05/053>. arXiv:0903.1219 [hep-ph]
38. ATLAS Collaboration, Measurement of the transverse momentum distribution of Drell–Yan lepton pairs in proton–proton collisions at $\sqrt{s} = 13\text{ TeV}$ with the ATLAS detector. *Eur. Phys. J. C* **80**, 616 (2020). <https://doi.org/10.1140/epjc/s10052-020-8001-z>. arXiv:1912.02844 [hep-ex]
39. ATLAS Collaboration, Modelling and computational improvements to the simulation of single vector-boson plus jet processes for the ATLAS experiment. *JHEP* **08**, 089 (2022). [https://doi.org/10.1007/JHEP08\(2022\)089](https://doi.org/10.1007/JHEP08(2022)089). arXiv:2112.09588 [hep-ex]
40. R. Frederix, E. Re, P. Torrielli, Single-top t -channel hadroproduction in the four-flavour scheme with POWHEG and aMC@NLO. *JHEP* **09**, 130 (2012). [https://doi.org/10.1007/JHEP09\(2012\)130](https://doi.org/10.1007/JHEP09(2012)130). arXiv:1207.5391 [hep-ph]
41. S. Frixione, E. Laenen, P. Motylinski, C. White, B.R. Webber, Single-top hadroproduction in association with a W boson. *JHEP* **07**, 029 (2008). <https://doi.org/10.1088/1126-6708/2008/07/029>. arXiv:0805.3067 [hep-ph]
42. ATLAS Collaboration, Measurements of Higgs boson production cross-sections in the $H \rightarrow \tau^+\tau^-$ decay channel in pp collisions at $\sqrt{s} = 13\text{ TeV}$ with the ATLAS detector. *JHEP* **08**, 175 (2022). [https://doi.org/10.1007/JHEP08\(2022\)175](https://doi.org/10.1007/JHEP08(2022)175). arXiv:2201.08269 [hep-ex]
43. ATLAS Collaboration, Studies of the muon momentum calibration and performance of the ATLAS detector with pp collisions at $\sqrt{s} = 13\text{ TeV}$. *Eur. Phys. J. C* **83**, 686 (2023). <https://doi.org/10.1140/epjc/s10052-023-11584-x>. arXiv:2212.07338 [hep-ex]
44. ATLAS Collaboration, Reconstruction of hadronic decay products of tau leptons with the ATLAS experiment. *Eur. Phys. J. C* **76**, 295 (2016). <https://doi.org/10.1140/epjc/s10052-016-4110-0>. arXiv:1512.05955 [hep-ex]
45. ATLAS Collaboration, The performance of missing transverse momentum reconstruction and its significance with the ATLAS detector using 140 fb^{-1} of $\sqrt{s} = 13\text{ TeV}$ pp collisions. (2024). arXiv:2402.05858 [hep-ex]
46. R. Ellis, I. Hinchliffe, M. Soldate, J. Van Der Bij, Higgs decay to $\tau^+\tau^-$ A possible signature of intermediate mass Higgs bosons at high energy hadron colliders. *Nucl. Phys. B* **297**, 221 (1988). [https://doi.org/10.1016/0550-3213\(88\)90019-3](https://doi.org/10.1016/0550-3213(88)90019-3)
47. ATLAS Collaboration, Jet reconstruction and performance using particle flow with the ATLAS detector. *Eur. Phys. J. C* **77**, 466 (2017). <https://doi.org/10.1140/epjc/s10052-017-5031-2>. arXiv:1703.10485 [hep-ex]
48. ATLAS Collaboration, Performance of the ATLAS muon triggers in Run 2. *JINST* **15**, P09015 (2020). <https://doi.org/10.1088/1748-0221/15/09/p09015>. arXiv:2004.13447 [physics.ins-det]
49. ATLAS Collaboration, Performance of the missing transverse momentum triggers for the ATLAS detector during Run-2 data taking. *JHEP* **08**, 080 (2020). [https://doi.org/10.1007/JHEP08\(2020\)080](https://doi.org/10.1007/JHEP08(2020)080). arXiv:2005.09554 [hep-ex]
50. ATLAS Collaboration, ATLAS flavour-tagging algorithms for the LHC Run 2 pp collision dataset. *Eur. Phys. J. C* **83**, 681 (2023). <https://doi.org/10.1140/epjc/s10052-023-11699-1>. arXiv:2211.16345 [physics.data-an]
51. ATLAS Collaboration, Jet energy scale and resolution measured in proton–proton collisions at $\sqrt{s} = 13\text{ TeV}$ with the ATLAS detector. *Eur. Phys. J. C* **81**, 689 (2021). <https://doi.org/10.1140/epjc/s10052-021-09402-3>. arXiv:2007.02645 [hep-ex]
52. ATLAS Collaboration, Precise measurements of W - and Z -boson transverse momentum spectra with the ATLAS detector using pp collisions at $\sqrt{s} = 5.02\text{ TeV}$ and 13 TeV . (2024). arXiv:2404.06204 [hep-ex]

ATLAS Collaboration*

- G. Aad¹⁰⁴, E. Aakvaag¹⁷, B. Abbott¹²³, S. Abdelhameed^{119a}, K. Abeling⁵⁶, N.J. Abicht⁵⁰, S.H. Abidi³⁰, M. Aboelela⁴⁶, A. Aboulhorma^{36e}, H. Abramowicz¹⁵⁵, Y. Abulaiti¹²⁰, B.S. Acharya^{70a,70b,n}, A. Ackermann^{64a}, C. Adam Bourdarios⁴, L. Adamczyk^{87a}, S. V. Addepalli¹⁴⁷, M. J. Addison¹⁰³, J. Adelman¹¹⁸, A. Adiguzel^{22c}, T. Adye¹³⁷, A. A. Affolder¹³⁹, Y. Afik⁴¹, M. N. Agaras¹³, A. Aggarwal¹⁰², C. Agheorghiesei^{28c}, F. Ahmadov^{40,ad}, S. Ahuja⁹⁷, X. Ai^{63e}, G. Aielli^{77a,77b}, A. Aikot¹⁶⁷, M. Ait Tamlihat^{36e}, B. Aitbenchikh^{36a}, M. Akbiyik¹⁰², T. P. A. Åkesson¹⁰⁰, A. V. Akimov¹⁴⁹, D. Akiyama¹⁷², N. N. Akolkar²⁵, S. Aktas^{22a}, G. L. Alberghi^{24b}, J. Albert¹⁶⁹, P. Albicocco⁵⁴, G. L. Albouy⁶¹, S. Alderweireldt⁵³, Z. L. Alegria¹²⁴, M. Aleksa³⁷, I. N. Aleksandrov⁴⁰, C. Alexa^{28b}, T. Alexopoulos¹⁰, F. Alfonsi^{24b}, M. Algren⁵⁷, M. Alhroob¹⁷¹, B. Ali¹³⁵, H. M. J. Ali^{93,w}, S. Ali³², S. W. Alibocus⁹⁴, M. Aliev^{34c}, G. Alimonti^{72a}, W. Alkakhi⁵⁶, C. Allaire⁶⁷, B. M. M. Allbrooke¹⁵⁰, J. S. Allen¹⁰³, J. F. Allen⁵³, C. A. Allendes Flores^{140f}, P. P. Allport²¹, A. Aloisio^{73a,73b}, F. Alonso⁹², C. Alpigiani¹⁴², Z. M. K. Alsolami⁹³, A. Alvarez Fernandez¹⁰², M. Alves Cardoso⁵⁷, M. G. Alviggi^{73a,73b}, M. Aly¹⁰³, Y. Amaral Coutinho^{84b}, A. Ambler¹⁰⁶, C. Amelung³⁷, M. Amerl¹⁰³, C. G. Ames¹¹¹, D. Amidei¹⁰⁸, B. Amini⁵⁵, K. Amirie¹⁵⁸, A. Amirkhanov³⁹, S. P. Amor Dos Santos^{133a}, K. R. Amos¹⁶⁷, D. Amperiadou¹⁵⁶, S. An⁸⁵, V. Ananiev¹²⁸, C. Anastopoulos¹⁴³, T. Andeen¹¹, J. K. Anders⁹⁴, A. C. Anderson⁶⁰, A. Andreazza^{72a,72b}, S. Angelidakis⁹, A. Angerami⁴³, A. V. Anisenkov³⁹, A. Annovi^{75a}, C. Antel⁵⁷, E. Antipov¹⁴⁹, M. Antonelli⁵⁴, F. Anulli^{76a}, M. Aoki⁸⁵, T. Aoki¹⁵⁷, M. A. Aparo¹⁵⁰, L. Aperio Bella⁴⁹, C. Appelt¹⁵⁵, A. Apyan²⁷, S. J. Arbiol Val⁸⁸, C. Arcangeletti⁵⁴, A. T. H. Arce⁵², J.-F. Arguin¹¹⁰, S. Argyropoulos¹⁵⁶, J.-H. Arling⁴⁹, O. Arnaez⁴, H. Arnold¹⁴⁹, G. Artoni^{76a,76b}, H. Asada¹¹³, K. Asai¹²¹, S. Asai¹⁵⁷, N. A. Asbah³⁷, R. A. Ashby Pickering¹⁷¹, A. M. Aslam⁹⁷, K. Assamagan³⁰, R. Astalos^{29a}, K. S. V. Astrand¹⁰⁰, S. Atashi¹⁶², R. J. Atkin^{34a}, H. Atmani^{36f}, P. A. Atmasiddha¹³¹, K. Augsten¹³⁵, A. D. Auriol⁴², V. A. Astrup¹⁰³, G. Avolio³⁷, K. Axiotis⁵⁷, G. Azuelos^{110,ah}, D. Baba^{29b}, H. Bachacou¹³⁸, K. Bachas^{156,r}, A. Bachiu³⁵, E. Bachmann⁵¹, A. Badea⁴¹, T. M. Baer¹⁰⁸, P. Bagnaia^{76a,76b}, M. Bahmani¹⁹, D. Bahner⁵⁵, K. Bai¹²⁶, J. T. Baines¹³⁷, L. Baines⁹⁶, O. K. Baker¹⁷⁶, E. Bakos¹⁶, D. Bakshi Gupta⁸, L. E. Balabram Filho^{84b}, V. Balakrishnan¹²³, R. Balasubramanian⁴, E. M. Baldin³⁹, P. Balek^{87a}, E. Ballabene^{24a,24b}, F. Balli¹³⁸, L. M. Baltes^{64a}, W. K. Balunas³³, J. Balz¹⁰², I. Bamwidhi^{119b}, E. Banas⁸⁸, M. Bandieramonte¹³², A. Bandyopadhyay²⁵, S. Bansal²⁵, L. Barak¹⁵⁵, M. Barakat⁴⁹, E. L. Barberio¹⁰⁷, D. Barberis^{58a,58b}, M. Barbero¹⁰⁴, M. Z. Barel¹¹⁷, T. Barillari¹¹², M-S. Barisits³⁷, T. Barklow¹⁴⁷, P. Baron¹²⁵, D. A. Baron Moreno¹⁰³, A. Baroncelli^{63a}, A. J. Barr¹²⁹, J. D. Barr⁹⁸, F. Barreiro¹⁰¹, J. Barreiro Guimaraes da Costa¹⁴, M. G. Barros Teixeira^{133a}, S. Barsov³⁹, F. Bartels^{64a}, R. Bartoldus¹⁴⁷, A. E. Barton⁹³, P. Bartos^{29a}, A. Basan¹⁰², M. Baselga⁵⁰, S. Bashiri⁸⁸, A. Bassalat^{67,b}, M. J. Basso^{159a}, S. Batatau⁴⁶, R. Bate¹⁶⁸, R. L. Bates⁶⁰, S. Batlamous¹⁰¹, M. Battaglia¹³⁹, D. Battulga¹⁹, M. Baucé^{76a,76b}, M. Bauer⁸⁰, P. Bauer²⁵, L. T. Bazzano Hurrell³¹, J. B. Beacham¹¹², T. Beau¹³⁰, J. Y. Beauchamp⁹², P. H. Beauchemin¹⁶¹, P. Bechtle²⁵, H. P. Beck^{20,q}, K. Becker¹⁷¹, A. J. Beddall⁸³, V. A. Bednyakov⁴⁰, C. P. Bee¹⁴⁹, L. J. Beemster¹⁶, M. Begalli^{84d}, M. Begel³⁰, J. K. Behr⁴⁹, J. F. Beirer³⁷, F. Beisiegel²⁵, M. Belfkir^{119b}, G. Bella¹⁵⁵, L. Bellagamba^{24b}, A. Bellerive³⁵, P. Bellos²¹, K. Beloborodov³⁹, D. Benchekroun^{36a}, F. Bendebba^{36a}, Y. Benhammou¹⁵⁵, K. C. Benkendorfer⁶², L. Beresford⁴⁹, M. Beretta⁵⁴, E. Bergeaas Kuutmann¹⁶⁵, N. Berger⁴, B. Bergmann¹³⁵, J. Beringer^{18a}, G. Bernardi⁵, C. Bernius¹⁴⁷, F. U. Bernlochner²⁵, F. Bernon³⁷, A. Berrocal Guardia¹³, T. Berry⁹⁷, P. Berta¹³⁶, A. Berthold⁵¹, S. Bethke¹¹², A. Betti^{76a,76b}, A. J. Bevan⁹⁶, N. K. Bhalla⁵⁵, S. Bharthuar¹¹², S. Bhatta¹⁴⁹, D. S. Bhattacharya¹⁷⁰, P. Bhattacharai¹⁴⁷, Z. M. Bhatti¹²⁰, K. D. Bhide⁵⁵, V. S. Bhopatkar¹²⁴, R. M. Bianchi¹³², G. Bianco^{24a,24b}, O. Biebel¹¹¹, M. Biglietti^{78a}, C. S. Billingsley⁴⁶, Y. Bimgni^{36f}, M. Bindi⁵⁶, A. Bingham¹⁷⁵, A. Bingul^{22b}, C. Bini^{76a,76b}, G. A. Bird³³, M. Birman¹⁷³, M. Biros¹³⁶, S. Biryukov¹⁵⁰, T. Bisanz⁵⁰, E. Bisceglie^{45a,45b}, J. P. Biswal¹³⁷, D. Biswas¹⁴⁵, I. Bloch⁴⁹, A. Blue⁶⁰, U. Blumenschein⁹⁶, J. Blumenthal¹⁰², V. S. Bobrovnikov³⁹, M. Boehler⁵⁵, B. Boehm¹⁷⁰, D. Bogavac³⁷, A. G. Bogdanchikov³⁹, L. S. Boggia¹³⁰, V. Boisvert⁹⁷, P. Bokan³⁷, T. Bold^{87a}, M. Bomben⁵, M. Bona⁹⁶, M. Boonekamp¹³⁸, A. G. Borbély⁶⁰, I. S. Bordulev³⁹, G. Borissov⁹³, D. Bortoletto¹²⁹, D. Boscherini^{24b}, M. Bosman¹³, K. Bouaouda^{36a}, N. Bouchhar¹⁶⁷, L. Boudet⁴, J. Boudreau¹³², E. V. Bouhova-Thacker⁹³, D. Boumediene⁴², R. Bouquet^{58a,58b}, A. Boveia¹²², J. Boyd³⁷, D. Boye³⁰, I. R. Boyko⁴⁰, L. Bozianu⁵⁷, J. Bracinik²¹, N. Brahimi⁴, G. Brandt¹⁷⁵, O. Brandt³³, B. Brau¹⁰⁵, J. E. Brau¹²⁶, R. Brener¹⁷³, L. Brenner¹¹⁷, R. Brenner¹⁶⁵, S. Bressler¹⁷³, G. Brianti^{79a,79b}, D. Britton⁶⁰

- D. Britzger¹¹², I. Brock²⁵, R. Brock¹⁰⁹, G. Brooijmans⁴³, A. J. Brooks⁶⁹, E. M. Brooks^{159b}, E. Brost³⁰, L. M. Brown¹⁶⁹, L. E. Bruce⁶², T. L. Bruckler¹²⁹, P. A. Bruckman de Renstrom⁸⁸, B. Brüers⁴⁹, A. Bruni^{24b}, G. Brun^{24b}, D. Brunner^{48a,48b}, M. Bruschi^{24b}, N. Bruscino^{76a,76b}, T. Buanes¹⁷, Q. Buat¹⁴², D. Buchin¹¹², A. G. Buckley⁶⁰, O. Bulekov³⁹, B. A. Bullard¹⁴⁷, S. Burdin⁹⁴, C. D. Burgard⁵⁰, A. M. Burger³⁷, B. Burghgrave⁸, O. Burlayenko⁵⁵, J. Burleson¹⁶⁶, J. T. P. Burr³³, J. C. Burzynski¹⁴⁶, E. L. Busch⁴³, V. Büscher¹⁰², P. J. Bussey⁶⁰, J. M. Butler²⁶, C. M. Butta⁶⁰, J. M. Butterworth⁹⁸, W. Buttlinger¹³⁷, C. J. Buxo Vazquez¹⁰⁹, A. R. Buzykaev³⁹, S. Cabrera Urbán¹⁶⁷, L. Cadamuro⁶⁷, D. Caforio⁵⁹, H. Cai¹³², Y. Cai^{24a,24b,114c}, Y. Cai^{114a}, V. M. M. Cairo³⁷, O. Cakir^{3a}, N. Calace³⁷, P. Calafiura^{18a}, G. Calderini¹³⁰, P. Calfayan³⁵, G. Callea⁶⁰, L. P. Caloba^{84b}, D. Calvet⁴², S. Calvet⁴², R. Camacho Toro¹³⁰, S. Camarda³⁷, D. Camarero Munoz²⁷, P. Camarri^{77a,77b}, M. T. Camerlingo^{73a,73b}, D. Cameron³⁷, C. Camincher¹⁶⁹, M. Campanelli⁹⁸, A. Camplani⁴⁴, V. Canale^{73a,73b}, A. C. Canbay^{3a}, E. Canonero⁹⁷, J. Cantero¹⁶⁷, Y. Cao¹⁶⁶, F. Capocasa²⁷, M. Capua^{45a,45b}, A. Carbone^{72a,72b}, R. Cardarelli^{77a}, J. C. J. Cardenas⁸, M. P. Cardiff²⁷, G. Carducci^{45a,45b}, T. Carli³⁷, G. Carlino^{73a}, J. I. Carlotto¹³, B. T. Carlson^{132,s}, E. M. Carlson¹⁶⁹, J. Carmignani⁹⁴, L. Carminati^{72a,72b}, A. Carnelli¹³⁸, M. Carnesale³⁷, S. Caron¹¹⁶, E. Carquin^{140f}, I. B. Carr¹⁰⁷, S. Carrá^{72a}, G. CarratTA^{24a,24b}, A. M. Carroll¹²⁶, M. P. Casado^{13,i}, M. Caspar⁴⁹, F. L. Castillo⁴, L. Castillo Garcia¹³, V. Castillo Gimenez¹⁶⁷, N. F. Castro^{133a,133e}, A. Catinaccio³⁷, J. R. Catmore¹²⁸, T. Cavaliere⁴, V. Cavaliere³⁰, L. J. Caviedes Betancourt^{23b}, Y. C. Cekmecelioglu⁴⁹, E. Celebi⁸³, S. Cella³⁷, V. Cepaitis⁵⁷, K. Cerny¹²⁵, A. S. Cerqueira^{84a}, A. Cerri^{75a,75b}, L. Cerrito^{77a,77b}, F. Cerutti^{18a}, B. Cervato¹⁴⁵, A. Cervelli^{24b}, G. Cesarini⁵⁴, S. A. Cetin⁸³, P. M. Chabrillat¹³⁰, J. Chan^{18a}, W. Y. Chan¹⁵⁷, J. D. Chapman³³, E. Chapon¹³⁸, B. Chargeishvili^{153b}, D. G. Charlton²¹, C. Chauhan¹³⁶, Y. Che^{114a}, S. Chekanov⁶, S. V. Chekulaev^{159a}, G. A. Chelkov^{40,a}, B. Chen¹⁵⁵, B. Chen¹⁶⁹, H. Chen^{114a}, H. Chen³⁰, J. Chen^{63c}, J. Chen¹⁴⁶, M. Chen¹²⁹, S. Chen⁸⁹, S. J. Chen^{114a}, X. Chen^{63c}, X. Chen^{15,ag}, Y. Chen^{63a}, C. L. Cheng¹⁷⁴, H. C. Cheng^{65a}, S. Cheong¹⁴⁷, A. Cheplakov⁴⁰, E. Cheremushkina⁴⁹, E. Cherepanova¹¹⁷, R. Cherkoui El Moursli^{36e}, E. Cheu⁷, K. Cheung⁶⁶, L. Chevalier¹³⁸, V. Chiarella⁵⁴, G. Chiarelli^{75a}, N. Chiedde¹⁰⁴, G. Chiodini^{71a}, A. S. Chisholm²¹, A. Chitan^{28b}, M. Chitishvili¹⁶⁷, M. V. Chizhov^{40,t}, K. Choi¹¹, Y. Chou¹⁴², E. Y. S. Chow¹¹⁶, K. L. Chu¹⁷³, M. C. Chu^{65a}, X. Chu^{14,114c}, Z. Chubinidze⁵⁴, J. Chudoba¹³⁴, J. J. Chwastowski⁸⁸, D. Cieri¹¹², K. M. Ciesla^{87a}, V. Cindro⁹⁵, A. Ciocio^{18a}, F. Cirotto^{73a,73b}, Z. H. Citron¹⁷³, M. Citterio^{72a}, D. A. Ciubotaru^{28b}, A. Clark⁵⁷, P. J. Clark⁵³, N. Clarke Hall⁹⁸, C. Clarry¹⁵⁸, S. E. Clawson⁴⁹, C. Clement^{48a,48b}, Y. Coadou¹⁰⁴, M. Cobal^{70a,70c}, A. Coccaro^{58b}, R. F. Coelho Barrue^{133a}, R. Coelho Lopes De Sa¹⁰⁵, S. Coelli^{72a}, L. S. Colangeli¹⁵⁸, B. Cole⁴³, J. Collot⁶¹, P. Conde Muiño^{133a,133g}, M. P. Connell^{34c}, S. H. Connell^{34c}, E. I. Conroy¹²⁹, F. Conventi^{73a,ai}, H. G. Cooke²¹, A. M. Cooper-Sarkar¹²⁹, F. A. Corchia^{24a,24b}, A. Cordeiro Oudot Choi¹³⁰, L. D. Corpe⁴², M. Corradi^{76a,76b}, F. Corriveau^{106,ab}, A. Cortes-Gonzalez¹⁹, M. J. Costa¹⁶⁷, F. Costanza⁴, D. Costanzo¹⁴³, B. M. Cote¹²², J. Couthures⁴, G. Cowan⁹⁷, K. Cranmer¹⁷⁴, L. Cremer⁵⁰, D. Cremonini^{24a,24b}, S. Crépé-Renaudin⁶¹, F. Crescioli¹³⁰, M. Cristinziani¹⁴⁵, M. Cristoforetti^{79a,79b}, V. Croft¹¹⁷, J. E. Crosby¹²⁴, G. Crosetti^{45a,45b}, A. Cueto¹⁰¹, H. Cui⁹⁸, Z. Cui⁷, W. R. Cunningham⁶⁰, F. Curcio¹⁶⁷, J. R. Curran⁵³, P. Czodrowski³⁷, M. J. Da Cunha Sargedas De Sousa^{58a,58b}, J. V. Da Fonseca Pinto^{84b}, C. Da Via¹⁰³, W. Dabrowski^{87a}, T. Dado³⁷, S. Dahbi¹⁵², T. Dai¹⁰⁸, D. Dal Santo²⁰, C. Dallapiccola¹⁰⁵, M. Dam⁴⁴, G. D'amen³⁰, V. D'Amico¹¹¹, J. Damp¹⁰², J. R. Dandoy³⁵, D. Dannheim³⁷, M. Danninger¹⁴⁶, V. Dao¹⁴⁹, G. Darbo^{58b}, S. J. Das³⁰, F. Dattola⁴⁹, S. D'Auria^{72a,72b}, A. D'Avanzo^{73a,73b}, T. Davidek¹³⁶, I. Dawson⁹⁶, H. A. Day-hall¹³⁵, K. De⁸, C. De Almeida Rossi¹⁵⁸, R. De Asmundis^{73a}, N. De Biase⁴⁹, S. De Castro^{24a,24b}, N. De Groot¹¹⁶, P. de Jong¹¹⁷, H. De la Torre¹¹⁸, A. De Maria^{114a}, A. De Salvo^{76a}, U. De Sanctis^{77a,77b}, F. De Santis^{71a,71b}, A. De Santo¹⁵⁰, J. B. De Vivie De Regie⁶¹, J. Debevc⁹⁵, D. V. Dedovich⁴⁰, J. Degens⁹⁴, A. M. Deiana⁴⁶, J. Del Peso¹⁰¹, L. Delagrange¹³⁰, F. Deliot¹³⁸, C. M. Delitzsch⁵⁰, M. Della Pietra^{73a,73b}, D. Della Volpe⁵⁷, A. Dell'Acqua³⁷, L. Dell'Asta^{72a,72b}, M. Delmastro⁴, C. C. Delogu¹⁰², P. A. Delsart⁶¹, S. Demers¹⁷⁶, M. Demichev⁴⁰, S. P. Denisov³⁹, H. Denizli^{22a,l}, L. D'Eramo⁴², D. Derendarz⁸⁸, F. Derue¹³⁰, P. Dervan⁹⁴, K. Desch²⁵, C. Deutsch²⁵, F. A. Di Bello^{58a,58b}, A. Di Ciaccio^{77a,77b}, L. Di Ciaccio⁴, A. Di Domenico^{76a,76b}, C. Di Donato^{73a,73b}, A. Di Girolamo³⁷, G. Di Gregorio³⁷, A. Di Luca^{79a,79b}, B. Di Micco^{78a,78b}, R. Di Nardo^{78a,78b}, K. F. Di Petrillo⁴¹, M. Diamantopoulou³⁵, F. A. Dias¹¹⁷, T. Dias Do Vale¹⁴⁶, M. A. Diaz^{140a,140b}, A. R. Didenko⁴⁰, M. Didenko¹⁶⁷, E. B. Diehl¹⁰⁸, S. Díez Cornell⁴⁹, C. Diez Pardos¹⁴⁵, C. Dimitriadi¹⁴⁸, A. Dimitrieva²¹, A. Dimri¹⁴⁹, J. Dingfelder²⁵, T. Dingley¹²⁹, I-M. Dinu^{28b}, S. J. Dittmeier^{64b}, F. Dittus³⁷, M. Divisek¹³⁶, B. Dixit⁹⁴, F. Djama¹⁰⁴, T. Djobava^{153b}, C. Doglioni^{100,103}, A. Dohnalova^{29a}, Z. Dolezal¹³⁶, K. Domijan^{87a}, K. M. Dona⁴¹, M. Donadelli^{84d}, B. Dong¹⁰⁹, J. Donini⁴²

- A. D'Onofrio^{73a,73b}, M. D'Onofrio⁹⁴, J. Dopke¹³⁷, A. Doria^{73a}, N. Dos Santos Fernandes^{133a}, P. Dougan¹⁰³, M. T. Dova⁹², A. T. Doyle⁶⁰, M. A. Draguet¹²⁹, M. P. Drescher⁵⁶, E. Dreyer¹⁷³, I. Drivas-koulouris¹⁰, M. Drnevich¹²⁰, M. Drozdova⁵⁷, D. Du^{63a}, T. A. du Pree¹¹⁷, F. Dubinin³⁹, M. Dubovsky^{29a}, E. Duchovni¹⁷³, G. Duckeck¹¹¹, O. A. Ducu^{28b}, D. Duda⁵³, A. Dudarev³⁷, E. R. Duden²⁷, M. D'uffizi¹⁰³, L. Duflot⁶⁷, M. Dührssen³⁷, I. Duminica^{28g}, A. E. Dumitriu^{28b}, M. Dunford^{64a}, S. Dungs⁵⁰, K. Dunne^{48a,48b}, A. Duperrin¹⁰⁴, H. Duran Yildiz^{3a}, M. Düren⁵⁹, A. Durglishvili^{153b}, D. Duvnjak³⁵, B. L. Dwyer¹¹⁸, G. I. Dyckes^{18a}, M. Dyndal^{87a}, B. S. Dziedzic³⁷, Z. O. Earnshaw¹⁵⁰, G. H. Eberwein¹²⁹, B. Eckerova^{29a}, S. Eggebrecht⁵⁶, E. Egidio Purcino De Souza^{84e}, L. F. Ehrke⁵⁷, G. Eigen¹⁷, K. Einsweiler^{18a}, T. Ekelof¹⁶⁵, P. A. Ekman¹⁰⁰, S. El Farkh^{36b}, Y. El Ghazali^{63a}, H. El Jarrari³⁷, A. El Moussaouy^{36a}, V. Ellajosyula¹⁶⁵, M. Ellert¹⁶⁵, F. Ellinghaus¹⁷⁵, N. Ellis³⁷, J. Elmsheuser³⁰, M. Elsawy^{119a}, M. Elsing³⁷, D. Emeliyanov¹³⁷, Y. Enari⁸⁵, I. Ene^{18a}, S. Epari¹³, P. A. Erland⁸⁸, D. Ernani Martins Neto⁸⁸, M. Errenst¹⁷⁵, M. Escalier⁶⁷, C. Escobar¹⁶⁷, E. Etzion¹⁵⁵, G. Evans^{133a,133b}, H. Evans⁶⁹, L. S. Evans⁹⁷, A. Ezhilov³⁹, S. Ezzarqtouni^{36a}, F. Fabbri^{24a,24b}, L. Fabbri^{24a,24b}, G. Facini⁹⁸, V. Fadeev¹³⁹, R. M. Fakhruddinov³⁹, D. Fakoudis¹⁰², S. Falciano^{76a}, L. F. Falda Ulhoa Coelho^{133a}, F. Fallavollita¹¹², G. Falsetti^{45a,45b}, J. Faltova¹³⁶, C. Fan¹⁶⁶, K. Y. Fan^{65b}, Y. Fan¹⁴, Y. Fang^{14,114c}, M. Fanti^{72a,72b}, M. Faraj^{70a,70b}, Z. Farazpay⁹⁹, A. Farbin⁸, A. Farilla^{78a}, T. Farooque¹⁰⁹, J. N. Farr¹⁷⁶, S. M. Farrington^{137,53}, F. Fassi^{36e}, D. Fassouliotis⁹, M. Faucci Giannelli^{77a,77b}, W. J. Fawcett³³, L. Fayard⁶⁷, P. Federic¹³⁶, P. Federicova¹³⁴, O. L. Fedin^{39,a}, M. Feickert¹⁷⁴, L. Feligioni¹⁰⁴, D. E. Fellers¹²⁶, C. Feng^{63b}, Z. Feng¹¹⁷, M. J. Fenton¹⁶², L. Ferencz⁴⁹, R. A. M. Ferguson⁹³, P. Fernandez Martinez⁶⁸, M. J. V. Fernoux¹⁰⁴, J. Ferrando⁹³, A. Ferrari¹⁶⁵, P. Ferrari^{116,117}, R. Ferrari^{74a}, D. Ferrere⁵⁷, C. Ferretti¹⁰⁸, M. P. Fewell¹, D. Fiacco^{76a,76b}, F. Fiedler¹⁰², P. Fiedler¹³⁵, S. Filimonov³⁹, A. Filipčič⁹⁵, E. K. Filmer^{159a}, F. Filthaut¹¹⁶, M. C. N. Fiolhais^{133a,133c,c}, L. Fiorini¹⁶⁷, W. C. Fisher¹⁰⁹, T. Fitschen¹⁰³, P. M. Fitzhugh¹³⁸, I. Fleck¹⁴⁵, P. Fleischmann¹⁰⁸, T. Flick¹⁷⁵, M. Flores^{34d,ae}, L. R. Flores Castillo^{65a}, L. Flores Sanz De Aedo³⁷, F. M. Follega^{79a,79b}, N. Fomin³³, J. H. Foo¹⁵⁸, A. Formica¹³⁸, A. C. Forti¹⁰³, E. Fortin³⁷, A. W. Fortman^{18a}, L. Fountas^{9,j}, D. Fournier⁶⁷, H. Fox⁹³, P. Francavilla^{75a,75b}, S. Francescato⁶², S. Franchellucci⁵⁷, M. Franchini^{24a,24b}, S. Franchino^{64a}, D. Francis³⁷, L. Franco¹¹⁶, V. Franco Lima³⁷, L. Franconi⁴⁹, M. Franklin⁶², G. Frattari²⁷, Y. Y. Frid¹⁵⁵, J. Friend⁶⁰, N. Fritzsch³⁷, A. Froch⁵⁷, D. Froidevaux³⁷, J. A. Frost¹²⁹, Y. Fu¹⁰⁹, S. Fuenzalida Garrido^{140f}, M. Fujimoto¹⁰⁴, K. Y. Fung^{65a}, E. Furtado De Simas Filho^{84e}, M. Furukawa¹⁵⁷, J. Fuster¹⁶⁷, A. Gaa⁵⁶, A. Gabrielli^{24a,24b}, A. Gabrielli¹⁵⁸, P. Gadow³⁷, G. Gagliardi^{58a,58b}, L. G. Gagnon^{18a}, S. Gaid¹⁶⁴, S. Galantzan¹⁵⁵, J. Gallagher¹, E. J. Gallas¹²⁹, A. L. Gallen¹⁶⁵, B. J. Gallop¹³⁷, K. K. Gan¹²², S. Ganguly¹⁵⁷, Y. Gao⁵³, A. Garabaglu¹⁴², F. M. Garay Walls^{140a,140b}, B. Garcia³⁰, C. Garcia¹⁶⁷, A. Garcia Alonso¹¹⁷, A. G. Garcia Caffaro¹⁷⁶, J. E. Garcia Navarro¹⁶⁷, M. Garcia-Sciveres^{18a}, G. L. Gardner¹³¹, R. W. Gardner⁴¹, N. Garelli¹⁶¹, R. B. Garg¹⁴⁷, J. M. Gargan⁵³, C. A. Garner¹⁵⁸, C. M. Garvey^{34a}, V. K. Gassmann¹⁶¹, G. Gaudio^{74a}, V. Gautam¹³, P. Gauzzi^{76a,76b}, J. Gavranovic⁹⁵, I. L. Gavrilenco³⁹, A. Gavrilyuk³⁹, C. Gay¹⁶⁸, G. Gaycken¹²⁶, E. N. Gazis¹⁰, A. Gekow¹²², C. Gemme^{58b}, M. H. Genest⁶¹, A. D. Gentry¹¹⁵, S. George⁹⁷, W. F. George²¹, T. Geralis⁴⁷, A. A. Gerwin¹²³, P. Gessinger-Befurt³⁷, M. E. Geyik¹⁷⁵, M. Ghani¹⁷¹, K. Ghorbanian⁹⁶, A. Ghosal¹⁴⁵, A. Ghosh¹⁶², A. Ghosh⁷, B. Giacobbe^{24b}, S. Giagu^{76a,76b}, T. Giani¹¹⁷, A. Giannini^{63a}, S. M. Gibson⁹⁷, M. Gignac¹³⁹, D. T. Gil^{87b}, A. K. Gilbert^{87a}, B. J. Gilbert⁴³, D. Gillberg³⁵, G. Gilles¹¹⁷, L. Ginabat¹³⁰, D. M. Gingrich^{2,ah}, M. P. Giordani^{70a,70c}, P. F. Giraud¹³⁸, G. Giugliarelli^{70a,70c}, D. Giugni^{72a}, F. Giuli^{77a,77b}, I. Gkialas^{9,j}, L. K. Gladilin³⁹, C. Glasman¹⁰¹, G. Glemža⁴⁹, M. Glisic¹²⁶, I. Gnesi^{45b}, Y. Go³⁰, M. Goblirsch-Kolb³⁷, B. Gocke⁵⁰, D. Godin¹¹⁰, B. Gokturk^{22a}, S. Goldfarb¹⁰⁷, T. Golling⁵⁷, M. G. D. Gololo^{34c}, D. Golubkov³⁹, J. P. Gombas¹⁰⁹, A. Gomes^{133a,133b}, G. Gomes Da Silva¹⁴⁵, A. J. Gomez Delegido¹⁶⁷, R. Gonçalo^{133a}, L. Gonella²¹, A. Gongadze^{153c}, F. Gonnella²¹, J. L. Gonski¹⁴⁷, R. Y. González Andana⁵³, S. González de la Hoz¹⁶⁷, R. Gonzalez Lopez⁹⁴, C. Gonzalez Renteria^{18a}, M. V. Gonzalez Rodrigues⁴⁹, R. Gonzalez Suarez¹⁶⁵, S. Gonzalez-Sevilla⁵⁷, L. Goossens³⁷, B. Gorini³⁷, E. Gorini^{71a,71b}, A. Gorišek⁹⁵, T. C. Gosart¹³¹, A. T. Goshaw⁵², M. I. Gostkin⁴⁰, S. Goswami¹²⁴, C. A. Gottardo³⁷, S. A. Gotz¹¹¹, M. Gouighri^{36b}, A. Goussiou¹⁴², N. Govender^{34c}, R. P. Grabarczyk¹²⁹, I. Grabowska-Bold^{87a}, K. Graham³⁵, E. Gramstad¹²⁸, S. Grancagnolo^{71a,71b}, C. M. Grant^{1,138}, P. M. Gravila^{28f}, F. G. Gravili^{71a,71b}, H. M. Gray^{18a}, M. Greco¹¹², M. J. Green¹, C. Grefe²⁵, A. S. Grefsrud¹⁷, I. M. Gregor⁴⁹, K. T. Greif¹⁶², P. Grenier¹⁴⁷, S. G. Grewe¹¹², A. A. Grillo¹³⁹, K. Grimm³², S. Grinstein^{13,x}, J. -F. Grivaz⁶⁷, E. Gross¹⁷³, J. Grosse-Knetter⁵⁶, L. Guan¹⁰⁸, J. G. R. Guerrero Rojas¹⁶⁷, G. Guerrieri³⁷, R. Gugel¹⁰², J. A. M. Guhit¹⁰⁸, A. Guida¹⁹, E. Guilloton¹⁷¹, S. Guindon³⁷, F. Guo^{14,114c}, J. Guo^{63c}, L. Guo⁴⁹, L. Guo^{114b,v}, Y. Guo¹⁰⁸, A. Gupta⁵⁰, R. Gupta¹³², S. Gurbuz²⁵, S. S. Gurdasani⁴⁹, G. Gustavino^{76a,76b}

- P. Gutierrez¹²³, L. F. Gutierrez Zagazeta¹³¹, M. Gutsche⁵¹, C. Gutschow⁹⁸, C. Gwenlan¹²⁹, C. B. Gwilliam⁹⁴, E. S. Haaland¹²⁸, A. Haas¹²⁰, M. Habedank⁶⁰, C. Haber^{18a}, H. K. Hadavand⁸, A. Hadef⁵¹, A. I. Hagan⁹³, J. J. Hahn¹⁴⁵, E. H. Haines⁹⁸, M. Haleem¹⁷⁰, J. Haley¹²⁴, G. D. Hallewell¹⁰⁴, L. Halser²⁰, K. Hamano¹⁶⁹, M. Hamer²⁵, E. J. Hampshire⁹⁷, J. Han^{63b}, L. Han^{114a}, L. Han^{63a}, S. Han^{18a}, K. Hanagaki⁸⁵, M. Hance¹³⁹, D. A. Hangal⁴³, H. Hanif¹⁴⁶, M. D. Hank¹³¹, J. B. Hansen⁴⁴, P. H. Hansen⁴⁴, D. Harada⁵⁷, T. Harenberg¹⁷⁵, S. Harkusha¹⁷⁷, M. L. Harris¹⁰⁵, Y. T. Harris²⁵, J. Harrison¹³, N. M. Harrison¹²², P. F. Harrison¹⁷¹, N. M. Hartman¹¹², N. M. Hartmann¹¹¹, R. Z. Hasan^{97,137}, Y. Hasegawa¹⁴⁴, F. Haslbeck¹²⁹, S. Hassan¹⁷, R. Hauser¹⁰⁹, C. M. Hawkes²¹, R. J. Hawkings³⁷, Y. Hayashi¹⁵⁷, D. Hayden¹⁰⁹, C. Hayes¹⁰⁸, R. L. Hayes¹¹⁷, C. P. Hays¹²⁹, J. M. Hays⁹⁶, H. S. Hayward⁹⁴, F. He^{63a}, M. He^{14,114c}, Y. He⁴⁹, Y. He⁹⁸, N. B. Heatley⁹⁶, V. Hedberg¹⁰⁰, A. L. Heggelund¹²⁸, C. Heidegger⁵⁵, K. K. Heidegger⁵⁵, J. Heilman³⁵, S. Heim⁴⁹, T. Heim^{18a}, J. G. Heinlein¹³¹, J. J. Heinrich¹²⁶, L. Heinrich^{112,af}, J. Hejbal¹³⁴, A. Held¹⁷⁴, S. Hellesund¹⁷, C. M. Helling¹⁶⁸, S. Hellman^{48a,48b}, R. C. W. Henderson⁹³, L. Henkelmann³³, A. M. Henriques Correia³⁷, H. Herde¹⁰⁰, Y. Hernández Jiménez¹⁴⁹, L. M. Herrmann²⁵, T. Herrmann⁵¹, G. Herten⁵⁵, R. Hertenberger¹¹¹, L. Hervas³⁷, M. E. Hesping¹⁰², N. P. Hessey^{159a}, J. Hessler¹¹², M. Hidaoui^{36b}, N. Hidic¹³⁶, E. Hill¹⁵⁸, S. J. Hillier²¹, J. R. Hinds¹⁰⁹, F. Hinterkeuser²⁵, M. Hirose¹²⁷, S. Hirose¹⁶⁰, D. Hirschbuehl¹⁷⁵, T. G. Hitchings¹⁰³, B. Hiti⁹⁵, J. Hobbs¹⁴⁹, R. Hobincu^{28e}, N. Hod¹⁷³, M. C. Hodgkinson¹⁴³, B. H. Hodgkinson¹²⁹, A. Hoecker³⁷, D. D. Hofer¹⁰⁸, J. Hofer¹⁶⁷, M. Holzbock³⁷, L. B. A. H. Hommels³³, B. P. Honan¹⁰³, J. J. Hong⁶⁹, J. Hong^{63c}, T. M. Hong¹³², B. H. Hooberman¹⁶⁶, W. H. Hopkins⁶, M. C. Hoppesch¹⁶⁶, Y. Horii¹¹³, M. E. Horstmann¹¹², S. Hou¹⁵², M. R. Housenga¹⁶⁶, A. S. Howard⁹⁵, J. Howarth⁶⁰, J. Hoya⁶, M. Hrabovsky¹²⁵, T. Hrynová⁴, P. J. Hsu⁶⁶, S. -C. Hsu¹⁴², T. Hsu⁶⁷, M. Hu^{18a}, Q. Hu^{63a}, S. Huang³³, X. Huang^{14,114c}, Y. Huang¹³⁶, Y. Huang^{114b}, Y. Huang¹⁰², Y. Huang¹⁴, Z. Huang¹⁰³, Z. Hubacek¹³⁵, M. Huebner²⁵, F. Huegging²⁵, T. B. Huffman¹²⁹, M. Hufnagel Maranha De Faria^{84a}, C. A. Hugli⁴⁹, M. Huhtinen³⁷, S. K. Huberts¹⁷, R. Hulskens¹⁰⁶, C. E. Hultquist^{18a}, N. Huseynov^{12,g}, J. Huston¹⁰⁹, J. Huth⁶², R. Hyneman⁷, G. Iacobucci⁵⁷, G. Iakovidis³⁰, L. Iconomou-Fayard⁶⁷, J. P. Iddon³⁷, P. Iengo^{73a,73b}, R. Iguchi¹⁵⁷, Y. Iiyama¹⁵⁷, T. Iizawa¹²⁹, Y. Ikegami⁸⁵, D. Iliadis¹⁵⁶, N. Ilic¹⁵⁸, H. Imam^{84c}, G. Inacio Goncalves^{84d}, S. A. Infante Cabanas^{140c}, T. Ingebretsen Carlson^{48a,48b}, J. M. Inglis⁹⁶, G. Introzzi^{74a,74b}, M. Iodice^{78a}, V. Ippolito^{76a,76b}, R. K. Irwin⁹⁴, M. Ishino¹⁵⁷, W. Islam¹⁷⁴, C. Issever¹⁹, S. Istiin^{22a,am}, H. Ito¹⁷², R. Iuppa^{79a,79b}, A. Ivina¹⁷³, V. Izzo^{73a}, P. Jacka¹³⁴, P. Jackson¹, C. S. Jagfeld¹¹¹, G. Jain^{159a}, P. Jain⁴⁹, K. Jakobs⁵⁵, T. Jakoubek¹⁷³, J. Jamieson⁶⁰, W. Jang¹⁵⁷, M. Javurkova¹⁰⁵, P. Jawahar¹⁰³, L. Jeanty¹²⁶, J. Jejelava^{153a}, P. Jenni^{55,f}, C. E. Jessiman³⁵, C. Jia^{63b}, H. Jia¹⁶⁸, J. Jia¹⁴⁹, X. Jia^{14,114c}, Z. Jia^{114a}, C. Jiang⁵³, Q. Jiang^{65b}, S. Jiggins⁴⁹, J. Jimenez Pena¹³, S. Jin^{114a}, A. Jinaru^{28b}, O. Jinnouchi¹⁴¹, P. Johansson¹⁴³, K. A. Johns⁷, J. W. Johnson¹³⁹, F. A. Jolly⁴⁹, D. M. Jones¹⁵⁰, E. Jones⁴⁹, K. S. Jones⁸, P. Jones³³, R. W. L. Jones⁹³, T. J. Jones⁹⁴, H. L. Joos^{37,56}, R. Joshi¹²², J. Jovicevic¹⁶, X. Ju^{18a}, J. J. Junggeburth³⁷, T. Junkermann^{64a}, A. Juste Rozas^{13,x}, M. K. Juzek⁸⁸, S. Kabana^{140e}, A. Kaczmar ska⁸⁸, M. Kado¹¹², H. Kagan¹²², M. Kagan¹⁴⁷, A. Kahn¹³¹, C. Kahra¹⁰², T. Kaji¹⁵⁷, E. Kajomovitz¹⁵⁴, N. Kakati¹⁷³, I. Kalaitzidou⁵⁵, N. J. Kang¹³⁹, D. Kar^{34g}, K. Karava¹²⁹, E. Karentzos²⁵, O. Karkout¹¹⁷, S. N. Karpov⁴⁰, Z. M. Karpova⁴⁰, V. Kartvelishvili⁹³, A. N. Karyukhin³⁹, E. Kasimi¹⁵⁶, J. Katzy⁴⁹, S. Kaur³⁵, K. Kawade¹⁴⁴, M. P. Kawale¹²³, C. Kawamoto⁸⁹, T. Kawamoto^{63a}, E. F. Kay³⁷, F. I. Kaya¹⁶¹, S. Kazakos¹⁰⁹, V. F. Kazanin³⁹, Y. Ke¹⁴⁹, J. M. Keaveney^{34a}, R. Keeler¹⁶⁹, G. V. Kehris⁶², J. S. Keller³⁵, J. J. Kempster¹⁵⁰, O. Kepka¹³⁴, J. Kerr^{159b}, B. P. Kerridge¹³⁷, B. P. Kerševan⁹⁵, L. Keszeghova^{29a}, R. A. Khan¹³², A. Khanov¹²⁴, A. G. Kharlamov³⁹, T. Kharlamova³⁹, E. E. Khoda¹⁴², M. Kholodenko^{133a}, T. J. Khoo¹⁹, G. Khoriauli¹⁷⁰, J. Khubua^{153b,*}, Y. A. R. Khwaira¹³⁰, B. Kibirige^{34g}, D. Kim⁶, D. W. Kim^{48a,48b}, Y. K. Kim⁴¹, N. Kimura⁹⁸, M. K. Kingston⁵⁶, A. Kirchhoff⁵⁶, C. Kirlfel²⁵, F. Kirlfel²⁵, J. Kirk¹³⁷, A. E. Kiryunin¹¹², S. Kita¹⁶⁰, C. Kitsaki¹⁰, O. Kivernyk²⁵, M. Klassen¹⁶¹, C. Klein³⁵, L. Klein¹⁷⁰, M. H. Klein⁴⁶, S. B. Klein⁵⁷, U. Klein⁹⁴, A. Klimentov³⁰, T. Klioutchnikova³⁷, P. Kluit¹¹⁷, S. Kluth¹¹², E. Kneringer⁸⁰, T. M. Knight¹⁵⁸, A. Knue⁵⁰, D. Kobylanski¹⁷³, S. F. Koch¹²⁹, M. Kocian¹⁴⁷, P. Kodyš¹³⁶, D. M. Koeck¹²⁶, P. T. Koenig²⁵, T. Koffas³⁵, O. Kolay⁵¹, I. Koletsou⁴, T. Komarek⁸⁸, K. Köneke⁵⁶, A. X. Y. Kong¹, T. Kono¹²¹, N. Konstantinidis⁹⁸, P. Kontaxakis⁵⁷, B. Konya¹⁰⁰, R. Kopeliansky⁴³, S. Koperny^{87a}, K. Korcyl⁸⁸, K. Kordas^{156,e}, A. Korn⁹⁸, S. Korn⁵⁶, I. Korolkov¹³, N. Korotkova³⁹, B. Kortman¹¹⁷, O. Kortner¹¹², S. Kortner¹¹², W. H. Kostecka¹¹⁸, V. V. Kostyukhin¹⁴⁵, A. Kotsokechagia³⁷, A. Kotwal⁵², A. Koumouris³⁷, A. Kourkoumelis-Charalampidi^{74a,74b}, C. Kourkoumelis⁹, E. Kourlitis¹¹², O. Kovanda¹²⁶, R. Kowalewski¹⁶⁹, W. Kozanecki¹²⁶, A. S. Kozhin³⁹, V. A. Kramarenko³⁹, G. Kramberger⁹⁵, P. Kramer²⁵, M. W. Krasny¹³⁰, A. Krasznahorkay¹⁰⁵, A. C. Kraus¹¹⁸

- J. W. Kraus¹⁷⁵, J. A. Kremer⁴⁹, T. Kresse⁵¹, L. Kretschmann¹⁷⁵, J. Kretzschmar⁹⁴, K. Kreul¹⁹, P. Krieger¹⁵⁸, K. Krizka²¹, K. Kroeninger⁵⁰, H. Kroha¹¹², J. Kroll¹³⁴, J. Kroll¹³¹, K. S. Krowpmann¹⁰⁹, U. Kruchonak⁴⁰, H. Krüger²⁵, N. Krumnack⁸², M. C. Kruse⁵², O. Kuchinskaia³⁹, S. Kuday^{3a}, S. Kuehn³⁷, R. Kuesters⁵⁵, T. Kuhl⁴⁹, V. Kukhtin⁴⁰, Y. Kulchitsky⁴⁰, S. Kuleshov^{140d,140b}, M. Kumar^{34g}, N. Kumari⁴⁹, P. Kumari^{159b}, A. Kupco¹³⁴, T. Kupfer⁵⁰, A. Kupich³⁹, O. Kuprash⁵⁵, H. Kurashige⁸⁶, L. L. Kurchaninov^{159a}, O. Kurdysh⁶⁷, Y. A. Kurochkin³⁸, A. Kurova³⁹, M. Kuze¹⁴¹, A. K. Kvam¹⁰⁵, J. Kvita¹²⁵, N. G. Kyriacou¹⁰⁸, L. A. O. Laatu¹⁰⁴, C. Lacasta¹⁶⁷, F. Lacava^{76a,76b}, H. Lacker¹⁹, D. Lacour¹³⁰, N. N. Lad⁹⁸, E. Ladygin⁴⁰, A. Lafarge⁴², B. Laforge¹³⁰, T. Lagouri¹⁷⁶, F. Z. Lahbab^{36a}, S. Lat⁵⁶, J. E. Lambert¹⁶⁹, S. Lammers⁶⁹, W. Lampl⁷, C. Lampoudis^{156,e}, G. Lamprinoudis¹⁰², A. N. Lancaster¹¹⁸, E. Lançon³⁰, U. Landgraf⁵⁵, M. P. J. Landon⁹⁶, V. S. Lang⁵⁵, O. K. B. Langrekken¹²⁸, A. J. Lankford¹⁶², F. Lanni³⁷, K. Lantzsch²⁵, A. Lanza^{74a}, M. Lanzac Berrocal¹⁶⁷, J. F. Laporte¹³⁸, T. Lari^{72a}, F. Lasagni Manghi^{24b}, M. Lassnig³⁷, V. Latonova¹³⁴, S. D. Lawlor¹⁴³, Z. Lawrence¹⁰³, R. Lazaridou¹⁷¹, M. Lazzaroni^{72a,72b}, H. D. M. Le¹⁰⁹, E. M. Le Boulicaut¹⁷⁶, L. T. Le Pottier^{18a}, B. Leban^{24a,24b}, M. LeBlanc¹⁰³, F. Ledroit-Guillon⁶¹, S. C. Lee¹⁵², T. F. Lee⁹⁴, L. L. Leeuw^{34c,ak}, M. Lefebvre¹⁶⁹, C. Leggett^{18a}, G. Lehmann Miotti³⁷, M. Leigh⁵⁷, W. A. Leight¹⁰⁵, W. Leinonen¹¹⁶, A. Leisos^{156,u}, M. A. L. Leite^{84c}, C. E. Leitgeb¹⁹, R. Leitner¹³⁶, K. J. C. Leney⁴⁶, T. Lenz²⁵, S. Leone^{75a}, C. Leonidopoulos⁵³, A. Leopold¹⁴⁸, J. H. Lepage Bourbonnais³⁵, R. Les¹⁰⁹, C. G. Lester³³, M. Levchenko³⁹, J. Levêque⁴, L. J. Levinson¹⁷³, G. Levrini^{24a,24b}, M. P. Lewicki⁸⁸, C. Lewis¹⁴², D. J. Lewis⁴, L. Lewitt¹⁴³, A. Li³⁰, B. Li^{63b}, C. Li¹⁰⁸, C-Q. Li¹¹², H. Li^{63a}, H. Li^{63b}, H. Li^{114a}, H. Li¹⁵, H. Li^{63a}, H. Li^{63b}, J. Li^{63c}, K. Li¹⁴, L. Li^{63c}, R. Li¹⁷⁶, S. Li^{14,114c}, S. Li^{63d,63c,d}, T. Li⁵, X. Li¹⁰⁶, Z. Li¹⁵⁷, Z. Li^{14,114c}, Z. Li^{63a}, S. Liang^{14,114c}, Z. Liang¹⁴, M. Liberatore¹³⁸, B. Liberti^{77a}, K. Lie^{65c}, J. Lieber Marin^{84e}, H. Lien⁶⁹, H. Lin¹⁰⁸, L. Linden¹¹¹, R. E. Lindley⁷, J. H. Lindon², J. Ling⁶², E. Lipeles¹³¹, A. Lipniacka¹⁷, A. Lister¹⁶⁸, J. D. Little⁶⁹, B. Liu¹⁴, B. X. Liu^{114b}, D. Liu^{63c,63d}, E. H. L. Liu²¹, J. K. K. Liu³³, K. Liu^{63d}, K. Liu^{63d,63c}, M. Liu^{63a}, M. Y. Liu^{63a}, P. Liu¹⁴, Q. Liu^{63c,63d,142}, X. Liu^{63a}, X. Liu^{63b}, Y. Liu^{114b,114c}, Y. L. Liu^{63b}, Y. W. Liu^{63a}, S. L. Lloyd⁹⁶, E. M. Lobodzinska⁴⁹, P. Loch⁷, E. Lodhi¹⁵⁸, T. Lohse¹⁹, K. Lohwasser¹⁴³, E. Loiacono⁴⁹, J. D. Lomas²¹, J. D. Long⁴³, I. Longarini¹⁶², R. Longo¹⁶⁶, A. Lopez Solis⁴⁹, N. A. Lopez-canelas⁷, N. Lorenzo Martinez⁴, A. M. Lory¹¹¹, M. Losada^{119a}, G. Löschcke Centeno¹⁵⁰, O. Loseva³⁹, X. Lou^{48a,48b}, X. Lou^{14,114c}, A. Lounis⁶⁷, P. A. Love⁹³, G. Lu^{14,114c}, M. Lu⁶⁷, S. Lu¹³¹, Y. J. Lu¹⁵², H. J. Lubatti¹⁴², C. Luci^{76a,76b}, F. L. Lucio Alves^{114a}, F. Luehring⁶⁹, O. Lukianchuk⁶⁷, B. S. Lunday¹³¹, O. Lundberg¹⁴⁸, B. Lund-Jensen^{148,*}, N. A. Luongo⁶, M. S. Lutz³⁷, A. B. Lux²⁶, D. Lynn³⁰, R. Lysak¹³⁴, E. Lytken¹⁰⁰, V. Lyubushkin⁴⁰, T. Lyubushkina⁴⁰, M. M. Lyukova¹⁴⁹, M. Firdaus M. Soberi⁵³, H. Ma³⁰, K. Ma^{63a}, L. L. Ma^{63b}, W. Ma^{63a}, Y. Ma¹²⁴, J. C. MacDonald¹⁰², P. C. Machado De Abreu Farias^{84e}, R. Madar⁴², T. Madula⁹⁸, J. Maeda⁸⁶, T. Maeno³⁰, P. T. Mafa^{34c,k}, H. Maguire¹⁴³, V. Maiboroda¹³⁸, A. Maio^{133a,133b,133d}, K. Maj^{87a}, O. Majersky⁴⁹, S. Majewski¹²⁶, R. Makhmanazarov³⁹, N. Makovec⁶⁷, V. Maksimovic¹⁶, B. Malaescu¹³⁰, Pa. Malecki⁸⁸, V. P. Maleev³⁹, F. Malek^{61,p}, M. Mali⁹⁵, D. Malito⁹⁷, U. Mallik^{81,*}, S. Maltezos¹⁰, S. Malyukov⁴⁰, J. Mamuzic¹³, G. Mancini⁵⁴, M. N. Mancini²⁷, G. Manco^{74a,74b}, J. P. Mandalia⁹⁶, S. S. Mandarry¹⁵⁰, I. Mandic⁹⁵, L. Manhaes de Andrade Filho^{84a}, I. M. Maniatis¹⁷³, J. Manjarres Ramos⁹¹, D. C. Mankad¹⁷³, A. Mann¹¹¹, S. Manzoni³⁷, L. Mao^{63c}, X. Mapekula^{34c}, A. Marantis^{156,u}, G. Marchiori⁵, M. Marcisovsky¹³⁴, C. Marcon^{72a}, M. Marinescu²¹, S. Marium⁴⁹, M. Marjanovic¹²³, A. Markhoos⁵⁵, M. Markovitch⁶⁷, M. K. Maroun¹⁰⁵, E. J. Marshall⁹³, Z. Marshall^{18a}, S. Marti-Garcia¹⁶⁷, J. Martin⁹⁸, T. A. Martin¹³⁷, V. J. Martin⁵³, B. Martin dit Latour¹⁷, L. Martinelli^{76a,76b}, M. Martinez^{13,x}, P. Martinez Agullo¹⁶⁷, V. I. Martinez Outschoorn¹⁰⁵, P. Martinez Suarez¹³, S. Martin-Haugh¹³⁷, G. Martinovicova¹³⁶, V. S. Martoiu^{28b}, A. C. Martyniuk⁹⁸, A. Marzin³⁷, D. Mascione^{79a,79b}, L. Masetti¹⁰², J. Maslik¹⁰³, A. L. Maslennikov³⁹, S. L. Mason⁴³, P. Massarotti^{73a,73b}, P. Mastrandrea^{75a,75b}, A. Mastroberardino^{45a,45b}, T. Masubuchi¹²⁷, T. T. Mathew¹²⁶, J. Matousek¹³⁶, D. M. Mattern⁵⁰, J. Maurer^{28b}, T. Maurin⁶⁰, A. J. Maury⁶⁷, B. Maček⁹⁵, D. A. Maximov³⁹, A. E. May¹⁰³, R. Mazini^{34g}, I. Maznias¹¹⁸, M. Mazza¹⁰⁹, S. M. Mazza¹³⁹, E. Mazzeo^{72a,72b}, J. P. Mc Gowan¹⁶⁹, S. P. Mc Kee¹⁰⁸, C. A. Mc Lean⁶, C. C. McCracken¹⁶⁸, E. F. McDonald¹⁰⁷, A. E. McDougall¹¹⁷, L. F. Mcelhinney⁹³, J. A. Mcfayden¹⁵⁰, R. P. McGovern¹³¹, R. P. Mckenzie^{34g}, T. C. McLachlan⁴⁹, D. J. McLaughlin⁹⁸, S. J. McMahon¹³⁷, C. M. Mcpartland⁹⁴, R. A. McPherson^{169,ab}, S. Mehlhase¹¹¹, A. Mehta⁹⁴, D. Melini¹⁶⁷, B. R. Mellado Garcia^{34g}, A. H. Melo⁵⁶, F. Meloni⁴⁹, A. M. Mendes Jacques Da Costa¹⁰³, H. Y. Meng¹⁵⁸, L. Meng⁹³, S. Menke¹¹², M. Mentink³⁷, E. Meoni^{45a,45b}, G. Mercado¹¹⁸, S. Merianos¹⁵⁶, C. Merlassino^{70a,70c}, C. Meroni^{72a,72b}, J. Metcalfe⁶

- A. S. Mete⁶, E. Meuser¹⁰², C. Meyer⁶⁹, J-P. Meyer¹³⁸, R. P. Middleton¹³⁷, L. Mijović⁵³, G. Mikenberg¹⁷³, M. Mikestikova¹³⁴, M. Mikuž⁹⁵, H. Mildner¹⁰², A. Milic³⁷, D. W. Miller⁴¹, E. H. Miller¹⁴⁷, L. S. Miller³⁵, A. Milov¹⁷³, D. A. Milstead^{48a,48b}, T. Min^{114a}, A. A. Minaenko³⁹, I. A. Minashvili^{153b}, A. I. Mincer¹²⁰, B. Mindur^{87a}, M. Mineev⁴⁰, Y. Mino⁸⁹, L. M. Mir¹³, M. Miralles Lopez⁶⁰, M. Mironova^{18a}, M. C. Missio¹¹⁶, A. Mitra¹⁷¹, V. A. Mitsou¹⁶⁷, Y. Mitsumori¹¹³, O. Miú¹⁵⁸, P. S. Miyagawa⁹⁶, T. Mkrtchyan^{64a}, M. Mlinarevic⁹⁸, T. Mlinarevic⁹⁸, M. Mlynarikova³⁷, S. Mobius²⁰, P. Mogg¹¹¹, M. H. Mohamed Farook¹¹⁵, A. F. Mohammed^{14,114c}, S. Mohapatra⁴³, G. Mokgatitswane^{34g}, L. Moleri¹⁷³, B. Mondal¹⁴⁵, S. Mondal¹³⁵, K. Mönig⁴⁹, E. Monnier¹⁰⁴, L. Monsonis Romero¹⁶⁷, J. Montejano Berlingen¹³, A. Montella^{48a,48b}, M. Montella¹²², F. Montereali^{78a,78b}, F. Monticelli⁹², S. Monzani^{70a,70c}, A. Morancho Tarda⁴⁴, N. Morange⁶⁷, A. L. Moreira De Carvalho⁴⁹, M. Moreno Llácer¹⁶⁷, C. Moreno Martinez⁵⁷, J. M. Moreno Perez^{23b}, P. Morettini^{58b}, S. Morgenstern³⁷, M. Morii⁶², M. Morinaga¹⁵⁷, M. Moritsu⁹⁰, F. Morodei^{76a,76b}, P. Moschovakos³⁷, B. Moser¹²⁹, M. Mosidze^{153b}, T. Moskalets⁴⁶, P. Moskvitina¹¹⁶, J. Moss^{32,m}, P. Moszkowicz^{87a}, A. Moussa^{36d}, Y. Moyal¹⁷³, E. J. W. Moyse¹⁰⁵, O. Mtintsilana^{34g}, S. Muanza¹⁰⁴, J. Mueller¹³², D. Muenstermann⁹³, R. Müller³⁷, G. A. Mullier¹⁶⁵, A. J. Mullin³³, J. J. Mullin¹³¹, A. E. Mulski⁶², D. P. Mungo¹⁵⁸, D. Munoz Perez¹⁶⁷, F. J. Munoz Sanchez¹⁰³, M. Murin¹⁰³, W. J. Murray^{171,137}, M. Muškinja⁹⁵, C. Mwewa³⁰, A. G. Myagkov^{39,a}, A. J. Myers⁸, G. Myers¹⁰⁸, M. Myska¹³⁵, B. P. Nachman^{18a}, K. Nagai¹²⁹, K. Nagano⁸⁵, R. Nagasaka¹⁵⁷, J. L. Nagle^{30,aj}, E. Nagy¹⁰⁴, A. M. Nairz³⁷, Y. Nakahama⁸⁵, K. Nakamura⁸⁵, K. Nakkalil⁵, H. Nanjo¹²⁷, E. A. Narayanan⁴⁶, Y. Narukawa¹⁵⁷, I. Naryshkin³⁹, L. Nasella^{72a,72b}, S. Nasri^{119b}, C. Nass²⁵, G. Navarro^{23a}, J. Navarro-Gonzalez¹⁶⁷, A. Nayaz¹⁹, P. Y. Nechaeva³⁹, S. Nechaeva^{24a,24b}, F. Nechansky¹³⁴, L. Nedic¹²⁹, T. J. Neep²¹, A. Negri^{74a,74b}, M. Negrini^{24b}, C. Nellist¹¹⁷, C. Nelson¹⁰⁶, K. Nelson¹⁰⁸, S. Nemecek¹³⁴, M. Nessi^{37,h}, M. S. Neubauer¹⁶⁶, F. Neuhaus¹⁰², J. Newell⁹⁴, P. R. Newman²¹, Y. W. Y. Ng¹⁶⁶, B. Ngair^{119a}, H. D. N. Nguyen¹¹⁰, R. B. Nickerson¹²⁹, R. Nicolaïdou¹³⁸, J. Nielsen¹³⁹, M. Niemeyer⁵⁶, J. Niermann³⁷, N. Nikiforou³⁷, V. Nikolaenko^{39,a}, I. Nikolic-Audit¹³⁰, P. Nilsson³⁰, I. Ninca⁴⁹, G. Ninio¹⁵⁵, A. Nisati^{76a}, N. Nishu², R. Nisius¹¹², N. Nitika^{70a,70c}, J-E. Nitschke⁵¹, E. K. Nkadimeng^{34g}, T. Nobe¹⁵⁷, T. Nommensen¹⁵¹, M. B. Norfolk¹⁴³, B. J. Norman³⁵, M. Noury^{36a}, J. Novak⁹⁵, T. Novak⁹⁵, R. Novotny¹¹⁵, L. Nozka¹²⁵, K. Ntekas¹⁶², N. M. J. Nunes De Moura Junior^{84b}, J. Ocariz¹³⁰, A. Ochi⁸⁶, I. Ochoa^{133a}, S. Oerdekk^{49,y}, J. T. Offermann⁴¹, A. Ogodnik¹³⁶, A. Oh¹⁰³, C. C. Ohm¹⁴⁸, H. Oide⁸⁵, R. Oishi¹⁵⁷, M. L. Ojeda³⁷, Y. Okumura¹⁵⁷, L. F. Oleiro Seabra^{133a}, I. Oleksiyuk⁵⁷, S. A. Olivares Pino^{140d}, G. Oliveira Correa¹³, D. Oliveira Damazio³⁰, J. L. Oliver¹⁶², Ö. Ö. Öncel⁵⁵, A. P. O'Neil²⁰, A. Onofre^{133a,133e}, P. U. E. Onyisi¹¹, M. J. Oreglia⁴¹, D. Orestano^{78a,78b}, R. S. Orr¹⁵⁸, L. M. Osojnak¹³¹, Y. Osumi¹¹³, G. Otero y Garzon³¹, H. Otono⁹⁰, P. S. Ott^{64a}, G. J. Ottino^{18a}, M. Ouchrif^{36d}, F. Ould-Saada¹²⁸, T. Oysiannikova¹⁴², M. Owen⁶⁰, R. E. Owen¹³⁷, V. E. Ozcan^{22a}, F. Ozturk⁸⁸, N. Ozturk⁸, S. Ozturk⁸³, H. A. Pacey¹²⁹, K. Pachal^{159a}, A. Pacheco Pages¹³, C. Padilla Aranda¹³, G. Padovano^{76a,76b}, S. Pagan Griso^{18a}, G. Palacino⁶⁹, A. Palazzo^{71a,71b}, J. Pampel²⁵, J. Pan¹⁷⁶, T. Pan^{65a}, D. K. Panchal¹¹, C. E. Pandini¹¹⁷, J. G. Panduro Vazquez¹³⁷, H. D. Pandya¹, H. Pang¹³⁸, P. Pani⁴⁹, G. Panizzo^{70a,70c}, L. Panwar¹³⁰, L. Paolozzi⁵⁷, S. Parajuli¹⁶⁶, A. Paramonov⁶, C. Paraskevopoulos⁵⁴, D. Paredes Hernandez^{65b}, A. Pareti^{74a,74b}, K. R. Park⁴³, T. H. Park¹¹², F. Parodi^{58a,58b}, J. A. Parsons⁴³, U. Parzefall⁵⁵, B. Pascual Dias¹¹⁰, L. Pascual Dominguez¹⁰¹, E. Pasqualucci^{76a}, S. Passaggio^{58b}, F. Pastore⁹⁷, P. Patel⁸⁸, U. M. Patel⁵², J. R. Pater¹⁰³, T. Pauly³⁷, F. Pauwels¹³⁶, C. I. Pazos¹⁶¹, M. Pedersen¹²⁸, R. Pedro^{133a}, S. V. Peleganchuk³⁹, O. Penc³⁷, E. A. Pender⁵³, S. Peng¹⁵, G. D. Penn¹⁷⁶, K. E. Penski¹¹¹, M. Penzin³⁹, B. S. Peralva^{84d}, A. P. Pereira Peixoto¹⁴², L. Pereira Sanchez¹⁴⁷, D. V. Perepelitsa^{30,aj}, G. Perera¹⁰⁵, E. Perez Codina^{159a}, M. Perganti¹⁰, H. Pernegger³⁷, S. Perrella^{76a,76b}, O. Perrin⁴², K. Peters⁴⁹, R. F. Y. Peters¹⁰³, B. A. Petersen³⁷, T. C. Petersen⁴⁴, E. Petit¹⁰⁴, V. Petousis¹³⁵, C. Petridou^{156,e}, T. Petru¹³⁶, A. Petrukhin¹⁴⁵, M. Pettee^{18a}, A. Petukhov⁸³, K. Petukhova³⁷, R. Pezoa^{140f}, L. Pezzotti³⁷, G. Pezzullo¹⁷⁶, A. J. Pfleger³⁷, T. M. Pham¹⁷⁴, T. Pham¹⁰⁷, P. W. Phillips¹³⁷, G. Piacquadio¹⁴⁹, E. Pianori^{18a}, F. Piazza¹²⁶, R. Piegaia³¹, D. Pietreanu^{28b}, A. D. Pilkington¹⁰³, M. Pinamonti^{70a,70c}, J. L. Pinfold², B. C. Pinheiro Pereira^{133a}, J. Pinol Bel¹³, A. E. Pinto Pinoargote^{138,138}, L. Pintucci^{70a,70c}, K. M. Piper¹⁵⁰, A. Pirttikoski⁵⁷, D. A. Pizzi³⁵, L. Pizzimento^{65b}, M. -A. Pleier³⁰, V. Pleskot¹³⁶, E. Plotnikova⁴⁰, G. Poddar⁹⁶, R. Poettgen¹⁰⁰, L. Poggioli¹³⁰, S. Polacek¹³⁶, G. Polesello^{74a}, A. Poley^{146,159a}, A. Polini^{24b}, C. S. Pollard¹⁷¹, Z. B. Pollock¹²², E. Pompa Pacchi¹²³, N. I. Pond⁹⁸, D. Ponomarenko⁶⁹, L. Pontecorvo³⁷, S. Popa^{28a}, G. A. Popeneciu^{28d}, A. Poreba³⁷, D. M. Portillo Quintero^{159a}, S. Pospisil¹³⁵, M. A. Postill¹⁴³, P. Postolache^{28c}, K. Potamianos¹⁷¹, P. A. Potepa^{87a}, I. N. Potrap⁴⁰, C. J. Potter³³, H. Potti¹⁵¹

- J. Poveda¹⁶⁷, M. E. Pozo Astigarraga³⁷, A. Prades Ibanez^{77a,77b}, J. Pretel¹⁶⁹, D. Price¹⁰³, M. Primavera^{71a}, L. Primomo^{70a,70c}, M. A. Principe Martin¹⁰¹, R. Privara¹²⁵, T. Procter⁶⁰, M. L. Proffitt¹⁴², N. Proklova¹³¹, K. Prokofiev^{65c}, G. Proto¹¹², J. Proudfoot⁶, M. Przybycien^{87a}, W. W. Przygoda^{87b}, A. Psallidas⁴⁷, J. E. Puddefoot¹⁴³, D. Pudzha⁵⁵, D. Pyatiizbyantseva¹¹⁶, J. Qian¹⁰⁸, R. Qian¹⁰⁹, D. Qichen¹⁰³, Y. Qin¹³, T. Qiu⁵³, A. Quadt⁵⁶, M. Queitsch-Maitland¹⁰³, G. Quetant⁵⁷, R. P. Quinn¹⁶⁸, G. Rabanal Bolanos⁶², D. Rafanoharana⁵⁵, F. Raffaeli^{77a,77b}, F. Ragusa^{72a,72b}, J. L. Rainbolt⁴¹, J. A. Raine⁵⁷, S. Rajagopalan³⁰, E. Ramakoti³⁹, L. Rambelli^{58a,58b}, I. A. Ramirez-Berend³⁵, K. Ran^{49,114c}, D. S. Rankin¹³¹, N. P. Rapheeha^{34g}, H. Rasheed^{28b}, V. Raskina¹³⁰, D. F. Rassloff^{64a}, A. Rastogi^{18a}, S. Rave¹⁰², S. Ravera^{58a,58b}, B. Ravina³⁷, I. Ravinovich¹⁷³, M. Raymond³⁷, A. L. Read¹²⁸, N. P. Readioff¹⁴³, D. M. Rebuzzi^{74a,74b}, A. S. Reed¹¹², K. Reeves²⁷, J. A. Reidelsturz¹⁷⁵, D. Reikher¹²⁶, A. Rej⁵⁰, C. Rembser³⁷, H. Ren^{63a}, M. Renda^{28b}, F. Renner⁴⁹, A. G. Rennie¹⁶², A. L. Rescia⁴⁹, S. Resconi^{72a}, M. Ressegotti^{58a,58b}, S. Rettie³⁷, W. F. Rettie³⁵, J. G. Reyes Rivera¹⁰⁹, E. Reynolds^{18a}, O. L. Rezanova³⁹, P. Reznicek¹³⁶, H. Riani^{36d}, N. Ribaric⁵², E. Ricci^{79a,79b}, R. Richter¹¹², S. Richter^{48a,48b}, E. Richter-Was^{87b}, M. Ridel¹³⁰, S. Ridouani^{36d}, P. Rieck¹²⁰, P. Riedler³⁷, E. M. Riefel^{48a,48b}, J. O. Rieger¹¹⁷, M. Rijssenbeek¹⁴⁹, M. Rimoldi³⁷, L. Rinaldi^{24a,24b}, P. Rincke⁵⁶, M. P. Rinnagel¹¹¹, G. Ripellino¹⁶⁵, I. Riu¹³, J. C. Rivera Vergara¹⁶⁹, F. Rizatdinova¹²⁴, E. Rizvi⁹⁶, B. R. Roberts^{18a}, S. S. Roberts¹³⁹, D. Robinson³³, M. Robles Manzano¹⁰², A. Robson⁶⁰, A. Rocchi^{77a,77b}, C. Roda^{75a,75b}, S. Rodriguez Bosca³⁷, Y. Rodriguez Garcia^{23a}, A. M. Rodriguez Vera¹¹⁸, S. Roe³⁷, J. T. Roemer³⁷, O. Røhne¹²⁸, R. A. Rojas³⁷, C. P. A. Roland¹³⁰, J. Roloff³⁰, A. Romaniouk⁸⁰, E. Romano^{74a,74b}, M. Romano^{24b}, A. C. Romero Hernandez¹⁶⁶, N. Rompotis⁹⁴, L. Roos¹³⁰, S. Rosati^{76a}, B. J. Rosser⁴¹, E. Rossi¹²⁹, E. Rossi^{73a,73b}, L. P. Rossi⁶², L. Rossi⁵⁵, R. Rosten¹²², M. Rotaru^{28b}, B. Rottler⁵⁵, C. Rougier⁹¹, D. Rousseau⁶⁷, D. Rousseau⁴⁹, S. Roy-Garand¹⁵⁸, A. Rozanov¹⁰⁴, Z. M. A. Rozario⁶⁰, Y. Rozen¹⁵⁴, A. Rubio Jimenez¹⁶⁷, V. H. Ruelas Rivera¹⁹, T. A. Ruggeri¹, A. Ruggiero¹²⁹, A. Ruiz-Martinez¹⁶⁷, A. Rummel³⁷, Z. Rurikova⁵⁵, N. A. Rusakovich⁴⁰, H. L. Russell¹⁶⁹, G. Russo^{76a,76b}, J. P. Rutherford Colmenares³³, M. Rybar¹³⁶, E. B. Rye¹²⁸, A. Ryzhov⁴⁶, J. A. Sabater Iglesias⁵⁷, H. F-W. Sadrozinski¹³⁹, F. Safai Tehrani^{76a}, S. Saha¹, M. Sahinsoy⁸³, A. Saibel¹⁶⁷, M. Saimpert¹³⁸, M. Saito¹⁵⁷, T. Saito¹⁵⁷, A. Sala^{72a,72b}, D. Salamani³⁷, A. Salnikov¹⁴⁷, J. Salt¹⁶⁷, A. Salvador Salas¹⁵⁵, D. Salvatore^{45a,45b}, F. Salvatore¹⁵⁰, A. Salzburger³⁷, D. Sammel⁵⁵, E. Sampson⁹³, D. Sampsonidis^{156,c}, D. Sampsonidou¹²⁶, J. Sanchez¹⁶⁷, V. Sanchez Sebastian¹⁶⁷, H. Sandaker¹²⁸, C. O. Sander⁴⁹, J. A. Sandesara¹⁰⁵, M. Sandhoff¹⁷⁵, C. Sandoval^{23b}, L. Sanfilippo^{64a}, D. P. C. Sankey¹³⁷, T. Sano⁸⁹, A. Sansoni⁵⁴, L. Santi^{37,76b}, C. Santoni⁴², H. Santos^{133a,133b}, A. Santra¹⁷³, E. Sanzani^{24a,24b}, K. A. Saoucha¹⁶⁴, J. G. Saraiva^{133a,133d}, J. Sardain⁷, O. Sasaki⁸⁵, K. Sato¹⁶⁰, C. Sauer³⁷, E. Sauvan⁴, P. Savard^{158,ah}, R. Sawada¹⁵⁷, C. Sawyer¹³⁷, L. Sawyer⁹⁹, C. Sbarra^{24b}, A. Sbrizzi^{24a,24b}, T. Scanlon⁹⁸, J. Schaarschmidt¹⁴², U. Schäfer¹⁰², A. C. Schaffer^{67,46}, D. Schaille¹¹¹, R. D. Schamberger¹⁴⁹, C. Scharf¹⁹, M. M. Schefer²⁰, V. A. Schegelsky³⁹, D. Scheirich¹³⁶, M. Schernau^{140e}, C. Scheulen⁵⁷, C. Schiavi^{58a,58b}, M. Schioppa^{45a,45b}, B. Schlag¹⁴⁷, S. Schlenker³⁷, J. Schmeing¹⁷⁵, M. A. Schmidt¹⁷⁵, K. Schmieden¹⁰², C. Schmitt¹⁰², N. Schmitt¹⁰², S. Schmitt⁴⁹, L. Schoeffel¹³⁸, A. Schoening^{64b}, P. G. Scholer³⁵, E. Schopf¹²⁹, M. Schott²⁵, J. Schovancova³⁷, S. Schramm⁵⁷, T. Schroer⁵⁷, H-C. Schultz-Coulon^{64a}, M. Schumacher⁵⁵, B. A. Schumm¹³⁹, Ph. Schunke¹³⁸, H. R. Schwartz¹³⁹, A. Schwartzman¹⁴⁷, T. A. Schwarz¹⁰⁸, Ph. Schwemling¹³⁸, R. Schwienhorst¹⁰⁹, F. G. Sciacca²⁰, A. Sciandra³⁰, G. Sciolla²⁷, F. Scuri^{75a}, C. D. Sebastiani⁹⁴, K. Sedlaczek¹¹⁸, S. C. Seidel¹¹⁵, A. Seiden¹³⁹, B. D. Seidlitz⁴³, C. Seitz⁴⁹, J. M. Seixas^{84b}, G. Sekhniaidze^{73a}, L. Selem⁶¹, N. Semprini-Cesari^{24a,24b}, A. Semushin^{177,39}, D. Sengupta⁵⁷, V. Senthilkumar¹⁶⁷, L. Serin⁶⁷, M. Sessa^{77a,77b}, H. Severini¹²³, F. Sforza^{58a,58b}, A. Sfyrla⁵⁷, Q. Sha¹⁴, E. Shabalina⁵⁶, H. Shaddix¹¹⁸, A. H. Shah³³, R. Shaheen¹⁴⁸, J. D. Shahinian¹³¹, D. Shaked Renous¹⁷³, L. Y. Shan¹⁴, M. Shapiro^{18a}, A. Sharma³⁷, A. S. Sharma¹⁶⁸, P. Sharma³⁰, P. B. Shatalov³⁹, K. Shaw¹⁵⁰, S. M. Shaw¹⁰³, Q. Shen^{63c}, D. J. Sheppard¹⁴⁶, P. Sherwood⁹⁸, L. Shi⁹⁸, X. Shi¹⁴, S. Shimizu⁸⁵, C. O. Shimmin¹⁷⁶, I. P. J. Shipsey^{129,*}, S. Shirabe⁹⁰, M. Shiyakova^{40,z}, M. J. Shochet⁴¹, D. R. Shope¹²⁸, B. Shrestha¹²³, S. Shrestha^{122,al}, I. Shreyber³⁹, M. J. Shroff¹⁶⁹, P. Sicho¹³⁴, A. M. Sickles¹⁶⁶, E. Sideras Haddad^{34g,163}, A. C. Sidley¹¹⁷, A. Sidoti^{24b}, F. Siegert⁵¹, Dj. Sijacki¹⁶, F. Sili⁹², J. M. Silva⁵³, I. Silva Ferreira^{84b}, M. V. Silva Oliveira³⁰, S. B. Silverstein^{48a}, S. Simion⁶⁷, R. Simoniello³⁷, E. L. Simpson¹⁰³, H. Simpson¹⁵⁰, L. R. Simpson¹⁰⁸, S. Simsek⁸³, S. Sindhu⁵⁶, P. Sinervo¹⁵⁸, S. N. Singh²⁷, S. Singh³⁰, S. Sinha⁴⁹, S. Sinha¹⁰³, M. Sioli^{24a,24b}, K. Sioulas⁹, I. Siral³⁷, E. Sitnikova⁴⁹, J. Sjölin^{48a,48b}, A. Skaf⁵⁶, E. Skorda²¹, P. Skubic¹²³, M. Slawinska⁸⁸, I. Slazik¹⁷, V. Smakhtin¹⁷³, B. H. Smart¹³⁷, S. Yu. Smirnov³⁹, Y. Smirnov³⁹, L. N. Smirnova^{39,a}, O. Smirnova¹⁰⁰, A. C. Smith⁴³, D. R. Smith¹⁶²,

- E. A. Smith⁴¹, J. L. Smith¹⁰³, M. B. Smith³⁵, R. Smith¹⁴⁷, H. Smitmanns¹⁰², M. Smizanska⁹³, K. Smolek¹³⁵, A. A. Snesarev³⁹, H. L. Snoek¹¹⁷, S. Snyder³⁰, R. Sobie^{169,ab}, A. Soffer¹⁵⁵, C. A. Solans Sanchez³⁷, E. Yu. Soldatov³⁹, U. Soldevila¹⁶⁷, A. A. Solodkov³⁹, S. Solomon²⁷, A. Soloshenko⁴⁰, K. Solovieva⁵⁵, O. V. Solovyyanov⁴², P. Sommer⁵¹, A. Sonay¹³, W. Y. Song^{159b}, A. Sopczak¹³⁵, A. L. Sopio⁵³, F. Sopkova^{29b}, J. D. Sorenson¹¹⁵, I. R. Sotarriba Alvarez¹⁴¹, V. Sothilingam^{64a}, O. J. Soto Sandoval^{140c,140b}, S. Sottocornola⁶⁹, R. Soualah¹⁶⁴, Z. Soumaimi^{36e}, D. South⁴⁹, N. Soybelman¹⁷³, S. Spagnolo^{71a,71b}, M. Spalla¹¹², D. Sperlich⁵⁵, B. Spisso^{73a,73b}, D. P. Spiteri⁶⁰, M. Spousta¹³⁶, E. J. Staats³⁵, R. Stamen^{64a}, E. Stanecka⁸⁸, W. Stanek-Maslouska⁴⁹, M. V. Stange⁵¹, B. Stanislaus^{18a}, M. M. Stanitzki⁴⁹, B. Stapf⁴⁹, E. A. Starchenko³⁹, G. H. Stark¹³⁹, J. Stark⁹¹, P. Staroba¹³⁴, P. Starovoitov¹⁶⁴, R. Staszewski⁸⁸, G. Stavropoulos⁴⁷, A. Steffl³⁷, P. Steinberg³⁰, B. Stelzer^{146,159a}, H. J. Stelzer¹³², O. Stelzer-Chilton^{159a}, H. Stenzel⁵⁹, T. J. Stevenson¹⁵⁰, G. A. Stewart³⁷, J. R. Stewart¹²⁴, M. C. Stockton³⁷, G. Stoicea^{28b}, M. Stolarski^{133a}, S. Stonjek¹¹², A. Straessner⁵¹, J. Strandberg¹⁴⁸, S. Strandberg^{48a,48b}, M. Stratmann¹⁷⁵, M. Strauss¹²³, T. Strebler¹⁰⁴, P. Strizenec^{29b}, R. Ströhmer¹⁷⁰, D. M. Strom¹²⁶, R. Stroynowski⁴⁶, A. Strubig^{48a,48b}, S. A. Stucci³⁰, B. Stugu¹⁷, J. Stupak¹²³, N. A. Styles⁴⁹, D. Su¹⁴⁷, S. Su^{63a}, W. Su^{63d}, X. Su^{63a}, D. Suchy^{29a}, K. Sugizaki¹³¹, V. V. Sulin³⁹, M. J. Sullivan⁹⁴, D. M. S. Sultan¹²⁹, L. Sultanaliyeva³⁹, S. Sultansoy^{3b}, S. Sun¹⁷⁴, W. Sun¹⁴, O. Sunneborn Gudnadottir¹⁶⁵, N. Sur¹⁰⁴, M. R. Sutton¹⁵⁰, H. Suzuki¹⁶⁰, M. Svatos¹³⁴, M. Swiatlowski^{159a}, T. Swirski¹⁷⁰, I. Sykora^{29a}, M. Sykora¹³⁶, T. Sykora¹³⁶, D. Ta¹⁰², K. Tackmann^{49,y}, A. Taffard¹⁶², R. Tafirout^{159a}, J. S. Tafoya Vargas⁶⁷, Y. Takubo⁸⁵, M. Talby¹⁰⁴, A. A. Talyshев³⁹, K. C. Tam^{65b}, N. M. Tamir¹⁵⁵, A. Tanaka¹⁵⁷, J. Tanaka¹⁵⁷, R. Tanaka⁶⁷, M. Tanasini¹⁴⁹, Z. Tao¹⁶⁸, S. Tapia Araya^{140f}, S. Tapprogge¹⁰², A. Tarek Abouelfadl Mohamed¹⁰⁹, S. Tarem¹⁵⁴, K. Tariq¹⁴, G. Tarna^{28b}, G. F. Tartarelli^{72a}, M. J. Tartarin⁹¹, P. Tas¹³⁶, M. Tasevsky¹³⁴, E. Tassi^{45a,45b}, A. C. Tate¹⁶⁶, G. Tateno¹⁵⁷, Y. Tayalati^{36e,aa}, G. N. Taylor¹⁰⁷, W. Taylor^{159b}, P. Teixeira-Dias⁹⁷, J. J. Teoh¹⁵⁸, K. Terashi¹⁵⁷, J. Terron¹⁰¹, S. Terzo¹³, M. Testa⁵⁴, R. J. Teuscher^{158,ab}, A. Thaler⁸⁰, O. Theiner⁵⁷, T. Theveneaux-Pelzer¹⁰⁴, O. Thielmann¹⁷⁵, D. W. Thomas⁹⁷, J. P. Thomas²¹, E. A. Thompson^{18a}, P. D. Thompson²¹, E. Thomson¹³¹, R. E. Thornberry⁴⁶, C. Tian^{63a}, Y. Tian⁵⁷, V. Tikhomirov^{39,a}, Yu. A. Tikhonov³⁹, S. Timoshenko³⁹, D. Timoshyn¹³⁶, E. X. L. Ting¹, P. Tipton¹⁷⁶, A. Tishelman-Charny³⁰, S. H. Tlou^{34g}, K. Todome¹⁴¹, S. Todorova-Nova¹³⁶, S. Todt⁵¹, L. Toffolin^{70a,70c}, M. Togawa⁸⁵, J. Tojo⁹⁰, S. Tokár^{29a}, O. Toldaiev⁶⁹, G. Tolkachev¹⁰⁴, M. Tomoto^{85,113}, L. Tompkins^{147,o}, E. Torrence¹²⁶, H. Torres⁹¹, E. Torró Pastor¹⁶⁷, M. Toscani³¹, C. Tosciri⁴¹, M. Tost¹¹, D. R. Tovey¹⁴³, T. Trefzger¹⁷⁰, A. Tricoli³⁰, I. M. Trigger^{159a}, S. Trincaz-Duvold¹³⁰, D. A. Trischuk²⁷, A. Tropina⁴⁰, L. Truong^{34c}, M. Trzebinski⁸⁸, A. Trzupek⁸⁸, F. Tsai¹⁴⁹, M. Tsai¹⁰⁸, A. Tsiamis¹⁵⁶, P. V. Tsiareshka⁴⁰, S. Tsigaridas^{159a}, A. Tsirigotis^{156,u}, V. Tsiskaridze¹⁵⁸, E. G. Tskhadadze^{153a}, M. Tsopoulou¹⁵⁶, Y. Tsujikawa⁸⁹, I. I. Tsukerman³⁹, V. Tsulaia^{18a}, S. Tsuno⁸⁵, K. Tsuri¹²¹, D. Tsybychev¹⁴⁹, Y. Tu^{65b}, A. Tudorache^{28b}, V. Tudorache^{28b}, S. Turchikhin^{58a,58b}, I. Turk Cakir^{3a}, R. Turra^{72a}, T. Turtuvshin^{40,ac}, P. M. Tuts⁴³, S. Tzamarias^{156,e}, E. Tzovara¹⁰², F. Ukegawa¹⁶⁰, P. A. Ulloa Poblete^{140c,140b}, E. N. Umaka³⁰, G. Unal³⁷, A. Undrus³⁰, G. Unel¹⁶², J. Urban^{29b}, P. Urrejola^{140a}, G. Usai⁸, R. Ushioda¹⁴¹, M. Usman¹¹⁰, F. Ustuner⁵³, Z. Uysal⁸³, V. Vacek¹³⁵, B. Vachon¹⁰⁶, T. Vafeiadis³⁷, A. Vaikus⁹⁸, C. Valderanis¹¹¹, E. Valdes Santurio^{48a,48b}, M. Valente^{159a}, S. Valentinetto^{24a,24b}, A. Valero¹⁶⁷, E. Valiente Moreno¹⁶⁷, A. Vallier⁹¹, J. A. Valls Ferrer¹⁶⁷, D. R. Van Arneman¹¹⁷, T. R. Van Daalen¹⁴², A. Van Der Graaf⁵⁰, P. Van Gemmeren⁶, M. Van Rijnbach³⁷, S. Van Stroud⁹⁸, I. Van Vulpen¹¹⁷, P. Vana¹³⁶, M. Vanadia^{77a,77b}, U. M. Vande Voorde¹⁴⁸, W. Vandelli³⁷, E. R. Vandewall¹²⁴, D. Vannicola¹⁵⁵, L. Vannoli⁵⁴, R. Vari^{76a}, E. W. Varnes⁷, C. Varni^{18b}, D. Varouchas⁶⁷, L. Varriale¹⁶⁷, K. E. Varvell¹⁵¹, M. E. Vasile^{28b}, L. Vaslin⁸⁵, A. Vasyukov⁴⁰, L. M. Vaughan¹²⁴, R. Vavricka¹⁰², T. Vazquez Schroeder¹³, J. Veatch³², V. Vecchio¹⁰³, M. J. Veen¹⁰⁵, I. Veliseck³⁰, L. M. Veloce¹⁵⁸, F. Veloso^{133a,133c}, S. Veneziano^{76a}, A. Ventura^{71a,71b}, S. Ventura Gonzalez¹³⁸, A. Verbytskyi¹¹², M. Verducci^{75a,75b}, C. Vergis⁹⁶, M. Verissimo De Araujo^{84b}, W. Verkerke¹¹⁷, J. C. Vermeulen¹¹⁷, C. Vernieri¹⁴⁷, M. Vessella¹⁶², M. C. Vetterli^{146,ah}, A. Vgenopoulos¹⁰², N. Viaux Maira^{140f}, T. Vickey¹⁴³, O. E. Vickey Boeriu¹⁴³, G. H. A. Viehauser¹²⁹, L. Vigani^{64b}, M. Vigl¹¹², M. Villa^{24a,24b}, M. Villaplana Perez¹⁶⁷, E. M. Villhauer⁵³, E. Vilucchi⁵⁴, M. G. Vincter³⁵, A. Visible¹¹⁷, C. Vittori³⁷, I. Vivarelli^{24a,24b}, E. Voevodina¹¹², F. Vogel¹¹¹, J. C. Voigt⁵¹, P. Vokac¹³⁵, Yu. Volkotrub^{87b}, E. Von Toerne²⁵, B. Vormwald³⁷, K. Vorobev³⁹, M. Vos¹⁶⁷, K. Voss¹⁴⁵, M. Vozak¹¹⁷, L. Vozdecky¹²³, N. Vranjes¹⁶, M. Vranjes Milosavljevic¹⁶, M. Vreeswijk¹¹⁷, N. K. Vu^{63d,63c}, R. Vuillermet³⁷, O. Vujinovic¹⁰², I. Vukotic⁴¹, I. K. Vyas³⁵, S. Wada¹⁶⁰, C. Wagner¹⁴⁷, J. M. Wagner^{18a}, W. Wagner¹⁷⁵, S. Wahdan¹⁷⁵, H. Wahlberg⁹², C. H. Waits¹²³, J. Walder¹³⁷, R. Walker¹¹¹, W. Walkowiak¹⁴⁵, A. Wall¹³¹, E. J. Wallin¹⁰⁰

- T. Wamorkar^{18a}, A. Z. Wang¹³⁹, C. Wang¹⁰², C. Wang¹¹, H. Wang^{18a}, J. Wang^{65c}, P. Wang¹⁰³, P. Wang⁹⁸, R. Wang⁶², R. Wang⁶, S. M. Wang¹⁵², S. Wang¹⁴, T. Wang^{63a}, W. T. Wang⁸¹, W. Wang¹⁴, X. Wang¹⁶⁶, X. Wang^{63c}, Y. Wang^{114a}, Y. Wang^{63a}, Z. Wang¹⁰⁸, Z. Wang^{63d,52,63c}, Z. Wang¹⁰⁸, C. Wanotayaroj, A. Warburton¹⁰⁶, R. J. Ward²¹, A. L. Warnerbring¹⁴⁵, N. Warrack⁶⁰, S. Waterhouse⁹⁷, A. T. Watson²¹, H. Watson⁵³, M. F. Watson²¹, E. Watton^{60,137}, G. Watts¹⁴², B. M. Waugh⁹⁸, J. M. Webb⁵⁵, C. Weber³⁰, H. A. Weber¹⁹, M. S. Weber²⁰, S. M. Weber^{64a}, C. Wei^{63a}, Y. Wei⁵⁵, A. R. Weidberg¹²⁹, E. J. Weik¹²⁰, J. Weingarten⁵⁰, C. Weiser⁵⁵, C. J. Wells⁴⁹, T. Wenaus³⁰, B. Wendland⁵⁰, T. Wengler³⁷, N. S. Wenke¹¹², N. Wermes²⁵, M. Wessels^{64a}, A. M. Wharton⁹³, A. S. White⁶², A. White⁸, M. J. White¹, D. Whiteson¹⁶², L. Wickremasinghe¹²⁷, W. Wiedenmann¹⁷⁴, M. Wielers¹³⁷, C. Wiglesworth⁴⁴, D. J. Wilber¹²³, H. G. Wilkens³⁷, J. J. H. Wilkinson³³, D. M. Williams⁴³, H. H. Williams¹³¹, S. Williams³³, S. Willocq¹⁰⁵, B. J. Wilson¹⁰³, D. J. Wilson¹⁰³, P. J. Windischhofer⁴¹, F. I. Winkel³¹, F. Winklmeier¹²⁶, B. T. Winter⁵⁵, M. Wittgen¹⁴⁷, M. Wobisch⁹⁹, T. Wojtkowski⁶¹, Z. Wolffs¹¹⁷, J. Wollrath³⁷, M. W. Wolter⁸⁸, H. Wolters^{133a,133c}, M. C. Wong¹³⁹, E. L. Woodward⁴³, S. D. Worm⁴⁹, B. K. Wosiek⁸⁸, K. W. Woźniak⁸⁸, S. Wozniewski⁵⁶, K. Wraight⁶⁰, C. Wu²¹, M. Wu^{114b}, M. Wu¹¹⁶, S. L. Wu¹⁷⁴, X. Wu⁵⁷, X. Wu^{63a}, Y. Wu^{63a}, Z. Wu⁴, J. Wuerzinger^{112,af}, T. R. Wyatt¹⁰³, B. M. Wynne⁵³, S. Xella⁴⁴, L. Xia^{114a}, M. Xia¹⁵, M. Xie^{63a}, A. Xiong¹²⁶, J. Xiong^{18a}, D. Xu¹⁴, H. Xu^{63a}, L. Xu^{63a}, R. Xu¹³¹, T. Xu¹⁰⁸, Y. Xu¹⁴², Z. Xu⁵³, Z. Xu^{114a}, B. Yabsley¹⁵¹, S. Yacoob^{34a}, Y. Yamaguchi⁸⁵, E. Yamashita¹⁵⁷, H. Yamauchi¹⁶⁰, T. Yamazaki^{18a}, Y. Yamazaki⁸⁶, S. Yan⁶⁰, Z. Yan¹⁰⁵, H. J. Yang^{63c,63d}, H. T. Yang^{63a}, S. Yang^{63a}, T. Yang^{65c}, X. Yang³⁷, X. Yang¹⁴, Y. Yang⁴⁶, Y. Yang^{63a}, W.-M. Yao^{18a}, H. Ye⁵⁶, J. Ye¹⁴, S. Ye³⁰, X. Ye^{63a}, Y. Yeh⁹⁸, I. Yeletskikh⁴⁰, B. Yeo^{18b}, M. R. Yexley⁹⁸, T. P. Yıldırım¹²⁹, P. Yin⁴³, K. Yorita¹⁷², S. Younas^{28b}, C. J. S. Young³⁷, C. Young¹⁴⁷, N. D. Young¹²⁶, Y. Yu^{63a}, J. Yuan^{14,114c}, M. Yuan¹⁰⁸, R. Yuan^{63d,63c}, L. Yue⁹⁸, M. Zaazoua^{63a}, B. Zabinski⁸⁸, I. Zahir^{36a}, Z. K. Zak⁸⁸, T. Zakareishvili¹⁶⁷, S. Zambito⁵⁷, J. A. Zamora Saa^{140b,140d}, J. Zang¹⁵⁷, D. Zanzi⁵⁵, R. Zanzottera^{72a,72b}, O. Zaplatilek¹³⁵, C. Zeitnitz¹⁷⁵, H. Zeng¹⁴, J. C. Zeng¹⁶⁶, D. T. Zenger Jr²⁷, O. Zenin³⁹, T. Ženiš^{29a}, S. Zenz⁹⁶, S. Zerradi^{36a}, D. Zerwas⁶⁷, M. Zhai^{14,114c}, D. F. Zhang¹⁴³, J. Zhang^{63b}, J. Zhang⁶, K. Zhang^{14,114c}, L. Zhang^{63a}, L. Zhang^{114a}, P. Zhang^{14,114c}, R. Zhang¹⁷⁴, S. Zhang⁹¹, T. Zhang¹⁵⁷, X. Zhang^{63c}, Y. Zhang¹⁴², Y. Zhang⁹⁸, Y. Zhang^{63a}, Y. Zhang^{114a}, Z. Zhang^{18a}, Z. Zhang^{63b}, Z. Zhang⁶⁷, H. Zhao¹⁴², T. Zhao^{63b}, Y. Zhao³⁵, Z. Zhao^{63a}, Z. Zhao^{63a}, A. Zhemchugov⁴⁰, J. Zheng^{114a}, K. Zheng¹⁶⁶, X. Zheng^{63a}, Z. Zheng¹⁴⁷, D. Zhong¹⁶⁶, B. Zhou¹⁰⁸, H. Zhou⁷, N. Zhou^{63c}, Y. Zhou¹⁵, Y. Zhou^{114a}, Y. Zhou⁷, C. G. Zhu^{63b}, J. Zhu¹⁰⁸, X. Zhu^{63d}, Y. Zhu^{63c}, Y. Zhu^{63a}, X. Zhuang¹⁴, K. Zhukov⁶⁹, N. I. Zimine⁴⁰, J. Zinsser^{64b}, M. Ziolkowski¹⁴⁵, L. Živković¹⁶, A. Zoccoli^{24a,24b}, K. Zoch⁶², T. G. Zorbas¹⁴³, O. Zormpa⁴⁷, W. Zou⁴³, L. Zwalinski³⁷

¹ Department of Physics, University of Adelaide, Adelaide, Australia² Department of Physics, University of Alberta, Edmonton, AB, Canada³ ^(a)Department of Physics, Ankara University, Ankara, Türkiye; ^(b)Division of Physics, TOBB University of Economics and Technology, Ankara, Türkiye⁴ LAPP, Université Savoie Mont Blanc, CNRS/IN2P3, Annecy, France⁵ APC, Université Paris Cité, CNRS/IN2P3, Paris, France⁶ High Energy Physics Division, Argonne National Laboratory, Argonne, IL, USA⁷ Department of Physics, University of Arizona, Tucson, AZ, USA⁸ Department of Physics, University of Texas at Arlington, Arlington, TX, USA⁹ Physics Department, National and Kapodistrian University of Athens, Athens, Greece¹⁰ Physics Department, National Technical University of Athens, Zografou, Greece¹¹ Department of Physics, University of Texas at Austin, Austin, TX, USA¹² Institute of Physics, Azerbaijan Academy of Sciences, Baku, Azerbaijan¹³ Institut de Física d'Altes Energies (IFAE), Barcelona Institute of Science and Technology, Barcelona, Spain¹⁴ Institute of High Energy Physics, Chinese Academy of Sciences, Beijing, China¹⁵ Physics Department, Tsinghua University, Beijing, China¹⁶ Institute of Physics, University of Belgrade, Belgrade, Serbia¹⁷ Department for Physics and Technology, University of Bergen, Bergen, Norway¹⁸ ^(a)Physics Division, Lawrence Berkeley National Laboratory, Berkeley, CA, USA; ^(b)University of California, Berkeley, CA, USA¹⁹ Institut für Physik, Humboldt Universität zu Berlin, Berlin, Germany

- ²⁰ Albert Einstein Center for Fundamental Physics and Laboratory for High Energy Physics, University of Bern, Bern, Switzerland
- ²¹ School of Physics and Astronomy, University of Birmingham, Birmingham, UK
- ²² ^(a)Department of Physics, Bogazici University, Istanbul, Türkiye; ^(b)Department of Physics Engineering, Gaziantep University, Gaziantep, Türkiye; ^(c)Department of Physics, Istanbul University, Istanbul, Türkiye
- ²³ ^(a)Facultad de Ciencias y Centro de Investigaciones, Universidad Antonio Nariño, Bogotá, Colombia; ^(b)Departamento de Física, Universidad Nacional de Colombia, Bogotá, Colombia
- ²⁴ ^(a)Dipartimento di Fisica e Astronomia A. Righi, Università di Bologna, Bologna, Italy; ^(b)INFN Sezione di Bologna, Bologna, Italy
- ²⁵ Physikalisches Institut, Universität Bonn, Bonn, Germany
- ²⁶ Department of Physics, Boston University, Boston, MA, USA
- ²⁷ Department of Physics, Brandeis University, Waltham, MA, USA
- ²⁸ ^(a)Transilvania University of Brasov, Brasov, Romania ^(b)Horia Hulubei National Institute of Physics and Nuclear Engineering, Bucharest, Romania; ^(c)Department of Physics, Alexandru Ioan Cuza University of Iasi, Iasi, Romania ^(d)Physics Department, National Institute for Research and Development of Isotopic and Molecular Technologies, Cluj-Napoca, Romania; ^(e)National University of Science and Technology Politehnica, Bucharest, Romania; ^(f)West University in Timisoara, Timisoara, Romania; ^(g)Faculty of Physics, University of Bucharest, Bucharest, Romania
- ²⁹ ^(a)Faculty of Mathematics, Physics and Informatics, Comenius University, Bratislava, Slovakia; ^(b)Department of Subnuclear Physics, Institute of Experimental Physics of the Slovak Academy of Sciences, Kosice, Slovak Republic
- ³⁰ Physics Department, Brookhaven National Laboratory, Upton, NY, USA
- ³¹ Universidad de Buenos Aires, Facultad de Ciencias Exactas y Naturales, Departamento de Física, y CONICET, Instituto de Física de Buenos Aires (IFIBA), Buenos Aires, Argentina
- ³² California State University, Long Beach, CA, USA
- ³³ Cavendish Laboratory, University of Cambridge, Cambridge, UK
- ³⁴ ^(a)Department of Physics, University of Cape Town, Cape Town, South Africa; ^(b)iThemba Labs, Cape Town, Western Cape, South Africa; ^(c)Department of Mechanical Engineering Science, University of Johannesburg, Johannesburg, South Africa; ^(d)National Institute of Physics, University of the Philippines Diliman (Philippines), Quezon City, Philippines; ^(e)University of South Africa, Department of Physics, Pretoria, South Africa; ^(f)University of Zululand, KwaDlangezwa, Ongoye, South Africa; ^(g)School of Physics, University of the Witwatersrand, Johannesburg, South Africa
- ³⁵ Department of Physics, Carleton University, Ottawa, ON, Canada
- ³⁶ ^(a)Faculté des Sciences Ain Chock, Université Hassan II de Casablanca, Casablanca, Morocco; ^(b)Faculté des Sciences, Université Ibn-Tofail, Kenitra, Morocco; ^(c)Faculté des Sciences Semlalia, Université Cadi Ayyad, LPHEA-Marrakech, Marrakech, Morocco; ^(d)LPMR, Faculté des Sciences, Université Mohamed Premier, Oujda, Morocco; ^(e)Faculté des sciences, Université Mohammed V, Rabat, Morocco; ^(f)Institute of Applied Physics, Mohammed VI Polytechnic University, Ben Guerir, Morocco
- ³⁷ CERN, Geneva, Switzerland
- ³⁸ Affiliated with an Institute Formerly Covered by a Cooperation Agreement with CERN, Geneva, Switzerland
- ³⁹ Affiliated with an Institute Covered by a Cooperation Agreement with CERN, Geneva, Switzerland
- ⁴⁰ Affiliated with an International Laboratory Covered by a Cooperation Agreement with CERN, Geneva, Switzerland
- ⁴¹ Enrico Fermi Institute, University of Chicago, Chicago, IL, USA
- ⁴² LPC, Université Clermont Auvergne, CNRS/IN2P3, Clermont-Ferrand, France
- ⁴³ Nevis Laboratory, Columbia University, Irvington, NY, USA
- ⁴⁴ Niels Bohr Institute, University of Copenhagen, Copenhagen, Denmark
- ⁴⁵ ^(a)Dipartimento di Fisica, Università della Calabria, Rende, Italy; ^(b)INFN Gruppo Collegato di Cosenza, Laboratori Nazionali di Frascati, Frascati, Italy
- ⁴⁶ Physics Department, Southern Methodist University, Dallas, TX, USA
- ⁴⁷ National Centre for Scientific Research “Demokritos”, Agia Paraskevi, Greece
- ⁴⁸ ^(a)Department of Physics, Stockholm University, Stockholm, Sweden; ^(b)Oskar Klein Centre, Stockholm, Sweden
- ⁴⁹ Deutsches Elektronen-Synchrotron DESY, Hamburg and Zeuthen, Germany
- ⁵⁰ Fakultät Physik, Technische Universität Dortmund, Dortmund, Germany
- ⁵¹ Institut für Kern- und Teilchenphysik, Technische Universität Dresden, Dresden, Germany
- ⁵² Department of Physics, Duke University, Durham, NC, USA

- ⁵³ SUPA-School of Physics and Astronomy, University of Edinburgh, Edinburgh, UK
⁵⁴ INFN e Laboratori Nazionali di Frascati, Frascati, Italy
⁵⁵ Physikalisches Institut, Albert-Ludwigs-Universität Freiburg, Freiburg, Germany
⁵⁶ II. Physikalisches Institut, Georg-August-Universität Göttingen, Göttingen, Germany
⁵⁷ Département de Physique Nucléaire et Corpusculaire, Université de Genève, Geneva, Switzerland
⁵⁸ ^(a)Dipartimento di Fisica, Università di Genova, Genoa, Italy; ^(b)INFN Sezione di Genova, Genoa, Italy
⁵⁹ II. Physikalisches Institut, Justus-Liebig-Universität Giessen, Giessen, Germany
⁶⁰ SUPA-School of Physics and Astronomy, University of Glasgow, Glasgow, UK
⁶¹ LPSC, Université Grenoble Alpes, CNRS/IN2P3, Grenoble INP, Grenoble, France
⁶² Laboratory for Particle Physics and Cosmology, Harvard University, Cambridge, MA, USA
⁶³ ^(a)Department of Modern Physics and State Key Laboratory of Particle Detection and Electronics, University of Science and Technology of China, Hefei, China; ^(b)Institute of Frontier and Interdisciplinary Science and Key Laboratory of Particle Physics and Particle Irradiation (MOE), Shandong University, Qingdao, China; ^(c)School of Physics and Astronomy, Shanghai Jiao Tong University, Key Laboratory for Particle Astrophysics and Cosmology (MOE), SKLPPC, Shanghai, China; ^(d)Tsung-Dao Lee Institute, Shanghai, China; ^(e)School of Physics, Zhengzhou University, China
⁶⁴ ^(a)Kirchhoff-Institut für Physik, Ruprecht-Karls-Universität Heidelberg, Heidelberg, Germany; ^(b)Physikalisches Institut, Ruprecht-Karls-Universität Heidelberg, Heidelberg, Germany
⁶⁵ ^(a)Department of Physics, Chinese University of Hong Kong, Shatin, N.T., Hong Kong; ^(b)Department of Physics, University of Hong Kong, Pok Fu Lam, Hong Kong; ^(c)Department of Physics and Institute for Advanced Study, Hong Kong University of Science and Technology, Clear Water Bay, Kowloon, Hong Kong, China
⁶⁶ Department of Physics, National Tsing Hua University, Hsinchu, Taiwan
⁶⁷ IJCLab, Université Paris-Saclay, CNRS/IN2P3, 91405 Orsay, France
⁶⁸ Centro Nacional de Microelectrónica (IMB-CNM-CSIC), Barcelona, Spain
⁶⁹ Department of Physics, Indiana University, Bloomington, IN, USA
⁷⁰ ^(a)INFN Gruppo Collegato di Udine, Sezione di Trieste, Udine, Italy; ^(b)ICTP, Trieste, Italy; ^(c)Dipartimento Politecnico di Ingegneria e Architettura, Università di Udine, Udine, Italy
⁷¹ ^(a)INFN Sezione di Lecce, Lecce, Italy; ^(b)Dipartimento di Matematica e Fisica, Università del Salento, Lecce, Italy
⁷² ^(a)INFN Sezione di Milano, Milan, Italy; ^(b)Dipartimento di Fisica, Università di Milano, Milan, Italy
⁷³ ^(a)INFN Sezione di Napoli, Naples, Italy; ^(b)Dipartimento di Fisica, Università di Napoli, Naples, Italy
⁷⁴ ^(a)INFN Sezione di Pavia, Pavia, Italy; ^(b)Dipartimento di Fisica, Università di Pavia, Pavia, Italy
⁷⁵ ^(a)INFN Sezione di Pisa, Pisa, Italy; ^(b)Dipartimento di Fisica E. Fermi, Università di Pisa, Pisa, Italy
⁷⁶ ^(a)INFN Sezione di Roma, Rome, Italy; ^(b)Dipartimento di Fisica, Sapienza Università di Roma, Rome, Italy
⁷⁷ ^(a)INFN Sezione di Roma Tor Vergata, Rome, Italy; ^(b)Dipartimento di Fisica, Università di Roma Tor Vergata, Rome, Italy
⁷⁸ ^(a)INFN Sezione di Roma Tre, Rome, Italy; ^(b)Dipartimento di Matematica e Fisica, Università Roma Tre, Rome, Italy
⁷⁹ ^(a)INFN-TIFPA, Povo, Italy; ^(b)Università degli Studi di Trento, Trento, Italy
⁸⁰ Universität Innsbruck, Department of Astro and Particle Physics, Innsbruck, Austria
⁸¹ University of Iowa, Iowa City, IA, USA
⁸² Department of Physics and Astronomy, Iowa State University, Ames, IA, USA
⁸³ İstinye University, Sarıyer, İstanbul, Türkiye
⁸⁴ ^(a)Departamento de Engenharia Elétrica, Universidade Federal de Juiz de Fora (UFJF), Juiz de Fora, Brazil;
; ^(b)Universidade Federal do Rio De Janeiro COPPE/EE/IF, Rio de Janeiro, Brazil; ^(c)Instituto de Física, Universidade de São Paulo, São Paulo, Brazil; ^(d)Rio de Janeiro State University, Rio de Janeiro, Brazil; ^(e)Federal University of Bahia, Bahia, Brazil
⁸⁵ KEK, High Energy Accelerator Research Organization, Tsukuba, Japan
⁸⁶ Graduate School of Science, Kobe University, Kobe, Japan
⁸⁷ ^(a)Faculty of Physics and Applied Computer Science, AGH University of Krakow, Krakow, Poland; ^(b)Marian Smoluchowski Institute of Physics, Jagiellonian University, Krakow, Poland
⁸⁸ Institute of Nuclear Physics Polish Academy of Sciences, Krakow, Poland
⁸⁹ Faculty of Science, Kyoto University, Kyoto, Japan
⁹⁰ Research Center for Advanced Particle Physics and Department of Physics, Kyushu University, Fukuoka , Japan
⁹¹ L2IT, Université de Toulouse, CNRS/IN2P3, UPS, Toulouse, France
⁹² Instituto de Física La Plata, Universidad Nacional de La Plata and CONICET, La Plata, Argentina

- ⁹³ Physics Department, Lancaster University, Lancaster, UK
⁹⁴ Oliver Lodge Laboratory, University of Liverpool, Liverpool, UK
⁹⁵ Department of Experimental Particle Physics, Jožef Stefan Institute and Department of Physics, University of Ljubljana, Ljubljana, Slovenia
⁹⁶ School of Physics and Astronomy, Queen Mary University of London, London, UK
⁹⁷ Department of Physics, Royal Holloway University of London, Egham, UK
⁹⁸ Department of Physics and Astronomy, University College London, London, UK
⁹⁹ Louisiana Tech University, Ruston, LA, USA
¹⁰⁰ Fysiska institutionen, Lunds universitet, Lund, Sweden
¹⁰¹ Departamento de Física Teórica C-15 and CIAFF, Universidad Autónoma de Madrid, Madrid, Spain
¹⁰² Institut für Physik, Universität Mainz, Mainz, Germany
¹⁰³ School of Physics and Astronomy, University of Manchester, Manchester, UK
¹⁰⁴ CPPM, Aix-Marseille Université, CNRS/IN2P3, Marseille, France
¹⁰⁵ Department of Physics, University of Massachusetts, Amherst, MA, USA
¹⁰⁶ Department of Physics, McGill University, Montreal, QC, Canada
¹⁰⁷ School of Physics, University of Melbourne, Melbourne, VIC, Australia
¹⁰⁸ Department of Physics, University of Michigan, Ann Arbor, MI, USA
¹⁰⁹ Department of Physics and Astronomy, Michigan State University, East Lansing, MI, USA
¹¹⁰ Group of Particle Physics, University of Montreal, Montreal, QC, Canada
¹¹¹ Fakultät für Physik, Ludwig-Maximilians-Universität München, Munich, Germany
¹¹² Max-Planck-Institut für Physik (Werner-Heisenberg-Institut), Munich, Germany
¹¹³ Graduate School of Science and Kobayashi-Maskawa Institute, Nagoya University, Nagoya, Japan
¹¹⁴ ^(a)Department of Physics, Nanjing University, Nanjing, China; ^(b)School of Science, Shenzhen Campus of Sun Yat-sen University, Shenzhen, China; ^(c)University of Chinese Academy of Science (UCAS), Beijing, China
¹¹⁵ Department of Physics and Astronomy, University of New Mexico, Albuquerque, NM, USA
¹¹⁶ Institute for Mathematics, Astrophysics and Particle Physics, Radboud University/Nikhef, Nijmegen, The Netherlands
¹¹⁷ Nikhef National Institute for Subatomic Physics and University of Amsterdam, Amsterdam, The Netherlands
¹¹⁸ Department of Physics, Northern Illinois University, DeKalb, IL, USA
¹¹⁹ ^(a)New York University Abu Dhabi, Abu Dhabi, United Arab Emirates; ^(b)United Arab Emirates University, Al Ain, United Arab Emirates
¹²⁰ Department of Physics, New York University, New York, NY, USA
¹²¹ Ochanomizu University, Otsuka, Bunkyo-ku, Tokyo, Japan
¹²² Ohio State University, Columbus, OH, USA
¹²³ Homer L. Dodge Department of Physics and Astronomy, University of Oklahoma, Norman, OK, USA
¹²⁴ Department of Physics, Oklahoma State University, Stillwater, OK, USA
¹²⁵ Palacký University, Joint Laboratory of Optics, Olomouc, Czech Republic
¹²⁶ Institute for Fundamental Science, University of Oregon, Eugene, OR, USA
¹²⁷ Graduate School of Science, Osaka University, Osaka, Japan
¹²⁸ Department of Physics, University of Oslo, Oslo, Norway
¹²⁹ Department of Physics, Oxford University, Oxford, UK
¹³⁰ LPNHE, Sorbonne Université, Université Paris Cité, CNRS/IN2P3, Paris, France
¹³¹ Department of Physics, University of Pennsylvania, Philadelphia, PA, USA
¹³² Department of Physics and Astronomy, University of Pittsburgh, Pittsburgh, PA, USA
¹³³ ^(a)Laboratório de Instrumentação e Física Experimental de Partículas - LIP, Lisbon, Portugal; ^(b)Departamento de Física, Faculdade de Ciências, Universidade de Lisboa, Lisbon, Portugal; ^(c)Departamento de Física, Universidade de Coimbra, Coimbra, Portugal; ^(d)Centro de Física Nuclear da Universidade de Lisboa, Lisbon, Portugal; ^(e)Departamento de Física, Escola de Ciências, Universidade do Minho, Braga, Portugal; ^(f)Departamento de Física Teórica y del Cosmos, Universidad de Granada, Granada, Spain; ^(g)Departamento de Física, Instituto Superior Técnico, Universidade de Lisboa, Lisbon, Portugal
¹³⁴ Institute of Physics of the Czech Academy of Sciences, Prague, Czech Republic
¹³⁵ Czech Technical University in Prague, Prague, Czech Republic
¹³⁶ Faculty of Mathematics and Physics, Charles University, Prague, Czech Republic
¹³⁷ Particle Physics Department, Rutherford Appleton Laboratory, Didcot, UK

- ¹³⁸ IRFU, CEA, Université Paris-Saclay, Gif-sur-Yvette, France
¹³⁹ Santa Cruz Institute for Particle Physics, University of California Santa Cruz, Santa Cruz, CA, USA
¹⁴⁰ (a) Departamento de Física, Pontificia Universidad Católica de Chile, Santiago, Chile; (b) Millennium Institute for Subatomic physics at high energy frontier (SAPHIR), Santiago, Chile; (c) Instituto de Investigación Multidisciplinario en Ciencia y Tecnología, y Departamento de Física, Universidad de La Serena, La Serena, Chile; (d) Department of Physics, Universidad Andres Bello, Santiago, Chile; (e) Instituto de Alta Investigación, Universidad de Tarapacá, Arica, Chile
; (f) Departamento de Física, Universidad Técnica Federico Santa María, Valparaíso, Chile
¹⁴¹ Department of Physics, Institute of Science, Tokyo, Japan
¹⁴² Department of Physics, University of Washington, Seattle, WA, USA
¹⁴³ Department of Physics and Astronomy, University of Sheffield, Sheffield, UK
¹⁴⁴ Department of Physics, Shinshu University, Nagano, Japan
¹⁴⁵ Department Physik, Universität Siegen, Siegen, Germany
¹⁴⁶ Department of Physics, Simon Fraser University, Burnaby, BC, Canada
¹⁴⁷ SLAC National Accelerator Laboratory, Stanford, CA, USA
¹⁴⁸ Department of Physics, Royal Institute of Technology, Stockholm, Sweden
¹⁴⁹ Departments of Physics and Astronomy, Stony Brook University, Stony Brook, NY, USA
¹⁵⁰ Department of Physics and Astronomy, University of Sussex, Brighton, UK
¹⁵¹ School of Physics, University of Sydney, Sydney, Australia
¹⁵² Institute of Physics, Academia Sinica, Taipei, Taiwan
¹⁵³ (a) E. Andronikashvili Institute of Physics, Iv. Javakhishvili Tbilisi State University, Tbilisi, Georgia; (b) High Energy Physics Institute, Tbilisi State University, Tbilisi, Georgia; (c) University of Georgia, Tbilisi, Georgia
¹⁵⁴ Department of Physics, Technion, Israel Institute of Technology, Haifa, Israel
¹⁵⁵ Raymond and Beverly Sackler School of Physics and Astronomy, Tel Aviv University, Tel Aviv, Israel
¹⁵⁶ Department of Physics, Aristotle University of Thessaloniki, Thessaloniki, Greece
¹⁵⁷ International Center for Elementary Particle Physics and Department of Physics, University of Tokyo, Tokyo, Japan
¹⁵⁸ Department of Physics, University of Toronto, Toronto, ON, Canada
¹⁵⁹ (a) TRIUMF, Vancouver, BC, Canada; (b) Department of Physics and Astronomy, York University, Toronto, ON, Canada
¹⁶⁰ Division of Physics and Tomonaga Center for the History of the Universe, Faculty of Pure and Applied Sciences, University of Tsukuba, Tsukuba, Japan
¹⁶¹ Department of Physics and Astronomy, Tufts University, Medford, MA, USA
¹⁶² Department of Physics and Astronomy, University of California Irvine, Irvine, CA, USA
¹⁶³ University of West Attica, Athens, Greece
¹⁶⁴ University of Sharjah, Sharjah, United Arab Emirates
¹⁶⁵ Department of Physics and Astronomy, University of Uppsala, Uppsala, Sweden
¹⁶⁶ Department of Physics, University of Illinois, Urbana, IL, USA
¹⁶⁷ Instituto de Física Corpuscular (IFIC), Centro Mixto Universidad de Valencia-CSIC, Valencia, Spain
¹⁶⁸ Department of Physics, University of British Columbia, Vancouver, BC, Canada
¹⁶⁹ Department of Physics and Astronomy, University of Victoria, Victoria, BC, Canada
¹⁷⁰ Fakultät für Physik und Astronomie, Julius-Maximilians-Universität Würzburg, Würzburg, Germany
¹⁷¹ Department of Physics, University of Warwick, Coventry, UK
¹⁷² Waseda University, Tokyo, Japan
¹⁷³ Department of Particle Physics and Astrophysics, Weizmann Institute of Science, Rehovot, Israel
¹⁷⁴ Department of Physics, University of Wisconsin, Madison, WI, USA
¹⁷⁵ Fakultät für Mathematik und Naturwissenschaften, Fachgruppe Physik, Bergische Universität Wuppertal, Wuppertal, Germany
¹⁷⁶ Department of Physics, Yale University, New Haven, CT, USA
¹⁷⁷ Yerevan Physics Institute, Yerevan, Armenia

^a Also Affiliated with an Institute Covered by a Cooperation Agreement with CERN, Geneva, Switzerland

^b Also at An-Najah National University, Nablus, Palestine

^c Also at Borough of Manhattan Community College, City University of New York, New York, NY, USA

^d Also at Center for High Energy Physics, Peking University, China

^e Also at Center for Interdisciplinary Research and Innovation (CIRI-AUTH), Thessaloniki, Greece

^f Also at CERN, Geneva, Switzerland

^g Also at CMD-AC UNEC Research Center, Azerbaijan State University of Economics (UNEC), Baku, Azerbaijan

^h Also at Département de Physique Nucléaire et Corpusculaire, Université de Genève, Geneva, Switzerland

ⁱ Also at Departament de Física de la Universitat Autònoma de Barcelona, Barcelona, Spain

^j Also at Department of Financial and Management Engineering, University of the Aegean, Chios, Greece

^k Also at Department of Mathematical Sciences, University of South Africa, Johannesburg, South Africa

^l Also at Department of Physics, Bolu Abant Izzet Baysal University, Bolu, Türkiye

^m Also at Department of Physics, California State University, Sacramento, USA

ⁿ Also at Department of Physics, King's College London, London, UK

^o Also at Department of Physics, Stanford University, Stanford, CA, USA

^p Also at Department of Physics, Stellenbosch University, South Africa

^q Also at Department of Physics, University of Fribourg, Fribourg, Switzerland

^r Also at Department of Physics, University of Thessaly, Volos, Greece

^s Also at Department of Physics, Westmont College, Santa Barbara, USA

^t Also at Faculty of Physics, Sofia University, 'St. Kliment Ohridski', Sofia, Bulgaria

^u Also at Hellenic Open University, Patras, Greece

^v Also at Henan University, Kaifeng, China

^w Also at Imam Mohammad Ibn Saud Islamic University, Riyadh, Saudi Arabia

^x Also at Institutio Catalana de Recerca i Estudis Avancats, ICREA, Barcelona, Spain

^y Also at Institut für Experimentalphysik, Universität Hamburg, Hamburg, Germany

^z Also at Institute for Nuclear Research and Nuclear Energy (INRNE) of the Bulgarian Academy of Sciences, Sofia, Bulgaria

^{aa} Also at Institute of Applied Physics, Mohammed VI Polytechnic University, Ben Guerir, Morocco

^{ab} Also at Institute of Particle Physics (IPP), Toronto, Canada

^{ac} Also at Institute of Physics and Technology, Mongolian Academy of Sciences, Ulaanbaatar, Mongolia

^{ad} Also at Institute of Physics, Azerbaijan Academy of Sciences, Baku, Azerbaijan

^{ae} Also at National Institute of Physics, University of the Philippines Diliman (Philippines), Quezon Cit, Philippines

^{af} Also at Technical University of Munich, Munich, Germany

^{ag} Also at The Collaborative Innovation Center of Quantum Matter (CICQM), Beijing, China

^{ah} Also at TRIUMF, Vancouver, BC, Canada

^{ai} Also at Università di Napoli Parthenope, Naples, Italy

^{aj} Also at University of Colorado Boulder, Department of Physics, Colorado, USA

^{ak} Also at University of the Western Cape, Cape Town, South Africa

^{al} Also at Washington College, Chestertown, MD, USA

^{am} Also at Yeditepe University, Physics Department, Istanbul, Türkiye

* Deceased